SUBSECTION 2.5.3 TABLE OF CONTENTS

SUBSECTION 2.5.3 LIST OF FIGURES

SUBSECTION 2.5.3 LIST OF FIGURES (CONTINUED)

2.5.3 Surface Deformation

This section evaluates the potential for tectonic and non-tectonic surface deformation at the Clinch River Nuclear (CRN) Site. Information presented within this section has been developed in accordance with Regulatory Guide (RG) 1.208 and is intended to demonstrate compliance with 10 CFR 100.23, *Geologic and Seismic Siting Criteria*. Specifically, this subsection addresses the following issues:

- Potential surface deformation associated with active tectonism, including any significant neotectonic features (faults).

- Potential surface deformation associated with non-tectonic processes such as collapse structures (karst collapse), slope failures, and anthropogenic deformation (e.g., mine collapse).

RG 1.208 states, “Comprehensive geological, seismological, geophysical, and geotechnical engineering investigations should be performed.” It also states that these investigations should be performed at four levels with the degree of detail based on distance from the site. This is consistent with guidance provided in RG 1.206 Section C.I.2.5 with the site region being defined as within a radius of 320 kilometer (km) (200 mile [mi]) and documented in Subsection 2.5.1.1.

In addition, according to NUREG-0800, *Standard Review Plan for the Review of Safety Analysis Reports for Nuclear Power Plants: LWR Edition*, Section 2.5.3:

> “The applicant reports this information [geologic, seismic, geophysical, and geotechnical information with respect to surface deformation] in its application in each of three areas defined by radii of 40 km (25 mi), 8 km (5 mi), and 1 km (0.6 mi) around the site...However, applicants need to report any significant neotectonic features found beyond these distance ranges, which have a potential to impact the site safety.”

The term “significant neotectonic feature” is not clearly defined in NUREG-0800, nor is it defined in RG 1.208. NUREG-0800 does, however, state that:

> “Emphasis is placed on Quaternary-age features because evidence of surface deformation during the last approximately 2.6 million years generally indicates a potential for future surface deformation to occur.”

Consistent with earlier NRC guidance, the term “a significant tectonic feature” is defined in this Site Safety Analysis Report by the following criteria:

(1) Movement at or near the ground surface at least once within the Quaternary Period (within the past 2.6 million years);

(2) Macro-seismicity instrumentally determined with records of sufficient precision to demonstrate a direct relationship with the feature;

(3) A structural relationship to a seismogenic fault according to characteristics (1) or (2) above such that movement on one could be reasonably expected to be accompanied by movement on the other.

This section summarizes the evaluation of the site to the above criteria and will establish that there are no significant neotectonic features within the 200-mi CRN site region that have a potential to impact the site. Several features within the site region have been proposed to exhibit evidence for Quaternary deformation and are discussed in more detail in Subsection 2.5.3.7.

Likewise, there is negligible potential for tectonic surface rupture within the site vicinity (25-mi radius). The CRN Site is located in the Valley and Ridge province, which is characterized by sub-parallel northeast-trending ridges and valleys, with generally 100 to 300 feet (ft) of relief throughout eastern Tennessee. This characteristic physiography is directly related to the structural geology of the region (Figure 2.5.3-1); the Valley and Ridge consists of numerous northeast-striking southeast-dipping imbricate thrust faults that were emplaced during the late Paleozoic assembly of the supercontinent Pangea (described in more detail in Subsection 2.5.1.1.2). This thin-skinned deformation is associated with the Alleghenian orogeny (see Subsection 2.5.1.1.2).

The site lies within the Eastern Tennessee Seismic Zone (ETSZ), which is the second-most active seismic zone in eastern North America (see Subsection 2.5.2; Reference 2.5.3-1, Section 7.3.4.1.2). The majority of earthquake hypocenters occur at depths of 5 to 26 km (3 to 16 mi) and are below the basal Paleozoic detachment surface that underlies the Valley and Ridge province (Reference 2.5.3-2). No unequivocal evidence for historic surface rupture has ever been reported (Reference 2.5.3-4). Intraplate earthquakes are not well understood, and as such, the nature of the seismicity remains ambiguous and debated. No **M**>5 earthquakes have been recorded in the ETSZ since instrumental seismicity recordings began in 1973 (see Subsection 2.5.2.1).

Karst dissolution is the primary non-tectonic surface deformation hazard at the CRN Site. The site is underlain by moderately east-dipping sedimentary strata that are variably susceptible to karst dissolution; this variability is primarily a function of carbonate content and bed thickness (see Subsection 2.5.1.2.5). All stratigraphic units at the site are to some degree calcareous and contain karst features. The thicker and more pure carbonate units contain the larger and more abundant karst features. Cavities encountered in boreholes are most frequent at higher elevations near the ground surface and steadily decrease in frequency with decreasing elevation (Reference 2.5.3-3). The primary karst hazard at the site is cavities that may be encountered in the wall or floor of excavations for safety-related structures in the power block area (Figure 2.5.1-52). The dimensions and extent of cavities cannot be predicted from the borehole data; however, their presence is indicated by the scatter of cavities encountered (see Subsection 2.5.1.2.5). Borehole data combined with a site karst model and an understanding of the origin and nature of these cavities suggests that cavities might be encountered in carbonate beds projected downdip toward the excavations, and some may occur below the base of the planned excavations. More thorough discussions of karst features and processes at the CRN Site are presented in Subsection 2.5.1.2.5; these are summarized below where relevant to the issue of surface deformation. A discussion of detailed geologic excavation mapping is presented in Subsection 2.5.1.2.6.

2.5.3.1 Geological, Seismological, and Geophysical Investigations

Available information regarding the potential for surface deformation at the CRN Site was compiled from several primary sources:

- Geologic mapping published by the Tennessee Division of Geology
- Previous geologic studies of the site and site vicinity (e.g., Reference 2.5.3-5, 2.5.3-6, and 2.5.3-7)
- Unpublished geologic mapping (Reference 2.5.3-8)

In addition to incorporating these existing data, the following investigations were performed to assess the potential for tectonic and non-tectonic deformation within the 5-mi CRN Site radius:

- Interpretation of aerial photography
- Geologic field reconnaissance mapping
- Detailed geomorphic analysis of high-resolution LiDAR digital elevation data (0.5-ft pixel resolution that covers 168 square mi) acquired during this investigation; LiDAR data were also used to map karst features
- Subsurface borehole and downhole shear wave velocity investigation
- Analysis and interpretation of seismic reflection data
- Review of the EPRI et al. CEUS Seismic Source Characterization (Reference 2.5.3-1), which includes a seismicity catalog that covers the period from 1568 through 2008, and post-2008 seismicity derived from available catalogs (see Subsection 2.5.2.1.1)

2.5.3.1.1 Previous Site Investigations

The CRN Site was previously investigated as part of the Clinch River Breeder Reactor Project (CRBRP). A preliminary safety analysis report (PSAR) for the site was completed before the CRBRP was terminated in 1983 (Reference 2.5.3-5 and 2.5.3-6). Data from previous site investigations relevant to ground deformation, seismic, and non-seismic hazard data from regional studies have been incorporated as part of this early site permit application (ESPA) investigation and are discussed in Subsection 2.5.1.

2.5.3.1.2 Regional and Local Geologic Studies

In addition to the extensive site investigation related to the CRBRP, the CRN Site and vicinity have also been the focus of several other detailed geologic and hydrogeologic investigations because of its proximity to the Oak Ridge Reservation (ORR) (e.g., Reference 2.5.3-7) and the Melton Hill Dam (Reference 2.5.3-9).

An integrated study of the geology of the ORR is provided by Hatcher et al. (Reference 2.5.3-7). This study combines detailed mapping of the ORR area with exploratory boreholes and geophysical data (both seismic reflection and refraction); provides a very detailed report on the soils, bedrock stratigraphy, and structural geology of the region; and proposes a hydrogeologic model based on data collected for that report. Rubin and Lemiszki (Reference 2.5.3-10) built on the hydrogeologic model proposed in that study and demonstrated that lithology and structural geology of the Valley and Ridge province in the ORR area strongly controls the spatial development of karst features through the region. They suggested that cave systems tend to develop extensive along-strike networks that are the result of restricted groundwater flow in siliciclastic lithologies adjacent to carbonate units. The geologic map that was produced during the Hatcher et al. (Reference 2.5.3-7) investigation was updated by Lemiszki et al. (Reference 2.5.3-8) and is included in the compiled geologic map (Plate 1) in Part 8 of this Application.

Several recent studies in eastern Tennessee have focused on evaluating evidence of Quaternary surface deformation and its possible association with the ETSZ (Reference 2.5.3-12, 2.5.3-13, 2.5.3-14, and 2.5.3-15). The primary focus of these studies has been on Quaternary terrace deposits that surround Douglas Reservoir (approximately 50 mi from the CRN Site), as this area may contain conditions conducive for finding evidence for paleoliquefaction features. Vaughn et al. (Reference 2.5.3-11) reported evidence of minor surface faulting, fracturing, and disrupted features in terrace alluvium, along with minor paleoliquefaction, northeast of Knoxville, Tennessee. Similarly, studies along Douglas Reservoir document bleached fracture systems and

possible sandy intrusions in terrace deposits that they interpret as paleoseismic in origin, although the origin of these features is unclear. Howard et al. (Reference 2.5.3-15) and Warrell et al. (Reference 2.5.3-13) reported fractures, small faults, and displacements in Quaternary alluvium along Douglas Reservoir that they suggest resulted from earthquakes with magnitudes greater than 6.0 and 6.5 (magnitude scale unspecified). While a seismic origin for many of the observed features in these studies cannot be definitively confirmed or ruled out, there are multiple alternative hypotheses that can explain their origin (e.g., pedogenic processes, karst collapse, slope failure). See Subsection 2.5.2.2.6.1.3 for a discussion of ETSZ Maximum Magnitude (Mmax) sensitivity studies.

2.5.3.2 Geological Evidence, or Absence of Evidence, for Surface Deformation

2.5.3.2.1 Bedrock Faults

The CRN Site is located between two major late Paleozoic thrust faults: the Whiteoak Mountain fault approximately 2 mi to the northwest, and the Copper Creek fault approximately 0.25 mi to the south (Figure 2.5.1-35) (see Subsection 2.5.1.2.4). Both faults juxtapose lower Cambrian Rome Formation above Middle Ordovician Chickamauga Group rocks and sole into the basal Appalachian detachment at 3.5 to 4 km below the ground surface (Figure 2.5.1-35). Additionally, Lemiszki et al. (Reference 2.5.3-8) traced out a relatively small-displacement thrust fault (Chestnut Ridge fault) 0.6 mi to the west that juxtaposes Ordovician units of the Knox Group (Figure 2.5.1-35) (see Subsection 2.5.1.2.4). This fault is interpreted as a thrust fault that propagated from bedding-parallel slip within the Knox Group and likely does not sole into the basal Appalachian detachment. Seismic reflection surveys conducted at the site revealed no evidence for blind faults (see Subsection 2.5.1.2.4; Reference 2.5.3-3). A blind fault might be indicated by reflectors that are offset or truncated by a more steeply dipping reflector that propagates through the Paleozoic section but either (1) does not penetrate the ground surface or (2) is overlain by sediments to the extent that the surface trace is not mappable. This would differ from the expression of faults identified in nearby seismic reflection profiles that include fault traces that are mapped at the ground surface.

Several lines of evidence strongly support late Paleozoic emplacement of Valley and Ridge thrust faults:

- The youngest strata that Valley and Ridge faults offset are Carboniferous (Pennsylvanian) in age (e.g., Reference 2.5.3-16).
- $^{40}K/^{40}Ar$ and $^{40}Ar/^{39}Ar$ geochronologic analyses of fault gouge from the Copper Creek fault yielded ages of 280 to 290 and 279.5 ± 11.3 *mega annum* (Ma), respectively (Reference 2.5.3-6; Reference 2.5.3-17).
- In the central Pennsylvania Valley and Ridge, undeformed Mesozoic diabase dikes have been mapped that clearly crosscut Valley and Ridge structures (Reference 2.5.3-18).

Additionally, undeformed Quaternary river terraces in the CRN site vicinity overlie the traces of Valley and Ridge thrust faults (Subsection 2.5.3.2.5; Figures 2.5.3-2 and 2.5.3-3), which further supports the conclusion that they are inactive structures.

2.5.3.2.2 Shear-Fracture Zones

As discussed in Subsections 2.5.1.2.4 and 2.5.1.2.6, a structure loosely described as a “shear zone” was identified in the Eidson Member of the Lincolnshire Formation in the CRBRP PSAR (References 2.5.3-5 and 2.5.3-6). The “shear zone” was penetrated in 39 boreholes during the CRBRP investigation, and a surface exposure in the northeastern portion of the site was

described in the CRBRP PSAR (Reference 2.5.3-6). This zone is reported to range from 19 to 46 ft thick and is, on average, reported to be approximately 35 ft thick (Reference 2.5.3-6). The zone is roughly parallel to bedding and occurs in the same stratigraphic position where encountered (Reference 2.5.3-5). It is characterized as “a zone of interbed slippage characterized by a combination of slickensides, calcite veins, and 1-inch to 1-foot segments that are either severely warped or brecciated” (Reference 2.5.3-5). Interbed slippage in the zone is estimated to be on the order of inches (Reference 2.5.3-6), as no stratigraphic offset is demonstrable. Reference 2.5.3-6 clarifies that “the ‘shear zone’ is not a fault breccia nor a fault zone.”

Similar structures identified in the Lincolnshire (Eidson Member), Rockdell, and Benbolt Formations are defined as shear-fracture zones in the current subsurface investigation (see Subsections 2.5.1.2.4 and 2.5.1.2.6). These shear-fracture zones are located and characterized in 18 of the 100-, 200-, and 400-series boreholes (Table 2.5.1-17; Figure 2.5.1-60). Shear-fracture zones consist of fractured, calcite-healed zones that form parallel to bedding, with reported thicknesses up to 22 ft (see Subsections 2.5.1.2.4 and 2.5.1.2.6 for detailed descriptions of their structural attributes). These shear-fracture zones are interpreted to be the same structures that were encountered and described as “shear zones” in the CRBRP PSAR (References 2.5.3-5 and 2.5.3-6).

Eighteen boreholes penetrated shear-fracture zones during the subsurface investigation (Reference 2.5.3-3; see Table 2.5.1-17). Core recovered from 100-, 200-, and 400-series borings in shear-fracture zones is commonly described as calcite-healed, with rock quality generally described as high with moderate to high core recovery (Reference 2.5.3-3; see Subsection 2.5.1.2.6.4). These zones, and calcite veins within the zones, are truncated by bedding-parallel and subvertical stylolites, which indicates development during diagenesis and a tectonic overprint (see Subsection 2.5.3.4.2). Shear-fracture zones do not appear to be loci for contemporary dissolution relative to adjacent rock. As discussed in Subsection 2.5.1.2.4.3.4, these zones are interpreted to represent localized strain accommodated primarily via dissolution-precipitation process during both diagenesis and during shortening associated with the Alleghanian orogeny.

2.5.3.2.3 Karst

Carbonate dissolution features that occur at the CRN Site and within the site area (5-mi radius) were identified using new data acquired for this ESPA, including (1) detailed analysis of high-resolution LiDAR-based digital elevation data and aerial photography; (2) field reconnaissance mapping; (3) seismic refraction surveys at the site; and (4) analysis of soil and rock-core borings drilled at the site. New data were compiled with existing site-specific data developed for the CRBRP, local investigations, and reports (e.g., References 2.5.3-21, 2.5.3-5 and 2.5.3-6; 2.5.3-10; 2.5.3-7; and 2.5.3-3). A comprehensive evaluation of karst features is provided in Subsection 2.5.1.2.5.

Within the site area, a total of 2797 karst depressions were identified (Figure 2.5.1-47). Of these, 1210 were classified as sinkholes at least 2 ft deep with an area of 100 ft^2 (see Subsection 2.5.1.2.5). The occurrence of karst depressions is strongly controlled by lithology; geologic units that comprise the highest depression densities consist of thick, relatively pure carbonates. These include the Knox Group dolomites and more pure limestones of the Chickamauga and Conasauga Groups. Stratigraphic units that contain interbedded carbonate and siliciclastic lithologies (e.g., Benbolt and the upper Blackford formations of the Chickamauga Group) have a moderate to few number of depressions, and those dominated by siliciclastics (sandstone, siltstone, shale) have very few to no depressions. Additionally, geologic structures (e.g., fractures, folds) can exert a strong influence in the development of karst features (Reference 2.5.3-10).

Bedrock at the CRN Site location primarily consists of the Chickamauga Group, with Knox Group rocks in the northwest portion of the 0.6-mi radius (Figure 2.5.1-37). Rubin and Lemiszki (Reference 2.5.3-10) reported that, in this structural position within the Valley and Ridge (hanging wall of the Whiteoak Mountain thrust sheet), the Rockdell, Benbolt, and Witten formations are the purest and thickest carbonate units, and the Fleanor Shale is a major potential barrier to down-dip conduit development. Bedding dip, faults, and fractures in the carbonates act as infiltration pathways and sites for potential dissolution, while groundwater flow is constrained by the presence of siliciclastic units. This results in the development of laterally extensive strike-parallel cave systems (Reference 2.5.3-10). Twenty-four caves were identified in the karst inventory of the site area (see Subsection 2.5.1.2.5), all of which formed in the Copper Ridge Dolomite, Chepultepec Dolomite, or Maynardville Limestone (see Subsection 2.5.1.2.5).

Karst-related surface features at the site, identified during the CRBRP and during the current investigation, include large funnel- and dish-shaped sinkholes and small holes in the ground. Two major sinkhole clusters occur within the 0.6-mi site radius: one in the Knox Group (at the contact between the Kingsport Formation and Mascot Dolomite) and the other in the Chickamauga Group (Witten Formation) (see Subsection 2.5.1.2.5).

In addition to analysis of the ground surface, seismic refraction tomography profiles were reviewed to possibly identify features related to carbonate dissolution in the shallow subsurface (Reference 2.5.3-3) (see Figure 2.5.1-86). Seismic refraction surveys were conducted in areas that had been graded as part of CRBRP construction activities to map the depth of bedrock (Reference 2.5.3-3). The deep excavation of the site had been partially backfilled to create a planar ground surface following the termination of the project, and tomography models were generated primarily to delineate the margins of the fill and the top of bedrock in the graded portion where epikarst zones had been removed and partially backfilled. The seismic refraction data were additionally reviewed to possibly identify any anomalies that could represent potential large karst dissolution features at the site; no conspicuous features in these data were identified that can clearly be attributed to karst phenomena.

A total of 180 exploratory rock core borings have been collected at the site (104 for the CRBRP and 76 for the current investigation), 42 percent of which encountered one or more cavities. Cavities were encountered in every stratigraphic unit that was drilled underlying or adjacent to the power block area, including the Blackford Formation, Eidson Member, Fleanor Shale, Rockdell Formation, and Benbolt Formation. The frequency and size of cavities are observed to be greater in units with higher carbonate content and, generally, decrease with depth (see Subsection 2.5.1.2.5).

2.5.3.2.4 Slope failure

Reconnaissance geologic mapping, aerial photograph analysis, and slope analysis using high-resolution digital elevation data revealed no existing landslides or other slump-related hazards in the site location. Additionally, landslide hazard maps (Reference 2.5.3-22) and landslide incidence and susceptibility maps (Figures 2.4.9-5 and 2.5.1-22) indicate the site is located in an area of moderate susceptibility and low incidence (see Subsection 2.5.1.1.5).

2.5.3.2.5 Evaluation of the Presence or Absence of Surface Deformation along the Clinch River Arm of the Watts Bar Reservoir

The evaluation of any potential surface deformation features along the Clinch River arm of the Watts Bar Reservoir included a detailed geomorphic investigation supplemented with focused geologic field reconnaissance along exposed Quaternary fluvial terraces. The acquisition of LiDAR across the CRN site area offered the opportunity to reevaluate the evidence for surface faulting or the absence of surface faulting at the site. Evidence for surface faulting in the

Quaternary is often expressed by subtle deformation of geomorphic landforms, including river terraces, and can be delineated using anomalies in longitudinal stream and terrace profiles. The high-resolution LiDAR data (0.5 ft pixel resolution) allowed for detailed mapping of Clinch River terraces across the 5-mi radius site area (Figures 2.5.3-2 and 2.5.3-3) and evaluation of the relative ages of terrace levels using morphological correlation and longitudinal profiling (Figure 2.5.3-4). Analysis of longitudinal profiles of terrace elevations can provide a means to assess irregularities that could be associated with reactivation of faults and possible surface deformation. As such, an investigation of terraces along the Clinch River arm of the Watts Bar Reservoir in the site area was undertaken to evaluate potential evidence for Quaternary surface deformation (see Figure 2.5.1-25 for geologic field reconnaissance waypoint locations; (Figures 2.5.3-2, 2.5.3-3, and 2.5.3-4).

2.5.3.2.5.1 Quaternary Deposits

Holocene through Pleistocene alluvial terrace deposits are mapped along the Clinch River arm of the Watts Bar Reservoir and larger tributary valleys in the site area (Figure 2.5.3-2). Terraces along the Clinch River were delineated using high-resolution LiDAR digital elevation data and were checked during field reconnaissance. Holocene and Pleistocene terrace levels along the Clinch River are assigned based on geomorphology and relative topographic positions, with Qht0 representing the historical flood plain (now flooded and not shown on maps) and Qpt6 representing the highest and oldest terrace level. Tributary terraces of probable Pleistocene age were not assigned a relative terrace level.

Field reconnaissance of fluvial terrace deposits along the Clinch River arm of the Watts Bar Reservoir revealed subtle variations in soil development between interpreted Pleistocene and Holocene terraces. Soil profiles in the Holocene terraces are predominantly dark yellowish brown silt with some clay. Weak pedologic development in the form of soil mottling and blocky soil structure was evident in some Holocene deposits. Pleistocene terrace deposits evaluated in the site area consist of massive clayey silt and sandy silt deposits with few interbedded gravel-rich units exposed in cross section. Pleistocene terrace treads are frequently littered with abundant subrounded to rounded gravels located on the terrace surfaces regionally. Soil development on these terraces is moderate with often a bleached “E” horizon and a moderately developed “Bt” horizon. Some buried paleosols were visible in deposits along the reservoir margin. Soil profiles were predominantly yellowish brown to dark brown sandy to clayey silt deposits with trace rounded gravels. The Pleistocene terraces have a notable lack of oxidation and no evidence of potential paleoseismic features including fracturing or paleoliquefaction was observed.

Colluvial (Qc) deposits consist of weathered residuum transported by hillslope processes including slopewash and creep. No landslides were mapped within the site area. Colluvium is deposited at the toe of hillslopes and in hollows on the hillsides. Colluvium mapped in the site area is predominantly Holocene, although Pleistocene deposits are likely present. The thickness and areal extent of colluvial deposits varies significantly dependent on the subsurface bedrock unit. The Rome Formation, which erodes primarily by mechanical weathering, produces abundant colluvial deposits which blanket the lower angle slopes underlain by stratigraphically adjacent units. Alternatively, carbonate deposits, which erode primarily by chemical processes, tend to produce areally extensive colluvial deposits if they contain a significant percentage of chert, such as the Longview Dolomite. Colluvium was mapped primarily on the basis of topographic expression, and only larger bodies are included in Figure 2.5.3-2.

Holocene alluvium (Qha) deposits occur in hillside gullies and in the principle tributary valleys across the site area (Figure 2.5.3-2). Unit Qha includes channel bottom alluvium and low terrace deposits that are undivided at the scale of mapping. The unit is composed largely of silt, with sand and gravel present in varying amounts dependent on the local bedrock parent material.

Holocene alluvial fan (Qhf) deposits are present primarily at the mouths of the larger gullies incised into ridges underlain by the Rome Formation.

2.5.3.2.5.2 Clinch River Terraces

Clinch River terraces are extensively preserved within the site area and record a history of incision likely dating back to the early Pleistocene and possibly into the Tertiary, indicative of a broad, stable landscape. Terrace surfaces were delineated primarily based on topographic expression in the LiDAR digital elevation model and field observations from surfaces accessed during the field reconnaissance (Figure 2.5.3-2).

Longitudinal profiles of the modern Clinch River baseline and terraces Qht1 through Qpt6 are shown in Figure 2.5.3-4. The baseline longitudinal profile was developed to represent the modern Clinch River prior to the construction of the Watts Bar Dam using the map view baseline stream course shown in Figure 2.5.3-2 and elevation points extracted or inferred from historic USGS topographic maps that were created prior to impoundment of Watts Bar Dam. The slope of the modern Clinch River baseline was used to determine permissible gradients of the paleo-Clinch River. Terrace elevations were extracted from the LiDAR digital elevation data and projected onto the baseline shown in Figure 2.5.3-2. Relative terrace levels were initially assigned using the terrace elevation and position relative to neighboring surfaces and morphology of terrace surfaces. These preliminary terrace levels were then refined by fitting the elevation data from each terrace level with a linear regression and comparing the slope of each regression to the slope of the modern Clinch River baseline. With some analytical refinement, the terrace elevations clustered into groups with regression slopes within a permissible range (Figure 2.5.3-4).

The only known absolute age control of Clinch River terrace deposits was obtained from archaeological excavations during the CRBRP site investigation (Reference 2.5.3-5). The oldest material dated was obtained from organic materials in the alluvium that underlies the Clinch River floodplain and yielded an age of about 2500 years (Reference 2.5.3-5). Regional terrace studies and age along analogous rivers provide information to aid in the estimation of Clinch River terrace ages.

Regional terrace studies include an investigation by Delcourt (Reference 2.5.3-24) along the Little Tennessee River which found nine topographically unique terrace levels based on elevation profiles and field reconnaissance. The terraces range in elevation above the main channel from less than 4 to 26 m (13 to 85 ft). Age control was largely qualitative and based on weathering characteristics; however, several radiocarbon dates were obtained from the lowest terrace levels, T1 and T2, at 3.5 to 15 and 28 thousand years, respectively. The T1 age is consistent with the age of a Tennessee River T1 terrace described in an archaeological study near the Tellico Dam. It stands 6 m (20 ft) higher than the adjacent river and contains charcoal samples with calibrated radiocarbon ages of 9270 to 9475 calendar years before present (BP) and 9545 to 9745 calendar years BP (Reference 2.5.3-25). The Delcourt (Reference 2.5.3-24) T2 age is broadly consistent with radiocarbon dates of approximately 29 to 31 thousand years reported for a T2 terrace deposit beneath the Watts Bar Nuclear Plant adjacent to the Tennessee River (Reference 2.5.3-26). Although detailed mapping of this set of terraces is not available, this deposit is estimated to be 2 to 6 m (6 to 20 ft) above the modern river level.

The distinction between Holocene (Qht) and Pleistocene (Qpt) terraces in Figure 2.5.3-4 is qualitative based on terrace morphology and elevation above the modern Clinch River baseline. In order to better constrain the relative ages of terraces along the Clinch River, morphological correlation and longitudinal profiling of terrace elevations was completed along the Clinch River in the site area, downstream of the Melton Hill Dam (Figure 2.5.3-4). The oldest terrace assigned a Holocene age (Qht3) is only slightly dissected by gully erosion and typically has an intact,

continuous terrace riser separating it from Qht2, which suggest a Holocene age. In contrast, terraces mapped by Delcourt (Reference 2.5.3-24) and Garrow and Leigh (Reference 2.5.3-25) at similar elevations above the Little Tennessee and Tennessee Rivers, respectively, suggest a late Pleistocene age for Qht3.

The Qpt5 and Qpt6 terraces are the oldest and highest terraces mapped in the site area and lie about 30 to 40 m (100 to 130 ft) above the modern Clinch River baseline, respectively. The Qpt5 terraces may correlate with terraces mapped by Hatcher et al. (Reference 2.5.3-7) along the Clinch River near the Oak Ridge National Laboratory that were determined to be Wisconsin in age (18 to 25 thousand years) on the basis of soil surveys (Reference 2.5.3-7). However, this age range should be taken as an absolute minimum based on comparison with absolute ages of terraces at similar heights above rivers in the eastern U.S. Approximate Wisconsin age terraces typically lie less than 10 m above modern river elevations, whereas terraces 30 to 40 m above modern rivers are typically on the order of hundreds of thousands of years old. Therefore, the Qpt5 and Qpt6 terraces are likely at least 200 thousand years old.

2.5.3.2.5.3 Evaluation of Terrace Profiles and Quaternary Surface Deformation

Detailed mapping of fluvial terraces along the Clinch River from field reconnaissance and interpretation of recently acquired LiDAR was used to evaluate the presence or absence of Quaternary faulting at the CRN Site. Evidence for surface faulting in the Quaternary is often expressed by subtle deformation of geomorphic landforms, including river terraces, and is commonly recorded as anomalies in longitudinal stream and terrace profiles and gradients. LiDAR data permit detailed mapping of Clinch River terraces across the site area (Plates 2a-2d in Part 8 of the ESPA and Figure 2.5.3-2) and evaluation of the relative ages of terrace levels using morphological correlation and longitudinal profiling (Figure 2.5.3-4). Evidence of Quaternary surface faulting in the site area was evaluated in two ways: (1) examination of Pleistocene terrace surfaces that directly overlie the mapped trace of faults; and (2) evaluation of longitudinal terrace profiles for systematic irregularities that would suggest repeated fault displacements or deformation.

Fluvial terraces along the Clinch River overlie the concealed trace of each of the five mapped Alleghanian thrust faults within the site area (Plates 2a through 2d in Part 8 of the ESPA and Figure 2.5.3-2) as well as the projected trace of the shear-fracture zone feature discussed in Subsection 2.5.1.2.4.3.4. A fault surface rupture that post-dates the formation and deposition of the overlying terrace would deform the terrace surface. If these faults were reactivated in the contemporary regional stress regime of the CEUS (NE-SW principal stress axis), their orientation would predict right oblique reverse displacement. Cumulative displacement of the terrace would produce a topographic scarp or warp on the terrace surface.

Clinch River terrace surfaces overlie a portion of the concealed trace of each of the five mapped Alleghanian thrust faults within the site area (Plates 2a through 2d, Figures 2.5.3-2 and 2.5.3-6). The Copper Creek fault is directly overlain by Qht1, Qht2, and Qht3 terraces (Figure 2.5.3-3); the northeastern projection of the Chestnut Ridge fault is overlain by Qht2 within the site area and Qpt2 northeast of the 0.6-mile site radius (Figures 2.5.3-2 and 2.5.3-7); the Whiteoak Mountain fault is overlain by Qht2 and Qpt2 terraces; and two unnamed faults of Lemiszki (Reference 2.5.3-56) are overlain by Qht1, Qht2, Qht3, Qpt1, and Qpt2 terraces (Figure 2.5.3-8). The projected trace of the shear-fracture zone (in the Eidson Member of the Lincolnshire Formation) is overlain by Qpt2 (Figure 2.5.3-9). While each of these terrace surfaces have some amount of topographic erosion and anthropogenic alteration, none of them display any linear topographic features or warping of the terrace profile suggestive of surface deformation as a result of repeated faulting. Furthermore, interpretation of LiDAR data documents the absence of any geomorphic lineament, scarps, sag ponds, or other features typically associated with an active Quaternary fault within the site area.

As discussed above, absolute age data for terraces in the site area is sparse; however, relative age of terrace levels was interpreted from morphological position and longitudinal profiling (Figure 2.5.3-4). By analogy to absolute ages of fluvial terraces located in the eastern U.S., the oldest and highest Qpt6 terraces along the Clinch River are likely to be at least 200 thousand years old. The longitudinal profiles of terrace levels presented in Figure 2.5.3-4 provide another means to assess irregularities that could be associated with repeated fault surface rupture. Repeated thrust faulting and relative uplift of terraces by one or more of the faults crossed by the longitudinal profile would result in: (1) increased incision and terrace formation in the hanging wall of the faults; (2) progressively increasing vertical displacement of correlative terraces; and (3) progressively increasing paleo-river gradients yielded from linear regressions of correlative terrace surfaces. The consistent number of terrace levels with similar longitudinal profile slopes that can be correlated across the site area document the absence of discernible Quaternary displacement along all of the Alleghanian thrust faults in the site area. Similarly, the terrace gradients are best fit by single, straight-line regressions (Figure 2.5.3-4); no evidence for vertical separation is apparent across the faults crossed by the longitudinal profile. Finally, the linear regressions indicate minor, non-systematic variations in gradient through time and most likely record climatic and landscape evolution processes, consistent with observations of Pleistocene terraces near the Oak Ridge National Laboratory (Reference 2.5.3-7).

2.5.3.2.6 Proposed Quaternary Deformation Features Along Douglas Reservoir, TN

The CEUS SSC (Reference 2.5.3-1) includes a paleoliquefaction database developed from earlier compilations of paleoliquefaction data of the New Madrid seismic zone and surrounding area. The ETSZ was discussed in general terms by the CEUS SSC modelers as a zone of elevated seismicity and noted:

> "At locations east to northeast of Knoxville, Tennessee, with late Quaternary terrace deposits, Vaughn et al. [Reference 2.5.3-11] report the occurrence of outcrop-scale strike-slip, reverse, and normal faults and prevalent fractures; minor paleoliquefaction features; and anomalous fractured and disrupted features attributed to liquefaction and forceful expulsion of groundwater during one or more major late Quaternary earthquakes. These preliminary observations suggest that the ETSZ has produced surface faulting and generated one or more strong earthquakes during late Quaternary time. However, these preliminary results could not qualify that RLMEs had occurred in the ETSZ, and were therefore insufficient to determine whether the ETSZ could be considered an RLME zone and treated accordingly in the CEUS SSC Project." (Reference 2.5.3-1, Section 7.3.4.4).

The elevated seismicity rate that defines the ETSZ was included in the CEUS SSC model as part of the Paleozoic Extended Crust (PEZ) areal source zone. Spatial smoothing was used to retain the elevated rate of seismicity in the ETSZ region.

Since publication of the CEUS SSC report more recent published research formally presents the earlier findings from Vaughn et al. (Reference 2.5.3-11) as well as additional evidence for possible paleoseismic features within the ETSZ (References 2.5.3-12, 2.5.3-13, and 2.5.3-57). This more recent research documents field work conducted along the shoreline of Douglas Reservoir, which is located approximately 50 mi east-northeast of the CRN Site (see Figure 2.5.2-26). Guidance from the CEUS SSC (Reference 2.5.3-1, Appendix E) is used to evaluate the recently reported paleoseismic evidence in these new publications on the ETSZ (References 2.5.3-11, 2.5.3-12, 2.5.3-13, and 2.5.3-57).

2.5.3.2.6.1 Established Criteria for Evaluating Evidence for Paleoliquefaction and Other Paleoseismic Features

2.5.3.2.6.1.1 CEUS SSC Paleoliquefaction Database

For inclusion in the CEUS SSC paleoliquefaction database and consideration in the seismic source characterization as earthquake-induced liquefaction features, features are required to satisfy specific, well-established criteria as defined in References 2.5.3-58 and 2.5.3-59. These criteria are listed below:

1. Sedimentary characteristics consistent with case histories of earthquake-induced liquefaction.

2. Sedimentary characteristics indicative of sudden, strong, upwardly directed hydraulic force of short duration.

3. Occurrence of more than one type of liquefaction feature and of similar features at multiple locations.

4. Occurrence in geomorphic settings where hydraulic conditions described in (2) would not develop under nonseismic conditions.

5. Age data to support both contemporaneous and episodic formation of features over a large area.

These well-established criteria are adopted to maintain consistency between datasets considered for the paleoliquefaction database. The CEUS SSC Report (Reference 2.5.3-1, Appendix E) also describes the types of liquefaction features used to identify paleoearthquakes in regional studies that are consistent with the above criteria. Potential paleoliquefaction features include sand blows or sand-blow craters (with feeder dikes), sand dikes, sand sills, ball-and-pillow structures, basal erosion and sand diapirs, dish structures, load casts, and pseudo-nodules (Reference 2.5.3-1, Appendix E).

Sedimentary characteristics of paleoliquefaction described in Reference 2.5.3-1 (Appendix E) that are consistent with the criteria outlined above include:

- Sand blows or sand-blow craters (with feeder dikes)
  - Typically elliptical or linear, sometimes circular, in plan view
  - Connected to feeder dikes below
  - Often characterized by “cut-and-fill” structure and flow structures, and/or lineations, above the feeder dike
  - Vented sediment is typically fine to coarse sand, may include some silt and clay
  - Often becomes finer-grained up-section and laterally away from feeder dike/vent
  - Usually thins laterally away from feeder dike/vent
  - May comprise multiple fining-up depositional units related to a sequence of earthquakes; seismites may be separated by layers of fines such as silty clay or clay that accumulated between earthquakes

  - May contain clasts of host deposit, especially near feeder dike, clast size generally decreases with distance from vent
  - Volume of vented deposit should “make sense” relative to size and number of sand dikes
  - Subsidence structures may be seen near vent, including localized downwarping of surface soil and host strata and possible vertical displacement across feeder dikes
  - Sand-blow craters often form in organic-rich soils or clay-rich host deposits
  - Sand-blow craters contain vented sand deposits and clasts of host material; overlain by crater fill deposits and/or reworked material

- Sand dikes
  - Dike sidewalls typically subparallel, usually widen downward; also may broaden upward into vent structure at the ground surface (event horizon)
  - Typically a few meters to tens of meters long (in plan view); therefore, often, but not always, exposed in both walls of a trench
  - Sand within dikes often fines upward
  - Often characterized by flow structure or lineations
  - Often contain clasts of hostdeposit(s)
  - Near-vertical dikes may exhibit grading, with finer material along dike margins; inclined dikes may exhibit bedding
  - May be characterized by subsidiary dikes and/or sills
  - Source layer often lacks original sedimentary structure where fluidized, may exhibit flow structure or lineations as well as soft-sediment deformation structures such as ball-and-pillow structures and dish structures.

2.5.3.2.6.1.2 Counts and Obermeier Paleoseismic Criteria

While the criteria described in Reference 2.5.3-1 broadly apply to paleoliquefaction features, Reference 2.5.3-60 presents criteria for also identifying small-scale soft-sediment deformation features. These features are often characterized by small intrusions of sand into a fine-grained host, deformed and disrupted bedding from seismic shaking, or deformation from sill intrusions. Reference 2.5.3-60 states that at least one of the following criteria should be met in order to consider a seismic origin for a feature:

1. Intrusion is the result of suddenly applied pore-water force that (a) caused hydraulic fracturing of the fine-grained host; (b) is indicated by small pinching-together dikes in the fine-grained host; (c) is indicated by clasts from overlying fine-grained stratum that have been transported downwards into underlying sand; or (d) is indicated by sand sills between fine-grained strata in which nonseismic fluidization can be eliminated.

2. Intrusion is much younger than the host and cannot be the result of external forces (e.g., wave pounding or wave shear from overlying flood waters). Wave shear is the friction exerted by flowing water on the stream bed, or in the case of flood waters, on the flood terrace. Wave shear can result in the injection of bedload sediment into the underlying material.

3. Multiple sites with proximal features are documented and their regional pattern of occurrence cannot be explained by sedimentary characteristics. Small-scale features found proximal to large-scale, more readily apparent seismically induced features are ideal.

Reference 2.5.3-60 also presents additional criteria to consider when identifying ground fractures, including:

1. Above liquefied sediment: fractures cannot be explained by lithologic properties or geologic anisotropies of the host sediments, are found at multiple proximal sites, occur in a regional pattern, and are parallel locally and across a larger area. Reference 2.5.3-60 stated that nonparallel fractures can be caused by seismic shaking; however, such features require additional evidence supporting a seismic origin.

2. Above nonliquefied sediment: fractures extend for meters in length and depth can be parallel or not, cannot be explained by characteristics of the sediments or bedrock (e.g., jointing at depth, desiccation, weathering, slumping), are found at multiple proximal sites, and occur in a regional pattern.

2.5.3.2.6.1.3 Criteria to Evaluate the Origin of Clastic Dikes

Clastic dikes are sedimentary dikes in soil or rock consisting of clastic material such as sand or gravels. Clastic dikes are cited as either resulting from paleoearthquakes (References 2.5.3-60 and 2.5.3-61) or soil-forming processes (References 2.5.3-62, 2.5.3-63, and 2.5.3-64). Reference 2.5.3-62 describes problems in evaluating the development of clastic dikes, including determining the origin of the fractures, the source of the clastic material, and the method of emplacement of the dike material (whether infilling from above or liquefaction). Reference 2.5.3-61 states that, in order for a clastic dike to be considered a liquefaction feature resulting from a paleoearthquake, the following criteria must be met:

1. Details of individual clastic dikes conform with those of known seismic origin.

2. Both the pattern and location of dikes in plan view conform with a seismic origin, on a scale of tens to thousands of meters.

3. The size of dikes on a regional scale identifies a central “core region” of widest dikes, which conforms with severity of effects expected in the energy source region (the meizoseismal zone).

4. Other possible causes for the dikes are ruled out (References 2.5.3-61, 2.5.3-65).

2.5.3.2.6.2 Douglas Reservoir Terrace Mapping

In order to better constrain the relative ages of terraces along Douglas Reservoir, morphological correlation and longitudinal profiling of terrace elevations was completed along approximately 95 km of the French Broad River as part of the CRN Site investigation (Figures 2.5.3-10 and 2.5.3-11). Correlated terraces include the modern (prior to the construction of Douglas Dam) flood plain (T0) and seven older terraces (T1 to T5, including an intermediate, locally observed terrace T2.5, and an undifferentiated Pleistocene terrace designation [QPT]). Terrace surfaces mapped on the banks of tributaries of the French Broad River, including the Pigeon River, the

Little Pigeon River, and the Nolichucky River, were not correlated but instead designated as uncorrelated terraces (UT) due to different development histories.

A baseline longitudinal profile was developed to represent the incised French Broad River prior to the construction of Douglas Dam (Figure 2.5.3-11). Elevation points within the study area below the dam (~13 km) and above Douglas Reservoir were extracted from the DEM, fit with a linear regression, and extrapolated along ~95 km of the mapped French Broad River. Additionally, correlated terrace surfaces' location and elevation data were linearly regressed. The linear regressions for the modern French Broad River and terraces T2 to T5 have the same slope of $-5x10^{-4}$, and QPT has a slightly steeper slope of $-6x10^{-4}$ (Figure 2.5.3-11). Using these regression-derived slopes, terraces T2, T3, T4, and T5 are approximately 15 m, 25 m, 31 m, and 37 m above the modern French Broad River, respectively. These are slightly higher average terrace elevations when compared to Hatcher et al. (Reference 2.5.3-12). Undifferentiated Pleistocene terrace, QPT, has a slightly steeper profile slope, possibly resulting from a long-term change in uplift or incision rates, or the erroneous inclusion of unrelated older terrace surfaces under a single profile (Figure 2.5.3-11). QPT is approximately 46 to 56 m above the modern French Broad River.

Field reconnaissance along the Douglas Reservoir was performed primarily to observe and evaluate the proposed paleoseismic features of Hatcher et al. (Reference 2.5.3-12). In addition to field reconnaissance, longitudinal terrace profiles were developed to determine relative terrace ages. The profiles presented in Figure 2.5.3-11, similar to the Clinch River terrace profiles discussed in Subsection 2.5.3.2.5.3 and presented in Figure 2.5.3-4, provide a means to evaluate potential repeated fault surface rupture. The consistent number of terrace levels with similar longitudinal profile slopes fit by single, straight-line regressions that can be correlated along the profile do not support discernible Quaternary displacement along the reservoir. The linear regressions do, however, indicate minor, non-systematic variations in gradient through time and most likely record climatic and landscape evolution processes, similar to other terraces in the region (e.g., Reference 2.5.3-69).

2.5.3.2.6.3 Field Reconnaissance of Proposed Quaternary Deformation along Douglas Reservoir

Douglas Reservoir, located on the French Broad River in Eastern Tennessee, has been the site of extensive recent study by University of Tennessee Professor Robert Hatcher and his colleagues. Douglas Reservoir is significantly drawn down each winter, exposing wave-eroded soil and weathered bedrock along the shoreline. Hatcher et al. (Reference 2.5.3-12) completed an 18-month pilot study to search for paleoseismic features in the ETSZ that included field reconnaissance with a focus on six sites (DL-1 through DL-6) along the Douglas Reservoir near Dandridge, Tennessee. In that pilot study, Hatcher et al. (Reference 2.5.3-12) identified potential paleoseismic features that include possible faults, fissures, bleached clay fractures, evidence of paleoliquefaction, shale "boils," and disturbed sediments. These features were observed at different sites within fluvial terraces of the French Broad River at Douglas Reservoir (Figures 2.5.3-10, 2.5.3-12).

Warrell (Reference 2.5.3-13) also studied potential paleoliquefaction features at the sites presented in Reference 2.5.3-12 with an emphasis on Site DL-6 and Site DL-9 (not presented in Reference 2.5.3-12; Sites DL-7 or DL-8 are not mentioned in either reference). These seven sites were visited and evaluated to support the CRN Site ESPA. Professor Robert Hatcher and Mr. James Vaughn accompanied Technical Integrator (TI) Team members during field reconnaissance of Sites DL-1, DL-3, DL-4, DL-5, DL-6, and DL-9. The results of that reconnaissance are included in the descriptions below.

2.5.3.2.6.3.1 Site DL-1

Hatcher et al. Observations and Interpretations

Site DL-1 is the farthest upstream site in the Reference 2.5.3-12 study area (Figure 2.5.3-13). Hatcher et al. (Reference 2.5.3-12) report a clastic dike that is at least 1 m long in plan view and greater than 1 m high. This dike is reported to be filled with fine- to medium-grained sand that can be traced down to an underlying sand bed with similar texture. Hatcher et al. (Reference 2.5.3-12) interpret the fine grain size of the dike fill as evidence of seismic liquefaction. Small "dikelets" (3-15 cm), and associated sills are noted by Hatcher et al. (Reference 2.5.3-12) to cut through their interpreted T1 terrace (based on the location of the site relative to their Figure 5). Hatcher et al. (Reference 2.5.3-12) conclude that these features are seismic based on the presence of microfaults, sills, and clasts close to the base of the dike.

TI Team Observations, Interpretations, and Evaluation of Previous Work

Based on the results of field reconnaissance and longitudinal profiling of fluvial terraces, Site DL-1 is located on the T2 terrace (Figures 2.5.3-10, 2.5.3-13), and has the most well-preserved and easily observable terrace deposit of the Hatcher et al. (Reference 2.5.3-12) sites. The T1 terrace of Hatcher et al. (Reference 2.5.3-12) is correlative with the T2 terrace that was delineated during terrace mapping to support the CRN Site ESPA (Figure 2.5.3-13). Several small terraces identified by Hatcher et al. (T2 and T3, Reference 2.5.3-12) near Site DL-1 were not observed during field reconnaissance (see Figure 2.5.3-13).

Terrace deposits at Site DL-1 overlie the Sevier Shale, and consist of a fining upward sequence with coarse gravelly sand that grades upward to a silt and clay (loess?) cap. The Sevier Shale is well exposed in an approximately 12 m high bluff above the modern river level. Thin joints were observed within the Sevier Shale beds and are likely the result of volume changes or regional strain within the Sevier Shale.

The exposure of the fine to medium-grained sand dike in T2, described by Hatcher et al. (Reference 2.5.3-12) as extending downward to an underlying sand bed with very small dikelets and micro-faults, was not located during reconnaissance with Professor Hatcher and James Vaughn. Review of photographic evidence (Reference 2.5.3-12, their Figure 15) suggests the interpreted paleoseismic fracture could easily have formed as the result of slope failure. In this alternative, gravity driven block rotation along the well exposed bluff produced an extensional fracture or fissure. The fissure was infilled by medium- to fine-grained sand that is locally abundant on the ground surface, and appears to have been transported aerially, which is supported by local loess deposits. Micro-fractures with soil bleaching were observed within the terrace deposits in T2, which appear to be pedogenic cutans (Reference 2.5.3-64) or other weathering phenomenon (References 2.5.3-62, 2.5.3-63) based on: 1) the fractures do not appear to disrupt bedding at the site; 2) similarity between fracture fill and host material; and 3) their relative abundance in the upper portions of the exposure. The consensus of the TI Team is that there is not sufficient evidence to support a seismic component to the origin of any of the features observed at DL-1. All of the features observed at DL-1 can be attributed to commonly occurring geomorphic and pedogenic processes.

2.5.3.2.6.3.2 Site DL-2

Site DL-2 is the next site downstream of site DL-1. The location of this site is shown by Hatcher et al. (Reference 2.5.3-12) to be on the south side of Douglas Reservoir. However, Hatcher et al. (Reference 2.5.3-12) do not discuss the presence or lack of potential seismogenic features within the text. Professor Hatcher and James Vaughn did not accompany the TI Team to this site during their field reconnaissance.

Site DL-2 occurs on the T1 and T2 terraces (Figure 2.5.3-10). Terrace deposits consist of mottled clay with ~10% sand and few pebbles, with ~25 cm and ~10 cm of modern surficial lacustrine material on terraces T1 and T2, respectively. No bleached fractures, boils, or other potential paleoliquefaction features were located during field reconnaissance at this site.

2.5.3.2.6.3.3 Site DL-3

Hatcher et al. Observations and Interpretations

Site DL-3 is located on the south side of Douglas Reservoir near the Tennessee Highway 92 bridge (Figure 2.5.3-10). East of the bridge at Site DL-3, Hatcher et al. (Reference 2.5.3-12) report an ~80 cm long bleached fracture that includes weathered Sevier Shale clasts in the undisturbed T3 terrace. These shale clasts are interpreted by Hatcher et al. (Reference 2.5.3-12) to be carried upward by “fluid moving through the fracture as it formed (possible hydrofracture?)”. Hatcher et al. (Reference 2.5.3-12) conclude that this feature is not related to any karst processes, based on their interpretation that the shale fragments were carried from below through undeformed terrace deposits.

TI Team Observations, Interpretations, and Evaluation of Previous Work

Site DL-3 is located on a wave-cut exposure of the T3 terrace and consists of predominantly reddish mottled clay with no apparent fluvial structures (Figure 2.5.3-10). Weathered Sevier Shale clasts were observed in the terrace deposit during field reconnaissance at this site. The thin fracture described by Hatcher et al. (Reference 2.5.3-12) as the conduit for shale clasts to travel upward from depth was not observed during field reconnaissance with Professor Hatcher and James Vaughn because of surficial sediment cover. Within the terrace deposit, several irregularly shaped, clay-lined fractures in contact with weathered shale clasts appear to curve around the clasts, rather than involve them. This implies the in-situ shale clasts within the terrace deposit are unrelated to the fractures. Additionally, anastomosing bleached fractures exposed at this site resemble pedogenic cutans similar to those described at Site DL-1 (Subsection 2.5.3.2.6.3.1). The consensus of the TI Team was that the bleached fractures can be more easily explained by pedogenic processes and the presence of Sevier Shale clasts is a function of deposition of the T3 terrace.

2.5.3.2.6.3.4 Site DL-4

Hatcher et al. Observations and Interpretations

Site DL-4 is located directly southwest of the Tennessee Highway 92 bridge over Douglas Reservoir (Figures 2.5.3-10, 2.5.3-14). Hatcher et al. (Reference 2.5.3-12) report bleached clay-filled fractures in their T2, T3, and T4 terraces, which are truncated by an overlying 1-2 m colluvial unit that yielded an OSL age >73.4 ka. Hatcher et al. (Reference 2.5.3-12) state that this OSL age provides a minimum age for deformation event(s) that may have involved coseismic deformation, mass movement, karst collapse, or a combination of these processes. The observed fractures have various orientations, with some isolated, branching, or intersecting. The host material is oxidized alluvium that contains rounded vein quartz and quartzite pebbles derived from the Blue Ridge and locally derived Knox Group angular chert pebbles (Reference 2.5.3-12).

TI Team Observations, Interpretations, and Evaluation of Previous Work

Based on the field assessment of the TI Team, Site DL-4 is located in the T3 terrace, similar to Site DL-3 (Figures 2.5.3-10, 2.5.3-14). This terrace deposit (near DL-4b and DL-4c) contains mottled silty clay with trace sand and lenses of rounded gravel. Bleached, vertically trending

clay-rich fractures described by Hatcher et al. (Reference 2.5.3-12) were observed during field reconnaissance with Professor Hatcher and James Vaughn. These bleached fractures exhibit a gradation in color, with grayish interior and darker red borders (Figure 2.5.3-14). They appear to crosscut one another and often pinch out at depth (Figure 2.5.3-14). Collectively, these attributes support the interpretation of these features as pedogenic cutans versus evidence for liquefaction or paleoseismicity.

Field reconnaissance confirms that these bleached fractures do not penetrate into the thin, overlying colluvium that was dated using OSL (>73.4 ka; Reference 2.5.3-12). Therefore, the depositional age of the colluvium represents the minimum age of the fractures (Reference 2.5.3-12). Hatcher et al. (Reference 2.5.3-12) correlate this colluvial OSL age from Site DL-5 to other sites surrounding Douglas Reservoir, and conclude that where proposed paleoseismic features penetrate the Bt horizons of ultisols in terrace deposits (specifically at Site DL-6), the proposed features represent a seismogenic event younger than 73.4 ka. The resulting conclusion that “two strong shocks occurred sometime after ~73 ka, and possibly much later than 73 ka” (Reference 2.5.3-12) is speculative based on the lack of terrace correlations. Field reconnaissance indicates that correlation of colluvial or soil units between sites around Douglas Reservoir, with respect to age and origin, is inherently uncertain and has not been sufficiently demonstrated at this time. Reconnaissance observations indicate that colluvium exposed at DL-4 and surficial materials at DL-6 have significantly different physical properties and soil development characteristics. Therefore, not only does this stratigraphic correlation (and the resulting conclusion) remain suspect, the interpreted paleoseismic features at DL-4 are better explained by pedogenic processes.

2.5.3.2.6.3.5 Site DL-5

Hatcher et al. Observations and Interpretations

Site DL-5 is located east of the Tennessee Highway 92 bridge along Douglas Reservoir (Figure 2.5.3-15). Hatcher et al. (Reference 2.5.3-12) report shale-clay “boils” and an anastomosing bleached clay-filled fracture array in the T3 terrace that is offset ~25 cm by a sinistral fault at Site DL-5. The orientations of these fractures vary from regional joint data sets in the Valley and Ridge and the western Blue Ridge Foothills (Reference 2.5.3-12). Hatcher et al. (Reference 2.5.3-12) obtained an OSL age of >104.5 ka from alluvium in the lower part of the T3 terrace. Observed fractures at this site crosscut this alluvium, and Hatcher et al. (Reference 2.5.3-12) suggest the OSL age of >104.5 ka represents a maximum age of the fractures, and that they may be as young as Pleistocene (Wisconsin stage) or Holocene. Hatcher et al. (Reference 2.5.3-13) note the presence of Knox Group carbonates and Sevier Shale (Reference 2.5.3-66) beneath DL-5 and suggests the features described above may be related to karst collapse.

Additionally, Warrell (Reference 2.5.3-13) identifies an outcrop of Lenoir Limestone that lies structurally above highly fractured Sevier Shale saprolite at Site DL-5c. Trenching across this contact exposed Sevier Shale and layered terrace alluvium that Warrell (Reference 2.5.3-13) interprets to be a paleolandslide deposit buttressed at its toe against an exposure of Lenoir Limestone. Warrell (Reference 2.5.3-13) concludes that a seismic or aseismic origin for this landslide could not be determined.

TI Team Observations, Interpretations, and Evaluation of Previous Work

Site DL-5 occurs on the wave cut exposure of the T3 terrace between the Tennessee Highway 92 bridge and Site DL-3 (Figures 2.5.3-10, 2.5.3-15). Along the wave cut surface, potential Quaternary alluvium landslide deposits were observed buttressed against an outcrop of Lenoir Limestone, as described in Reference 2.5.3-13. Additionally, rounded gravels and cobbles that

had eroded from the overlying terrace deposits are imbedded in the soft clay-rich Sevier Shale saprolite all along the shoreline at Sites DL-3 and 5.

Examples of shale chips, shale “boils,” and the anastomosing bleached clay-filled fracture array described by Hatcher et al. (Reference 2.5.3-12) were observed during field reconnaissance with Professor Hatcher and James Vaughn. The specific shale “boil” presented in Figure 10c of Hatcher et al. (Reference 2.5.3-12) was covered by lacustrine sediment and not exposed during the field reconnaissance. Reportedly similar shale chip features were observed up-river, approximately 30 m near the boat dock walkway. The shale chips are located within a mottled reddish clay matrix with little to no sand, similar to terrace deposits at Site DL-4. The shale chip “boil” reported by Hatcher et al. (Reference 2.5.3-12) occurs very close to the underlying contact with Sevier Shale and resembles classic soil mottling (redoximorphic features) described above. Another possible interpretation is that these shale “boils” are rip-up clasts that resulted from fluvial processes during terrace deposition.

No clastic dikes were observed during field reconnaissance with Professor Hatcher and James Vaughn. However, bleached fractures similar to Site DL-4 were observed. Hatcher et al. (Reference 2.5.3-12) also cites slickensides as evidence for possible displacement along fractures, although slickensides on clay-filled fractures may be related to repeated clay soil expansion and differential forces rather than tectonic microfaulting at this site. These types of slickensides are referred to as stress cutans and are the result of soil processes resulting in the concentration of particular soil constituents or in situ modification due to differential forces as described above (Reference 2.5.3-64).

Hatcher et al. (Reference 2.5.3-12) suggest that a well-developed ultisol with a very long development history (Wisconsin stage and Holocene) that contains bleached fractures is evidence for young paleoseismic activity. It is not clear if these bleached fractures postdate soil development or the secondary soil development post-dates the fractures. The relative age uncertainty described by Hatcher et al. (Reference 2.5.3-12), as well as the uncertainty regarding the formation of the fractures by either soil processes or suggested ground shaking, makes any conclusions regarding number of earthquakes or earthquake timing at Site DL-5 highly uncertain. It was the opinion of the TI Team that the features observed at Site DL-5 were most likely related to pedogenic or depositional processes.

Additionally, during field reconnaissance, Professor Hatcher and James Vaughn showed the location of an OSL sample, collected downslope of DL-5 on the T2 terrace, that yielded an age of ~200 ka. This age is inconsistent with the T2 terrace OSL age of ~27 ka near Site DL-1, which highlights (1) the uncertainty in the available terrace ages; (2) the potential limits of applying OSL dating to sites within Douglas Reservoir; and (3) the need for additional age control.

2.5.3.2.6.3.6 Site DL-6

Hatcher et al. and Warrell Observations and Interpretations

Site DL-6 is located on the north side of Douglas Reservoir, ~5 km southwest of Dandridge, Tennessee, on a partially eroded south-facing T3 terrace slope (Reference 2.5.3-12). Hatcher et al. (Reference 2.5.3-12) and Warrell (Reference 2.5.3-13) document potential paleoseismic features at this site that include: (1) thrust and sinistral faults that cut Sevier Shale and terrace alluvium; (2) alluvium filled fissures; (3) clastic dikes and sills; (4) fracture arrays; and (5) anomalous fracture-bound, elongate “boat” structures that Hatcher et al. (Reference 2.5.3-12) attribute to liquefaction and fluidization. Hatcher et al. (Reference 2.5.3-12) interpret crosscutting relationships of these structural and proposed paleoliquefaction and fluidization features as evidence for at least two strong paleoearthquakes in the ETSZ. Hatcher et al.(Reference 2.5.3-12) also suggest coseismic fracturing may have occurred along with

expulsion of overpressured groundwater through bedrock fractures, as well as liquefaction and fluidization of sandy alluvium.

TI Team Observations, Interpretations, and Evaluation of Previous Work

At site DL-6 (Figures 2.5.3-10, 2.5.3-16, 2.5.3-17, 2.5.3-18, 2.5.3-19), a significant portion of Trench 2 presented in Reference 2.5.3-12 and Reference 2.5.3-13 had been re-excavated and cleaned by Dr. Hatcher's colleagues and students prior to field reconnaissance by the TI Team. The TI Team cleaned, logged, and photographed the east wall of Trench 2, and cleaned and photographed the west wall (Figure 2.5.3-17). Geomorphic and geologic mapping was performed in the area of DL-6 to gain better perspective on the relationship of the slopes and bedding with possible paleoseismic features observed at the site (Figure 2.5.3-16).

The most conspicuous evidence for possible paleoseismic features among all the sites described by Hatcher and his colleagues along the Douglas Reservoir is located at Site DL-6. The two most prominent features include (1) a shallow-dipping shear plane, exposed in Trench 2 and visible at the ground surface for approximately 25 m on the shore of Douglas Reservoir; and (2) an alluvium-filled fracture also exposed in Trench 2 and at the ground surface that is truncated at depth by the shear plane (Figure 2.5.3-17).

The shear plane is marked by a relatively thin (0.5 – 1.5 cm) seam of reddish, soft, moist clay along a bedding plane within the Sevier Shale. No sand or Sevier Shale clasts were visible along the shear plane. The clay seam is probably derived from the Sevier Shale and has been oxidized by movement of meteoric water along the surface. The shear plane strikes N55°E and dips between 10 and 45 degrees, and is coincident with a gently dipping bedding plane in the Sevier shale and has apparent thrust motion (Figure 2.5.3-17). The shear plane becomes listric and steepens as it approaches the ground surface, but it is parallel to bedding lower in the trench and does not appear to cross cut the shale bedding. A small splay off the main shear plane accommodates minor displacement where the plane becomes listric. This splay also parallels bedding and does not appear to be rooted at depth to the main shear plane, which is inconsistent with the interpreted reverse motion. During field reconnaissance with Professor Hatcher and James Vaughn, no slickensides or rake marks on the shear plane were confidently identified. However, stress cutans were observed at several locations within the clay-rich shear plane. Where exposed at the ground surface and excavated to shallow depth, these stress cutans exhibited a dendritic or radial pattern which precludes their origin as fault or landslide slickensides or rake marks.

The shear plane in Trench 2 juxtaposes weathered sandy clay alluvial terrace materials and deeply to completely weathered (saprolite) Sevier Shale bedrock (Figure 2.5.3-17). Two near vertical, 15 to 40 cm wide alluvium-filled fissures occur in the hanging wall block above the shear plane (Figure 2.5.3-17). The fissures terminate at the shear plane 1 m below the ground surface, and do not occur in the footwall. The trench was subsequently deepened during field reconnaissance in an attempt to locate the basal portion of the purported offset filled fissure. However, no equivalent fissure material that might have been offset along the shear plane was found in the footwall. If the fissure fill is offset by approximately 1 m, as interpreted by Hatcher et al. (Reference 2.5.3-12) and Warrell (Reference 2.5.3-13), the offset equivalent in the footwall would have been uncovered. The base of the filled fissure and the shear plane are also visible at the ground surface, approximately 18 m southwest of Trench 2.

The apparent thrust displacement along the shear plane of about 1 m is based on the juxtaposition and apparent offset of the contact between the Sevier Shale bedrock and the terrace deposits (Figure 2.5.3-17). There are questions and fundamental concerns regarding this interpretation, including:

- If this fault is a secondary coseismic feature, how can ground motion from a deep earthquake thrust a block of material approximately 1m up a slope (as interpreted in Reference 2.5.3-12)? In particular, the downslope projection of the purported thrust fault would daylight in the canyon wall of the French Broad River. If the thrust fault post-dates formation of terrace T3, and thus daylights out of the canyon wall at the time of its purported displacement, there is no driving mechanism or lateral force to push this block of material up slope.

- If this thrust fault is the result of liquefaction (Reference 2.5.3-12), where is the liquefiable material that is reportedly *stratigraphically beneath or within the Sevier Shale*?

- What is the nature of the wide alluvium-filled fissure, and why is it not present in the footwall?

- If this fault is seismogenic, where does the relatively shallow, bedding plane parallel shear plane root to a more vertically oriented shear zone? If it does not, this feature should daylight further downslope, sub-aerially within Douglas Reservoir.

If the shear plane represents a thrust fault with a pure dip-slip vector parallel to the wall in Trench 2 (Figure 2.5.3-17) and the filled fracture predates the shear plane, then (1) the filled fracture should be found down-dip in the footwall and (2) the overlying material on the bedrock surface should match across the fault (Units 5 and 6c on Figure 2.5.3-17). The absence of the alluvium-filled fracture in the footwall does not support the hypothesis that this shear plane represents a thrust fault that offsets a pre-existing fracture as suggested by Hatcher et al. (Reference 2.5.3-12) and Warrell (Reference 2.5.3-13). Additionally, Units 5 and 6c appear to be different facies of the same material, which requires a significant component of lateral slip (out of the trench wall plane) to explain their spatial relationship exposed in Trench 2. These observations highlight the uncertainty regarding the proposed interpretations of thrust displacement at Site DL-6.

The geometry and sense of displacement of the offset bedrock is not well enough defined to provide a piercing point for accurate displacement measurements. The overlying material on the bedrock surface, as well as the character of the bedrock surface, do not match across the trench. The different material properties, such as grain size, sorting, and depositional structures of the overlying units (Units 5 and 6; Figure 2.5.3-17), indicate a significant component of lateral slip may have occurred, regardless of whether Unit 6c may have undergone potential fluidization. Lateral slip on a shallowdipping shear plane that is coincident to dip-slope bedding is more indicative of gravitational slope processes than compressional seismogenic processes.

Given the considerable uncertainty regarding the thrust-fault hypothesis for this feature, alternative explanations include in order of likelihood: (1) a lateral margin of a landslide (SE-directed movement) that locally juxtaposes the bedrock/alluvial contact in an apparent reverse separation in Trench 2 (Figure 2.5.3-18), (2) reverse movement at the toe of an ancient landslide within a paleo-landscape, and (3) deformation related to karst dissolution processes, as several closed depressions occur close to the site (Figure 2.5.3-19). Results from the TI Team assessment of the features observed at Site DL-6 are that they are likely the result of nontectonic processes and, therefore, do not represent paleo-earthquakes. The absence of the alluvium-filled fracture beneath the shear plane suggests it is either contemporaneous with or post-dates initial movement on the underlying shear plane (Figure 2.5.3-18). The filled fracture likely developed during extension of a pre-existing subvertical joint or fracture (striking N33°E) in the Sevier Shale that opened as a result of gravitational block sliding along the pre-existing, bedding parallel, basal shear plane. Subsequent infilling of the fracture with packages of alluvial material likely occurred shortly after extension (Figure 2.5.3-18). This interpretation is consistent with the orientation of the modern hillslope approximately parallel to the dip of bedding in the shale. Several linear features interpreted as slickenlines (Reference 2.5.3-13, their Figure 4-5)

along the shear plane are oriented normal to the fissure, which also supports downslope movement of a gravitational block. To definitively determine the temporal relationship of the filled fracture, whether it post- or pre-dates the shear plane, the basal portion of the fracture in the footwall should be located (if it exists below the floor of the trench that was deepened during field reconnaissance) to resolve its origin and determine the possible sense and amount of slip along the shear plane.

The reported “boat structure” at site DL-6 was not observed during field reconnaissance, as Trench 1 had been backfilled and not re-excavated. Some evidence for paleofluidization-liquefaction was discussed at the north end of the exposed Trench 2 during the reconnaissance visit with Professor Hatcher and James Vaughn (Figure 2.5.3-17). This evidence included a poorly sorted alluvial deposit containing clasts of completely weathered Sevier Shale up to 1-2 cm in diameter, suspended in a mottled reddish brown clay matrix. The deposit does not exhibit the typical sedimentary characteristics of the well-established paleoliquefaction criteria, as defined in References 2.5.3-58, 2.5.3-59, and 2.5.3-60, and described in Subsection 2.5.3.2.6.1. Several diagnostic criteria that are critical to the interpretation of these features as a result of liquefaction are absent from these exposures, including sand sills, fining upward sand dikes, and flow structures. An alternative explanation for this poorly sorted deposit, supported by the absence of these key criteria, is that it is the result of a channelized debris flow of terrace sediments at some point in the past.

Hatcher et al. (Reference 2.5.3-12) postulate that the suspended Sevier Shale clasts visible in alluvium in the north side of Trench 2 (Units 6b and 6c; Figure 2.5.3-17) were expelled from the shear plane by the forceful expulsion of ground water. The soft clay within the shear plane does not resemble the matrix of the alluvium, nor are there any clasts of Sevier Shale within the clay-rich shear plane, which would be expected given this interpretation. The small shear splay in the footwall of the shear zone forms an acute angle, which graphically resembles a point of discharge (Figure 2.5.3-17). However, based on our detailed logging of the trench, the shear splay does not appear to connect with the main shear plane at depth (Figure 2.5.3-17). Additionally, the shear splay is clearly visible in the alluvium and, therefore, would have formed after any expulsion event (Figure 2.5.3-17).

2.5.3.2.6.3.7 Site DL-9

Warrell Observations and Interpretations

In addition to the six sites included in Reference 2.5.3-12, Warrell (Reference 2.5.3-13) includes observations at Site DL-9, located on the south side of Douglas Reservoir across from and ~1 km southwest of DL-6. Warrell (Reference 2.5.3-13) reports two OSL ages for this site: (1) DL-9-01, sampled from sediment filling a branching fissure, yielded an OSL age of 15,865 ± 1,735 y; DL-9-02, sampled from undisturbed terrace material near the site, yielded an OSL age of 21,765 ± 1,445 y.

TI Team Observations, Interpretations, and Evaluation of Previous Work

At site DL-9 (Figures 2.5.3-10, 2.5.3-20), numerous alluvium-filled fractures (similar to site DL-6) were observed on a moderately dipping slope within Sevier Shale bedrock. These alluvium-filled fractures are up to approximately 30 cm wide and strike in two conjugate orientations of about N35°E and N10°W. Bedrock at DL-9 dips gently to the southeast. T3 terrace deposits are located upslope and no fractures or deformation were observed in these deposits. The age of the terrace deposits at DL-9 is reported to be approximately 15 ka (Reference 2.5.3-13), based on the OSL age determined using alluvium sampled from the filled fractures. However, the terrace elevation is the same as site DL-6 (T3) and well-developed Fe-Mn soil concretions up to about 60 cm in

diameter were observed in this same deposit several hundred meters west of site DL-9, which indicates much older age, possibly on the order of hundreds of thousands of years.

The relationship between the orientation of the alluvium-filled fractures, the modern slope aspect and dip, and the shallow dipping slope-parallel bedding indicates that these fractures likely developed along pre-existing planes of weakness (joints), which were subjected to extension during down-slope rotational block sliding (see Figure 2.5.3-20). This interpretation is consistent with the modern geomorphologic conditions. Similar to site DL-6, the fractures do not extend into the overlying terrace deposits and are confined to the Sevier bedrock.

2.5.3.2.7 Evaluation of the Presence or Absence of Surface Deformation along the Tellico Reservoir

Following the construction of the Tellico Dam in the 1970s, Tellico Reservoir flooded the Little Tennessee River. Along 54 km of this river, Delcourt (Reference 2.5.3-24; Reference 2.5.3-68) mapped and developed longitudinal topographic profiles for the modern flood plain (T0) and nine older fluvial terrace surfaces (T1 through T9; Reference 2.5.3-69). This terrace mapping included development of five, 1- to 3-km-long trenches at 10-km intervals perpendicular to the river and descriptions and samples of the terrace depositional units from the trench exposures. Radiocarbon dates were obtained on samples collected from terraces T0 through T2, with age results of 3.5 ka, 15 to 3.5 ka, and approximately 28 ka, respectively (Reference 2.5.3-69). The radiocarbon age of T2 is comparable to dates of 29 to 31 ka of correlative terraces of the Tennessee River at the Watts Bar Nuclear Power Plant (Reference 2.5.3-69). Mills and Delcourt (Reference 2.5.3-69) concluded that these terrace ages indicated peak aggradation of sediment occurred at glacial/interglacial or stadial/interstadial transitions rather than solely during peak-glacial intervals as proposed by King (Reference 2.5.3-70). While no radiocarbon dating was performed for terraces T3 through T9, Mills and Delcourt (Reference 2.5.3-69) postulated that these older terraces formed during similar climatic transitions earlier in the Quaternary.

Terrace surfaces along the flooded Little Tennessee River (Tellico Reservoir) were observed and reviewed as part of the field reconnaissance in an effort to: (1) draw comparisons between these terraces and those observed within and adjacent to Douglas Reservoir, and (2) search for potential paleoliquefaction features. The construction of the Tellico Dam, however, resulted in the flooding of the majority of the mapped terraces of Delcourt (Reference 2.5.3-24), leaving only dissected remnant terraces T6 to T9 exposed in select locations. Below is a report of the observations of these terraces along Tellico Reservoir.

Near the Fort Loudon Dam and along the Little Tennessee River, a sequence of terraces, T6, T7, and T9 (as mapped by Delcourt, Reference 2.5.3-24), was observed (Waypoints 240, 242, 243, Figure 2.5.3-21). The T8 terrace does not appear to be preserved in this area. The T6 and T7 terraces were easily distinguishable by their near-horizontal, planar treads (Figure 2.5.3-22A) with relatively small (approximately 1- to 2-m-high) sharp risers. Extensive exposures of the 4-m-high riser between the T7 and T9 treads include well rounded gravel horizons interbedded with strongly oxidized reddish sandy clay terrace deposits (Figure 2.5.3-22B). T9 terrace deposits appear to be approximately 3 to 4 m thick. Small gravel-rich fans emanating from T9 and deposited on T7 were evident. No evidence of potential paleoseismic features, such as fractures, clastic dikes, or paleoliquefaction, was found in these terrace deposits.

2.5.3.3 Correlation of Earthquakes with Capable Tectonic Sources

The CRN Site is located within the ETSZ, an approximately 300-km-long (186 mi) and less than 50-km-wide (31 mi) northeasterly trending, elongate band of seismicity within the Valley and Ridge and westernmost Blue Ridge physiographic provinces; it underlies parts of eastern Tennessee, North Carolina, Georgia, and Alabama (e.g., References 2.5.3-27, 2.5.3-28, 2.5.3-2,

and 2.5.3-29). After the New Madrid seismic zone, the ETSZ has the second highest rate of small (i.e., moment magnitude **(M)**<5) earthquakes in the eastern United States (Reference 2.5.3-1, Section 7.3.4.1.2). Within the CRN site vicinity, two **M**>4 have been recorded in recent history (4.01, 3 November 1973, and 4.03, 27 March 1987; Reference 2.5.3-1). Twenty-eight earthquakes between **M**2.9 and 4.0 have been recorded within the site vicinity; of these 28, four have occurred within the site area (Figure 2.5.3-5).

Instrumentally located epicenters within the ETSZ indicate that the overwhelming majority of earthquake hypocenters are located in Neoproterozoic (approximately 1.1 Ga) basement rocks beneath the 5-km (3 mi) thick Paleozoic foreland fold-thrust belt (Reference 2.5.3-2). The mean focal depth of earthquakes within the ETSZ is approximately 15 km (9 mi) (Reference 2.5.3-2). These earthquakes have been correlated with potential aeromagnetic anomalies (mostly the NY-AL lineament) and associated with alternative tectonic models (References 2.5.3-30; 2.5.3-27; 2.5.3-28; 2.5.3-2; 2.5.3-31; 2.5.3-32; 2.5.3-29; and 2.5.3-33). The vast majority of ETSZ earthquakes with instrumental hypocenters have depths below the detachment (approximately 3 km [2 mi] below the site), and, of the few known to have more shallow depths, none have been correlated with known faults exposed near the ground surface.

2.5.3.4 Ages of Most Recent Deformation

2.5.3.4.1 Bedrock Faults

Multiple lines of evidence suggest bedrock thrust faults in the Valley and Ridge were active during the late Paleozoic Alleghanian orogeny (discussed in Subsections 2.5.1.1.2, 2.5.1.1.4, 2.5.1.2.4, and 2.5.3.2.1). $^{40}K/^{40}Ar$ and $^{40}Ar/^{39}Ar$ geochronologic analyses of fault gouge from the Copper Creek fault yielded ages of 280 to 290 and 279.5 ± 11.3 Ma, respectively, which support this timing (Reference 2.5.3-6; Reference 2.5.3-17). In the site vicinity, there is no evidence for later reactivation of these structures. Mesozoic faults, basin fill, and volcanic intrusions associated with the breakup of Pangea are generally restricted to areas more proximal to the Atlantic coast at the latitude of the site, which prohibits the direct observation of any crosscutting relationship near the site. However, several undeformed diabase dikes crosscut Valley and Ridge structures in the central Appalachians (central Virginia and Pennsylvania), which supports thrusting along those faults and associated folding occurred prior to approximately 200 Ma (see Subsection 2.5.1.1.4.1.3). Additionally, high-resolution LiDAR data yielded no evidence of deformation where Pleistocene and Holocene river terraces overlie major bedrock thrust faults in the site area, lending further support to the hypothesis that these faults are not active. Based on the available data, the most recent deformation of Valley and Ridge thrust faults within the site region occurred during the late Paleozoic.

The CRBRP PSAR also evaluated the potential for surface faulting along these structures, and, based on similar evidence presented herein (fault gouge geochronology, crosscutting relationships with surficial material), determined that they were not capable tectonic sources and likely last active during the Alleghanian orogeny (Reference 2.5.3-6). The safety evaluation report issued by the NRC in response to the licensing application for the CRBRP agreed with this conclusion (Reference 2.5.3-34).

2.5.3.4.2 Shear-Fracture Zones

The observed orientations and crosscutting relationships of stylolites, among other structures, are key to understanding the timing of deformation within the shear-fracture zones (see Subsection 2.5.1.2.4.3.4). Truncation of the shear-fracture zones, or calcite veins within the zones, by bedding parallel stylolites demonstrates pre- to syn-diagenetic development of these zones and precipitation of calcite in veins. Truncation of calcite veins within the shear-fracture zones by steeply dipping and subvertical stylolites, folding and deformation of calcite veins, and

slickenlined vein and bedding surfaces, demonstrate a tectonic overprint on the zone, likely related to Alleghanian shortening related to emplacement of Valley and Ridge thrust faults.

While it is permissible that tectonic stylolites in Valley and Ridge carbonate rocks in eastern Tennessee developed during the Mesozoic breakup of Pangea, it is more likely that they developed during intense shortening related to the Alleghanian orogeny. Evidence for compressional deformation associated with Pangea breakup (related to the rift-to-drift transition) is mostly confined to Mesozoic rift basins in the southern Appalachians (Reference 2.5.3-37, 2.5.3-39, and 2.5.3-41), whereas evidence for compressional deformation related to the Alleghanian orogeny extends well into the continental interior (Reference 2.5.3-43). Additionally, shortening in the Valley and Ridge province in central-eastern Tennessee is estimated to be greater than 50 percent, based on palinspastic restoration of balanced cross sections (Reference 2.5.3-71).

Quaternary terrace profiles across the projected trace of the shear-fracture zone show no evidence of linear topographic features or warping of the terrace profile suggestive of surface deformation as a result of movement along the shear-fracture zone (Figure 2.5.3-9). This, and the crosscutting relationships discussed above, support the interpretation that the shear-fracture zones accommodated shortening during the late Paleozoic Alleghanian orogeny and emplacement of foreland fold-thrust belt thrust sheets in the Valley and Ridge Province.

2.5.3.4.3 Karst Collapse

Carbonate dissolution and the development of karst features are ongoing processes. Subsidence of Quaternary terrace material within the site area that overlies carbonate units indicates these processes have locally been active through the Holocene (see Subsection 2.5.1.2.5 for more detailed discussion of karst features).

2.5.3.5 Relationship of Tectonic Structures in the Site Area to Regional Tectonic Sources

Alleghanian bedrock faults that occur within the CRN site area (Copper Creek and Whiteoak Mountain faults, Figure 2.5.1-35) are part of the more regional Valley and Ridge foreland fold-thrust belt system. Faults of this nature (northeast-striking, southeast-dipping thrust faults) occur along orogenic strike from northeastern Alabama to eastern Pennsylvania (see Subsection 2.5.1.1.4). These faults are demonstrably late Paleozoic in age, and the evidence for this timing is discussed thoroughly in Subsection 2.5.1 and Subsections 2.5.3.2.1 and 2.5.3.4.1. Valley and Ridge thrust faults exposed at the ground surface generally have a listric geometry (shallow with depth) and sole into the master Appalachian detachment at the base of the Paleozoic passive margin sedimentary section (see Subsections 2.5.1.1.4 and 2.5.1.2.4 for more detailed discussion). Earthquakes associated with the ETSZ occur in crystalline basement rocks below the Appalachian detachment, 5 to 26 km (3 to 16 mi) deep (Reference 2.5.3-38). Therefore, Alleghanian bedrock thrust faults exposed in the site area are not related to seismicity associated with the ETSZ.

2.5.3.6 Characterization of Capable Tectonic Sources

Based on the analysis and results presented in Subsections 2.5.1, 2.5.3.2, and 2.5.3.5, there is no evidence for significant neotectonic features within the 200-mi CRN site region radius that have a potential to impact site safety. Alleghanian bedrock faults in the valley and ridge are demonstrably late Paleozoic in age, and the evidence for this timing is discussed thoroughly in Subsection 2.5.1 and Subsections 2.5.3.2.1 and 2.5.3.4.1. Regional geologic mapping and longitudinal profiles along the Clinch River using high-resolution LiDAR data (described in Subsection 2.5.3.2.5) indicate that there has not been discernible displacement resulting from

Quaternary movement along faults in the site area. Additionally, there is no evidence that ETSZ earthquakes are related to faults at the ground surface.

Seismicity in the site region is elevated near the CRN Site and is associated with the ETSZ. Seismicity within the ETSZ is included in a larger seismic source area described in Subsection 2.5.2.2. Four earthquakes with **M** ≥ 2.9 and < 3.6 have been recorded within the CRN site area (Figure 2.5.3-5), three of which have occurred since 1982.

Earthquakes associated with the ETSZ are likely related to present-day compressive stresses present throughout eastern North America (Reference 2.5.3-36). Chapman et al. (Reference 2.5.3-38) found ETSZ focal mechanism solutions to be bimodal based on statistical analyses. One group includes right-lateral motion on north-trending nodal planes and left-lateral motion on east-trending nodal planes. The second group includes right-lateral motion on northeasterly trending nodal planes and left-lateral motion on southeasterly trending nodal planes. Chapman et al. (Reference 2.5.3-38) proposed: (1) that the earthquakes have occurred primarily through left-lateral motion on east-west trending faults that are east of and adjacent to the NY-AL lineament, and (2) that the preferred orientation of focal mechanism nodal planes and epicenter alignments suggest seismicity is distributed over a series of northeast-trending, en-echelon segments and is structurally controlled by basement faults. Chapman et al. (Reference 2.5.3-29) suggested that these linear segments and the locations of their terminations may reflect basement fault structure that is being reactivated in the modern stress regime by the presence of a weak lower crust and/or increased fluid pressures within the upper to middle crust, as indicated by the anomalously low velocities within the seismic zone. Chapman et al. (Reference 2.5.3-29) suggested a slight correlation may exist between the seismicity, the major drainage pattern, and the general topography of the region, which could result from a hydrological element linkage (Reference 2.5.3-40).

Steltenpohl et al. (Reference 2.5.3-33) attributed seismicity in the ETSZ to the N15°E magnetic grain of hypothesized metasedimentary gneisses of the buried Ocoee block correlative with the Amish anomaly. Additionally, Steltenpohl et al. (Reference 2.5.3-33) proposed that the stress that initiated dextral motion along the NY-AL lineament and the modern stress field are compatible. Long and Zelt (Reference 2.5.3-42), Long and Kaufmann (Reference 2.5.3-44), and Kaufmann and Long (Reference 2.5.3-31) proposed an alternative interpretation of seismicity and velocity structures in the ETSZ, in which the majority of seismicity is concentrated in areas of low velocity at midcrustal depths and is not associated with major crustal features, such as distinct crustal blocks defined by the NY-AL lineament. This alternative model suggests intraplate earthquakes occur in midcrustal zones of weakness that may result from increased fluid content in the crust (Reference 2.5.3-42).

Investigations and subsequent evaluation of potential tectonic features associated with the ETSZ described by Hatcher et al. (Reference 2.5.3-12) and Warrell (References 2.5.3-13 and 2.5.3-14) are thoroughly discussed and evaluated in Subsections 2.5.2.2.5.1 and 2.5.2.2.6.1.3. Based on field inspection and review, nearly all the features interpreted as paleoseismic in origin can also be explained by other plausible, non-seismic processes.

2.5.3.7 Designation of Zones of Quaternary Deformation in the Site Region

There are no zones of Quaternary deformation associated with tectonic faults that require detailed investigation within the CRN site vicinity or site area (see Subsection 2.5.3.2). However, three possible Quaternary fault systems occur within the CRN site region (Kentucky River fault system, Rough Creek-Shawneetown fault system, and several unnamed Quaternary faults in western North Carolina; References 2.5.3-45 and 2.5.3-46). Van Arsdale (Reference 2.5.3-47) correlates the Kentucky River and Rough Creek-Shawneetown fault systems.

The Kentucky River fault system is an east-northeast-trending system in northeastern Kentucky (see Figure 2.5.1-18, Sheet 1); at its closest extent, the Kentucky River fault system is approximately 125 mi from the CRN Site. Zeng et. al. (Reference 2.5.3-48) demonstrated the Kentucky River fault system was active as a growth fault during the Carboniferous based on thickening sequences of carbonate strata buttressed against the fault zone. Van Arsdale (Reference 2.5.3-47) indicated that faults appear to offset Pliocene-Pleistocene terrace deposits in a reverse sense, based on evidence from exploratory trenches at several sites in north-central Kentucky (Reference 2.5.3-47). Crone and Wheeler (Reference 2.5.3-45) suggest evidence of Quaternary deformation from exploratory trenches on the Kentucky River fault system could also be related to karst collapse of underlying carbonate bedrock. Crone and Wheeler (Reference 2.5.3-45) classified the Kentucky River fault system as a Class B feature, which is defined as follows:

> "Geologic evidence demonstrates the existence of a fault or suggests Quaternary deformation, but either (1) the fault might not extend deeply enough to be a potential source of significant earthquakes, or (2) the currently available geologic evidence is too strong to confidently assign the feature to Class C but not strong enough to assign it to Class A."

The Rough Creek-Shawneetown fault system occurs in west-central Kentucky, approximately 125 mi northwest of the CRN Site (see Figure 2.5.1-18, Sheet 1). Bedrock steps beneath Pliocene(?)-Holocene alluvium have been suggested to represent Holocene reactivation of Neoproterozoic-early Paleozoic Rough Creek graben normal faults (see Reference 2.5.3-45 and references therein). However, no evidence of Quaternary faulting has been reported in the Rough Creek-Shawneetown fault system, and Krausse and Treworgy (Reference 2.5.3-49) and Thomas (Reference 2.5.3-50) suggest a late Paleozoic age (see Subsection 2.5.1.1.4.1.1). The Rough Creek-Shawneetown fault system is therefore classified by Crone and Wheeler (Reference 2.5.3-45) as Class C, meaning:

> "Geologic evidence is insufficient to demonstrate (1) the existence of tectonic fault, or (2) Quaternary slip or deformation associated with the feature."

Prowell (Reference 2.5.3-46) reported three localities small faults near Saluda, North Carolina, that appear to offset alluvial and colluvial deposits interpreted as Quaternary (Figure 2.5.1-18). These faults are described as reverse, strike-slip, tear and normal faults, with apparent vertical offsets of 4 m (reverse) and 5 m (normal) (Reference 2.5.3-46). These faults were originally identified by Conley and Drummond (Reference 2.5.3-51) and later revisited by York and Oliver (Reference 2.5.3-52). Although these are identified as Quaternary features, they were not evaluated by Crone and Wheeler (Reference 2.5.3-45) or Wheeler (Reference 2.5.3-53). The closest of this group of faults is approximately 118 mi southeast of the CRN Site (Figure 2.5.1-18).

2.5.3.8 Potential for Tectonic or Non-Tectonic Deformation at the Site

2.5.3.8.1 Potential for Tectonic Deformation

The potential for tectonic surface deformation at the CRN Site is negligible based on evidence presented herein. Although the site lies within the boundary of the ETSZ, earthquakes occur below the Paleozoic foreland-fold thrust belt, and no Quaternary tectonic faults are exposed within the site area or site vicinity. Detailed mapping of the excavation(s), as called for in Subsection 2.5.1.2.6, will help to confirm the negligible potential for tectonic deformation of the CRN Site.

2.5.3.8.2 Potential for Non-Tectonic Deformation

2.5.3.8.2.1 Karst-Related Deformation

The potential for non-tectonic surface deformation as a result of karst features represents the most significant geologic hazard to the CRN Site. A more comprehensive assessment of karst hazards at the CRN Site is addressed separately in Subsection 2.5.1.2.5.

The site consists of thick residual soils that cover an irregular bedrock surface of slots and pinnacles. Fifteen stratigraphic units, most of which are calcareous, comprise the bedrock geology at the site (see Figure 2.5.1-28). The planned site construction will bear on the middle Chickamauga to upper Knox Group bedrock units. Overburden soils and cavities associated with dissolution near the top of rock will be removed during the excavation process, thereby mitigating hazard of a cover-collapse or subsidence sinkhole. However, cavities have been observed in boreholes as deep as 660 ft elevation (see Subsection 2.5.1.2.5; Figure 2.5.1-52); these cavities and karst conditions pose four types of hazards to the proposed construction:

- The ground surface may experience collapse or subsidence from sinkholes. Cover-collapse and cover-subsidence sinkholes are present in the landscape (see Subsection 2.5.1.2.5), and additional sinkholes may develop during the lifetime of the plant. Construction activities such as grading, which thins the soil overburden; loading from buildings, roads, and waste ponds, or changes in groundwater levels, can trigger new sinkholes. The site area karst features inventory shows that several of the lithologic units are especially prone to sinkhole development (see Subsection 2.5.1.2.5).

- The potential presence of cavities in the excavation walls below the groundwater table may pose a hazard to the safety of the excavation. Groundwater may discharge from the cavities, making it difficult to maintain a dry excavation, and the water may affect slope stability. The CRBRP PSAR (References 2.5.3-5 and 2.5.3-6) anticipated this problem, although records indicate that excavation had been relatively dry (Reference 2.5.3-54). Subsections 2.5.1.2.5.1.3, 2.5.1.2.6.10, and 2.5.4.12 discuss mitigation strategies that will be employed prior to and during the excavation.

- The presence of cavities below the base of the foundation would compromise the structural stability of the foundation. As discussed in Subsection 2.5.1.2.5, slightly deeper cavities that cannot be seen may be detected using geophysical methods or boreholes in the finished excavation. Final conclusions regarding karst hazard should be based on detailed geologic mapping of the excavations and geophysical surveys at foundation level (see Subsection 2.5.1.2.6.10).

- The presence of cavities may enable rapid movement of groundwater through the underground karst drainage system.

2.5.3.8.2.2 Slope Failure

Reconnaissance geologic mapping, aerial photograph analysis, and slope analysis using high-resolution LiDAR digital elevation data revealed no existing landslides or other slump-related hazards at the CRN Site.

2.5.3.8.2.3 Anthropogenic Features

The CRN Site has never been commercially mined; there is no potential hazard from mine collapse (see Subsection 2.5.1.2.6.8). The previous grading and excavation of the CRBRP contain fill and will be evaluated for any future development.

2.5.3.9 References

2.5.3-1. Electric Power Research Institute (EPRI), Palo Alto, CA, U.S. DOE, and U.S. NRC, Central and Eastern United States Seismic Source Characterization for Nuclear Facilities, NUREG-2115, 2012.

2.5.3-2. Powell, C.A., G.A. Bollinger, M.C. Chapman, M.S. Sibol, A.C. Johnston, and R.L. Wheeler, *A seismotectonic model for the 300-kilometer–long Eastern Tennessee Seismic Zone*, *Science* Vol. 264, pp. 686–688, 1994.

2.5.3-3. AMEC Infrastructure and Environment, *Geotechnical Exploration and Testing, Clinch River SMR Project, Oak Ridge, Tennessee*, Data Report, Rev. 4, AMEC Project No. 6468-13-1072, submitted to Bechtel Power Corporation, October 2014.

2.5.3-4. Powell, C.A., and J.E. Beavers, The “unknown” hazard in East Tennessee and potential losses, in Beavers, J.E., ed., Multi-hazard Issues in the Central United States: Understanding the Hazards and Reducing the Losses: Reston, Virginia, American Society of Civil Engineers, 2009.

2.5.3-5. Project Management Corporation, Clinch River Breeder Reactor Project – Preliminary Safety Analysis Report, Vol. 2, p. 1982a.

2.5.3-6. Project Management Corporation, Clinch River Breeder Reactor Project – Preliminary Safety Analysis Report, Vol. 3, p. 1982b.

2.5.3-7. Hatcher, R.D., Jr., P.J. Lemiszki, R.B. Dreier, R.H. Ketelle, R.R. Lee, D.A. Lietzke, W.M. McMaster, J.L. Foreman, S.Y. Lee, *Status report on the geology of the Oak Ridge Reservation*, Oak Ridge National Laboratory (ORNL/TM-12074), Environmental Sciences Division Publication No. 3860, pp. 29–39, 1992.

2.5.3-8. Lemiszki, P.J., R.D. Hatcher, and R.H. Ketelle, *Preliminary Detailed Geologic Map of the Oak Ridge, TN Area*, DRAFT, scale 1:24,000, 2013.

2.5.3-9. Harrell, H.C., *Final Geologic Report for Melton Hill Project: Tennessee Valley Authority Division of Water Control Planning Geologic Branch*, May 1965.

2.5.3-10. Rubin, P.A., and P.J. Lemiszki, *Structural and stratigraphic controls on cave development in the Oak Ridge area, Tennessee*, in Gangaware, T., et al., (eds.), Seventh Tennessee Water Resources Symposium and Student Symposium, Tennessee Section of the American Water Resources Association, Nashville, Tennessee, pp. 1–6, 1992.

2.5.3-11. Vaughn, J.D., S.F. Obermeier, R.D. Hatcher, C.W. Howard, M.H. Mills, and S.C. Whisner, *Evidence for one or more major late-Quaternary earthquakes and surface faulting in the East Tennessee seismic zone*, Seismological Research Letters, Vol. 81, Issue 2, p. 323, 2010.

2.5.3-12. Hatcher, R.D., Jr., J.D. Vaughn, and S.F. Obermeier, *Large earthquake paleoseismology in the East Tennessee seismic zone: Results of an 18-month pilot study*, in Cox, R.T., M.P. Tuttle, O.S. Boyd, and J. Locat, (eds.), *Recent Advances in North American Paleoseismology and Neotectonics East of the Rockies*, Geological Society of America Special Paper No. 493, pp. 111–142, 2012.

2.5.3-13. Warrell, K.F., R.D. Hatcher, S.A. Blankenship, C.W. Howard, P.M. Derryberry, A.L. Wunderlich, S.F. Obermeier, R.C. Counts, and J.D. Vaughn, *Detailed geologic mapping of paleoseismic features: An added tool for seismic hazard assessment in the East Tennessee seismic zone*, Geological Society of America Abstracts with Programs Vol. 44, No. 4, p. 19, 2012.

2.5.3-14. Warrell, K.F., *Detailed Geologic Studies of Paleoseismic Features Exposed at Sites in the East Tennessee Seismic Zone: Evidence for Large, Prehistoric Earthquakes*, Master's Thesis, University of Tennessee, p. 131, 2013.

2.5.3-15. Howard, C.W., P.M. Derryberry, R.D. Hatcher, Jr., J.D. Vaughn, and S.F. Obermeier, *Detailed geologic maps of two sites south of Dandridge, Tennessee, record evidence of polyphase paleoseismic activity in the East Tennessee seismic zone*, Geological Society of America Abstracts with Programs Vol. 43, No. 2, p. 16-1, 2011.

2.5.3-16. Hatcher, R.D., Jr., *Developmental Model for the Southern Appalachians*, Geological Society of America Bulletin Vol. 83, pp. 2735–2760, 1972.

2.5.3-17. Hnat, J.S., and B.A. van der Pluijm, *Fault gouge dating in the southern Appalachians, USA*, Geological Society of America Bulletin No.126, pp. 639–651, 2014.

2.5.3-18. Hoskins, D.M., *Geologic map of the Millersburg 15-minute quadrangle, Dauphin, Juniata, Northumberland, Perry, and Snyder Counties, Pennsylvania,* Harrisburg, Pennsylvania Bureau of Topographic and Geologic Survey, scale 1:24,000, 1976.

2.5.3-19. Not used.

2.5.3-20. Not used.

2.5.3-21. Tennessee Valley Authority (TVA), Topography, Liquid Metal Fast Breeder Reactor, Clinch River site, nine plates at 1" = 100' scale, 90-MS-461 pp. 501-101–109, 1973.

2.5.3-22. Radbruch-Hall, D.H., R.B. Colton, W.E. Davies, I. Luchitta, B.A. Skipp, and D.J. Varnes, Landslide overview map of the conterminous United States, U.S. Geological Survey, Professional Paper 1183, 1982. Available at http://pubs.usgs.gov/pp/p1183/, accessed October 20, 2014.

2.5.3-23. Lietzke, D.A., S.Y. Lee, and R.E. Lambert, *Soils, Surficial Geology, and Geomorphology of the Bear Creek Valley Low-Level Waste Disposal. Development and Demonstration Program Site*, Oak Ridge National Lab, Environmental Sciences Division Publication No. 3017, 1988.

2.5.3-24. Delcourt, P.A., Quaternary alluvial terraces of the Little Tennessee River Valley, east Tennessee, in Chapman, J. (ed.), *The 1979 archaeological and geological investigation in the Tellico Reservoir*, University of Tennessee Department of Anthropology Report of Investigations No. 29, pp. 110–121 and 175–212, 1980.

2.5.3-25. Garrow, P., D.S. Leigh, *Phase II Archaeological testing of the Grigsby Bottom site 40LD132, Loudon County, Tennessee*, TVA, p. 15, 1999.

2.5.3-26. TVA, *Watts Bar Final Safety Analysis Report*, through Amendment 114.

2.5.3-27. Johnston, A.C., D.J. Reinbold, and S.I. Brewer, *Seismotectonics of the Southern Appalachians*, Seismological Society of America Bulletin No. 75, pp. 291–312, 1985.

2.5.3-28. Bollinger, G.A., A.C. Johnston, P. Talwani, L.T. Long, K.M. Shedlock, M. Sibol, and M.C. Chapman, *Seismicity of the southeastern United States*, pp. 1698–1986, in Slemmons, D.B., E.R. Engdahl, M.D. Zoback, and D.D. Blackwell (eds.), *Neotectonics of North America*, Geological Society of America, Decade Map No. 1, Series 16, pp. 291–308, 1991.

2.5.3-29. Chapman, M.C., C.A. Powell, S.C. Whisner, and J. Whisner, *The Eastern Tennessee Seismic Zone: Summary After 20 Years of Network Monitoring*, Seismological Research Letters Vol. 73, No. 2, p. 245, 2002.

2.5.3-30. King, E.R., and I. Zietz, *The New York-Alabama lineament: Geophysical evidence for a major crustal break in the basement beneath the Appalachian basin*, Geology 6, pp. 312–318.

2.5.3-31. Kaufmann, R.D., and L.T. Long, *Velocity structure and seismicity of southeastern Tennessee*, Journal of Geophysical Research Vol. 101, Issue B4, pp. 8531–8542, 1996.

2.5.3-32. Vlahovic, G., C.A. Powell, M.C. Chapman, and M. Sibol, *Joint hypocenter-velocity inversion for the eastern Tennessee seismic zone*, Journal of Geophysical Research, Vol. 103 Issue B3, pp. 4879–4896, 1998.

2.5.3-33. Steltenpohl, M.G., I. Zietz, J.W. Horton, Jr., D.L. Daniels, *New York-Alabama lineament: A buried right-slip fault bordering the Appalachians and mid-continent North America*, Geology, Vol. 38, No. 6, pp. 571–574, 2010.

2.5.3-34. NRC, Safety Evaluation Report related to the construction of the Clinch River Breeder Reactor Plant, NUREG-0986, Vol. 1, 1983.

2.5.3-35. Not used.

2.5.3-36. Mazzotti, S., and J. Townend, State of stress in central and eastern North American seismic zones: Lithosphere, Vol. 2, p. 76–83, 2010.

2.5.3-37. Manspeizer, W. et al., *The Geology of North America, The Appalachian-Ouachita Orogen in the United States, Chapter 6, Post-Paleozoic activity*: The Geological Society of America, pp. 319–374, 1989.

2.5.3-38. Chapman, M.C., C.A. Powell, G. Vlahovic, and M.S. Sibol, *A statistical analysis of earthquake focal mechanisms and epicenter locations in the Eastern Tennessee Seismic Zone*, Bulletin of the Seismological Society of America Vol. 87, No. 6, pp. 1522–1536, 1997.

2.5.3-39. Withjack, M.O., et al., *Diachronous Rifting, Drifting, and Inversion on the Passive Margin of Central Eastern North America: An analog for Other Passive Margins: The American Association of Petroleum Geologists*, AAPG Bulletin, Vol. 82, No. 5A, pp. 817–835, May 1998, Part A.

2.5.3-40. Costain, J.K., G.A. Bollinger, and J.A. Speer, *Hydroseismicity—A hypothesis for the role of water in the generation of intraplate seismicity*, Geology Vol. 15, pp. 618–621, 1987.

2.5.3-41. Schlische, R.W., et al., *Relative Timing of Camp, Rifting, Continental Breakup, and Basin Inversion: Tectonic Significance*, in Hames, W.E., G.C. McHone, P.R. Renne, and C. Ruppel, (eds.), *The Central Atlantic Magmatic Province*, American Geophysical Union Monograph, 2002.

2.5.3-42. Long, L.T., and K.-H. Zelt, *A local weakening of the brittle-ductile transition can explain some intraplate seismic zones*, Tectonophysics Vol. 186, pp. 175–192, 1991.

2.5.3-43. Craddock, J.P., and B.A., *Late Paleozoic deformation of the cratonic carbonate cover of eastern North America,* Geological Society of America, Geology, Vol. 17, pp. 416–419, 1989.

2.5.3-44. Long, L.T., and R.D. Kaufmann, *The velocity structure and seismotectonics of southeastern Tennessee*, Seismological Research Letters Vol. 65, Issue 3/4, pp. 211–231, 1994.

2.5.3-45. Crone, A.J., and R.L. Wheeler, *Data for Quaternary faults, liquefaction features, and possible tectonic features in the Central and Eastern United States, east of the Rocky Mountain front*, U.S. Geological Survey Open-File Report 00-260, p. 332, 2000.

2.5.3-46. Prowell, D.C., Index of Faults of Cretaceous and Cenozoic Age in the Eastern United States, U.S. Geological Survey miscellaneous field studies map MF-1269, 2 sheets, 1:2,500,000 scale, 1983.

2.5.3-47. Van Arsdale, R.B., *Quaternary displacement on faults within the Kentucky River fault system of east-central Kentucky,* Geological Society of America Bulletin, Vol. 97, pp. 1382–1392, 1986.

2.5.3-48. Zeng, M., F.R. Ettensohn, and W.B. Wilhelm, Upper Mississippian (Lower Carboniferous) carbonate stratigraphy and syndepositional faulting reveal likely Ouachita flexural forebulge effects, eastern Kentucky, U.S.A., Sedimentary Geology, Vol. 289, pp. 99–114, 2013.

2.5.3-49. Krausse, H.F., and C.G. Treworgy, *Major structures of the southern part of the Illinois basin*, in Palmer, J.E., and R.R. Dutcher, (eds.), *Depositional and structural history of the Pennsylvanian System in the Illinois basin*, Illinois State Geological Survey Guidebook No.15a, pp. 115–120, 1979.

2.5.3-50. Thomas, W.A., *Continental margins, orogenic belts, and intracratonic structures*, *Geology* Lecture Notes 11, pp. 270–272, 1983.

2.5.3-51. Conley, J.F., and K.M. Drummond, Faulted alluvial and colluvial deposits along the Blue Ridge front near Saluda, North Carolina: Southeastern Geology Vol. 7, No. 1: 35–39, 1965.

2.5.3-52. York, J.E., and J.E. Oliver, Cretaceous and Cenozoic faulting in eastern North America: Geological Society of America Bulletin Vol. 87, No. 8: 1105–1114, 1976.

2.5.3-53. Wheeler, R.L., Known or suggested Quaternary tectonic faulting, central and eastern United States – new and updated assessments for 2005: U.S. Geological Survey open-file report 2005–1336, 2005.

2.5.3-54. Kummerle, R.P., and D.A. Benvie, *Exploration, design and excavation of Clinch River Breeder Reactor Foundations*, 28th U.S. Symposium on Rock Mechanics, pp. 351–358, 1987.

2.5.3-55. Hardeman, W.D., *Geologic map of Tennessee*, scale 1:250,000, Tennessee Division of Geology, 1966.

2.5.3-56. Lemiszki, P. J., Geologic Map of the Elverton Quadrangle, Tennessee, Draft Open File Map, scale 1:24,000, 2015.

2.5.3-57. Obermeier, S.F., Vaughn, J.D., and Hatcher, R.D., Jr., Field Trip Guide – Paleoseismic Features in and Near Douglas Reservoir East Tennessee Seismic Zone, Northeastern Tennessee, Site Visit for the Nuclear Regulatory Commission and Other Agencies, University of Tennessee, 2010.

2.5.3-58. Obermeier, S.F., Use of liquefaction-induced features for paleoseismic analysis - An overview of how seismic liquefaction features can be distinguished from other features and how their regional distribution and properties of source sediment can be used to infer the location and strength of Holocene paleo-earthquakes, *Engineering Geology*, Volume 44, pp. 1-76, 1996.

2.5.3-59. Tuttle, M.P., The use of liquefaction features in paleoseismology: Lessons learned in the New Madrid seismic zone, central United States, *Journal of Seismology*, Volume 5, pp. 361-380, 2001.

2.5.3-60. Counts, R. and Obermeier, S.F., Seismic signatures: Small-scale features and ground fractures: in Cox, R.T., Tuttle, M.P., Boyd, O.S., and Locat, J. (editors), *Recent Advances in North American Paleoseismology and Neotectonics East of the Rockies*, Geological Society of America Special Paper 493, pp. 203–219, 2013.

2.5.3-61. Obermeier, S.F., Pond, E.C., Olson, S.M., Green, R.A., Stark, T.D., and Mitchell, J.K., Paleoliquefaction studies in continental settings: geologic and geotechnical factors in interpretations and back-analysis, *U.S. Geological Survey Open-File Report 01-29*, 72 pp, 2001.

2.5.3-62. Heron, S.D., Jr., Judd, J.B., Johnson, H.S., Jr., Clastic dikes associated with soil horizons in the North and South Carolina Coastal Plain, *Geological Society of America Bulletin* Vol. 82, No. 7, pp. 1801-1810, 1971.

2.5.3-63. Bechtel Power Corporation (Bechtel), Geologic Evaluation of Trench Exposure, Vogtle Nuclear Generating Plant, 1984.

2.5.3-64. Abbott, J.C., Gelinas, R.L., and Amick, D.C., Investigation of suspect liquefaction features at the Savannah River Site, South Carolina, U.S. Nuclear Regulatory Commission, NUREG/CR-5503 Appendix A, p. A-3 to A-26, 1999.

2.5.3-65. Obermeier, S.F., Liquefaction evidence for strong earthquakes of Holocene and latest Pleistocene ages in the states of Indiana and Illinois, USA, *Engineering Geology* 50, pp. 227-254, 1998.

2.5.3-66. Hatcher, R.D., Jr., and Bridge, J., Geologic Map of the Jefferson City Quadrangle, Tennessee, *Tennessee Division of Geology Geologic Map*, GM-163-SW, Scale 1:24,000, 1973.

2.5.3-67. Nicholson, S.W., Dicken, C.L., Horton, J.D., Labay, K.A., Foose, M.P., Mueller, J.A.L., 2005. Preliminary integrated geologic map database for the United States: Kentucky, Ohio, Tennessee, and West Virginia, U.S. Geological Survey Open-File Report 2005-1324, version 1.1, available at http://pubs.usgs.gov/of/2005/1324/, accessed on September 22, 2016.

2.5.3-68. Delcourt, P.A., H.R. Delcourt, P.A. Cridlebaugh, and J. Chapman, Holocene ethnobotanical and paleoecological record of human impact on vegetation in the Little Tennessee River Valley, Tennessee, U.S.A., *Quaternary Research* 25: 330-349, 1986.

2.5.3-69. Mills, H.M, and P.A. Delcourt, Quaternary geology of the Appalachian Highlands and Interior Low Plateaus, *Quaternary Nonglacial: Conterminous U.S., The Geology of North America*, Geological Society of America K-2: 611-628, 1991.

2.5.3-70. King, P.B., Geology of the Elkton area, Virginia, *U.S. Geological Professional Paper 230*: p. 82, 1950.

2.5.3-71. Hatcher, R.D., Jr., P.J. Lemiszki, and J.B. Whisner, Character of rigid boundaries and internal deformation of the southern Appalachian foreland fold-thrust belt, J.W. Sears, T.A. Harms, and C.A. Evenchick, (eds.), Whence the Mountains? Inquiries into the Evolution of Orogenic Systems: A Volume in Honor of Raymond A. Price: Boulder, Colorado, Geological Society of America Special Paper 433, pp. 243–276, 2007.

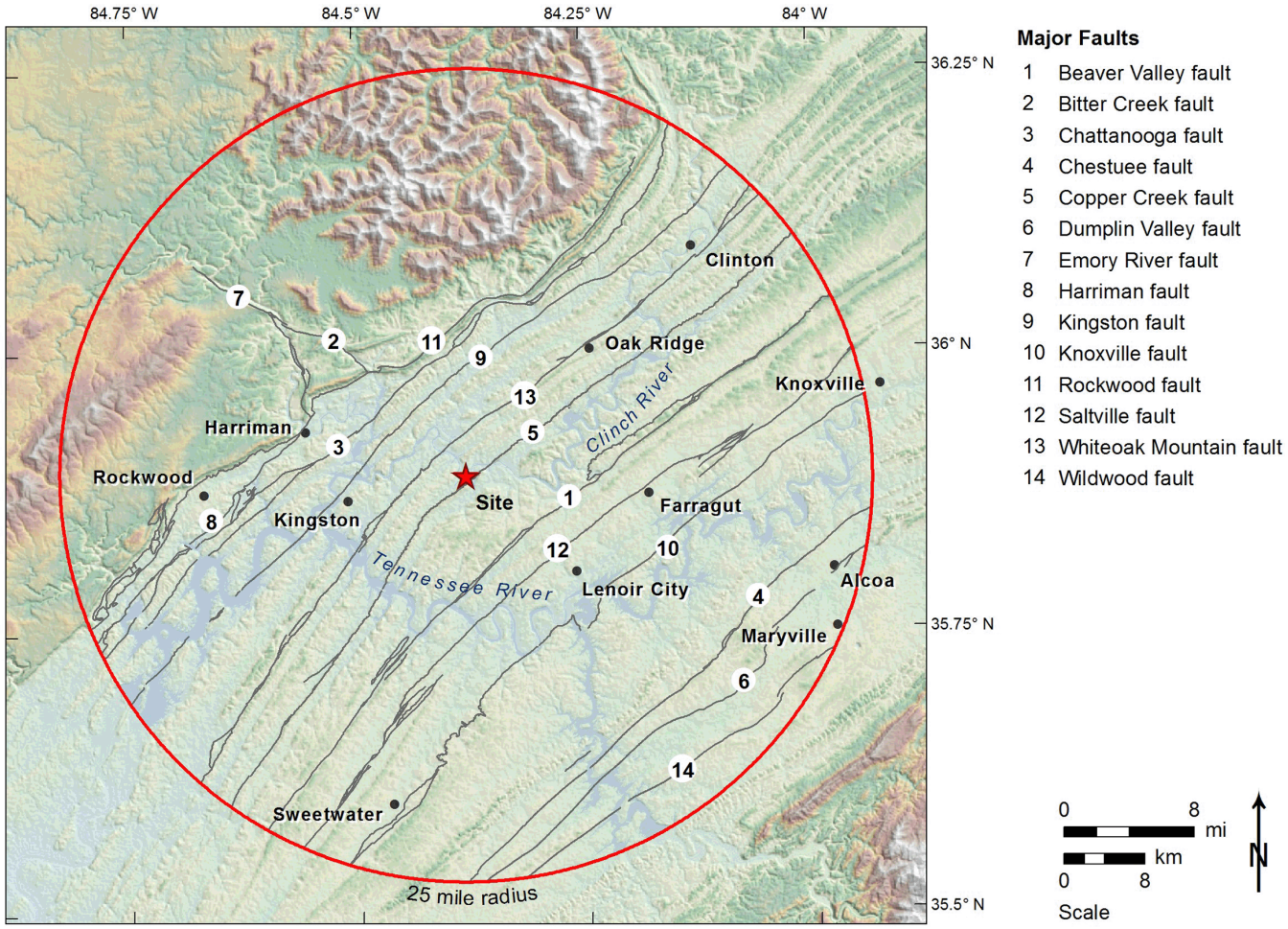

Source: Reference 2.5.3-55

Figure 2.5.3-1. Shaded Relief Map of the Site Vicinity Illustrating the Relationship Between Physiography and Major Thrust Faults of the Pennsylvanian to Permian Alleghanian Orogeny

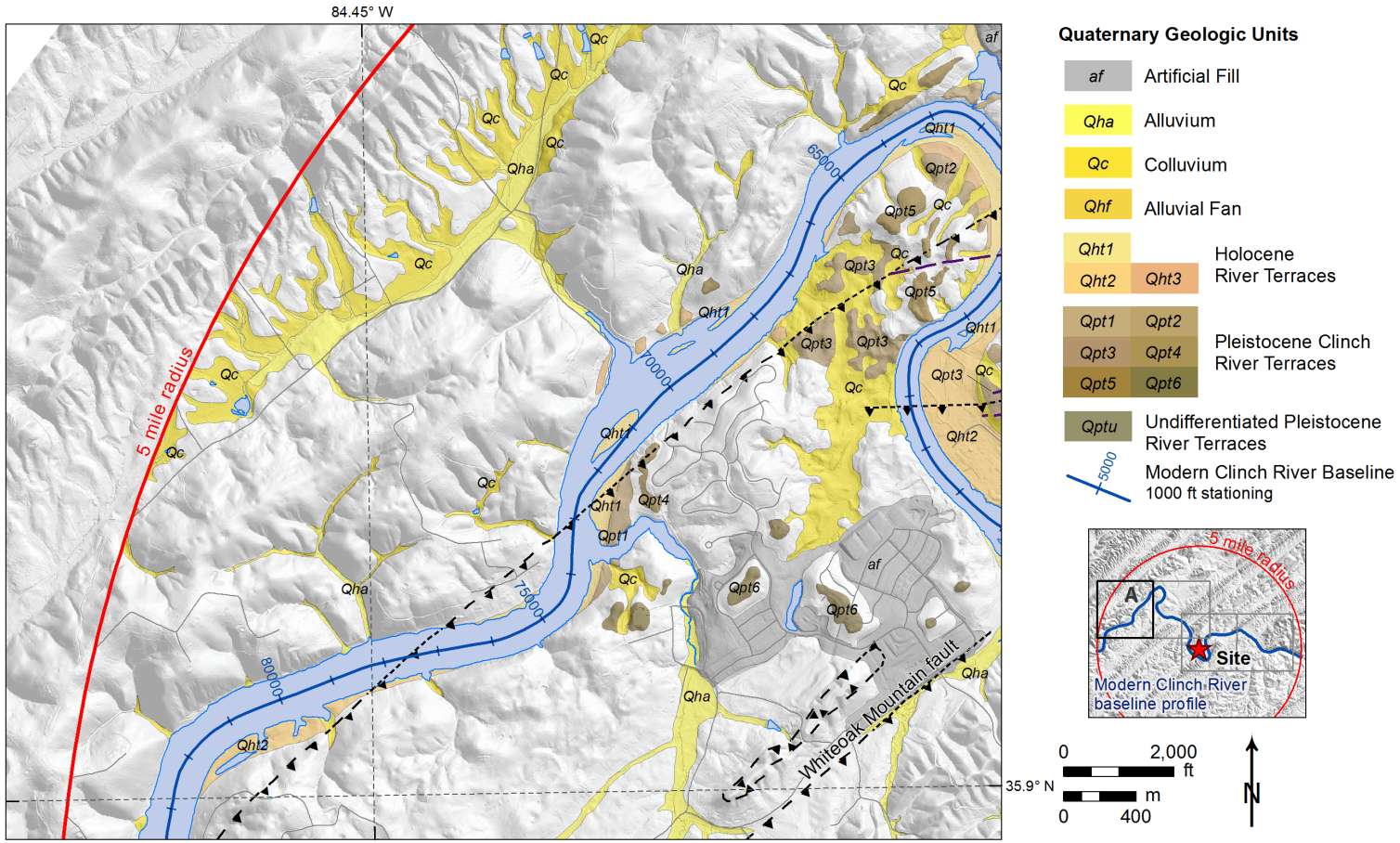

Figure 2.5.3-2. (Sheet 1 of 4) Quaternary Terrace Map Adjacent to the Clinch River Arm of the Watts Bar Reservoir Within the Clinch River Nuclear Site Area, Location A

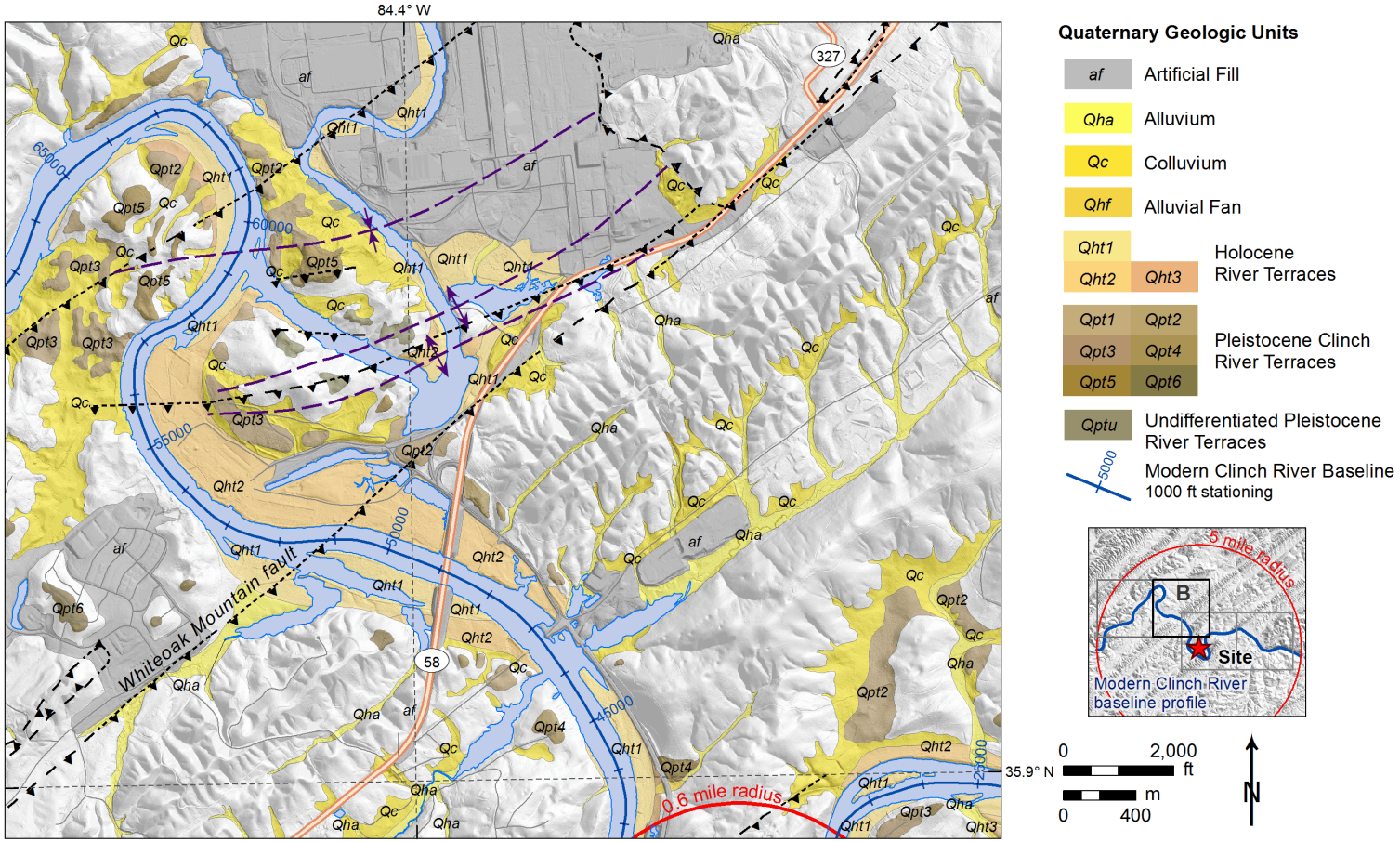

Figure 2.5.3-2. (Sheet 2 of 4) Quaternary Terrace Map Adjacent to the Clinch River Arm of the Watts Bar Reservoir Within the Clinch River Nuclear Site Area, Location B

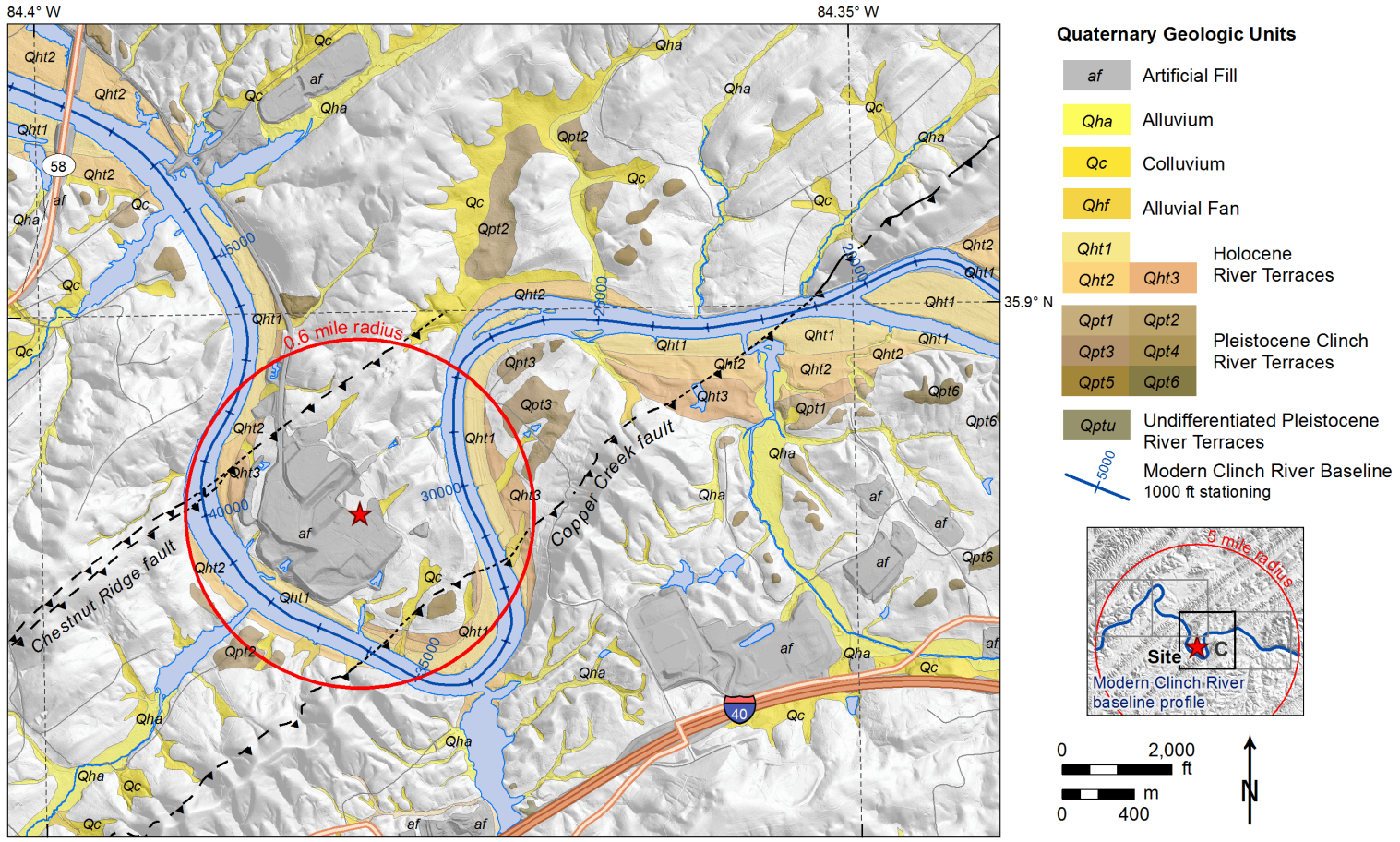

Figure 2.5.3-2. (Sheet 3 of 4) Quaternary Terrace Map Adjacent to the Clinch River Arm of the Watts Bar Reservoir Within the Clinch River Nuclear Site Area, Location C

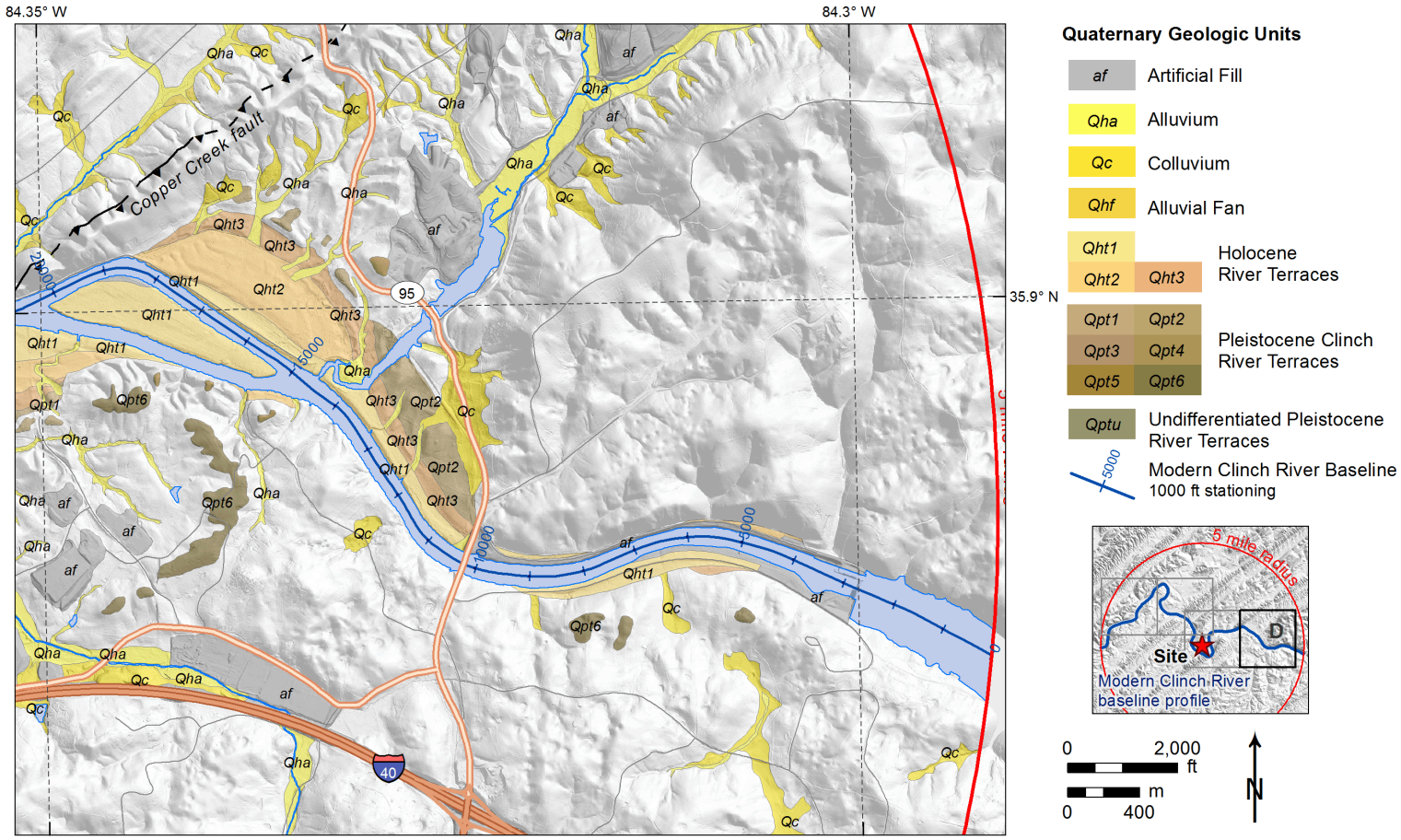

Figure 2.5.3-2. (Sheet 4 of 4) Quaternary Terrace Map Adjacent to the Clinch River Arm of the Watts Bar Reservoir Within the Clinch River Nuclear Site Area, Location D

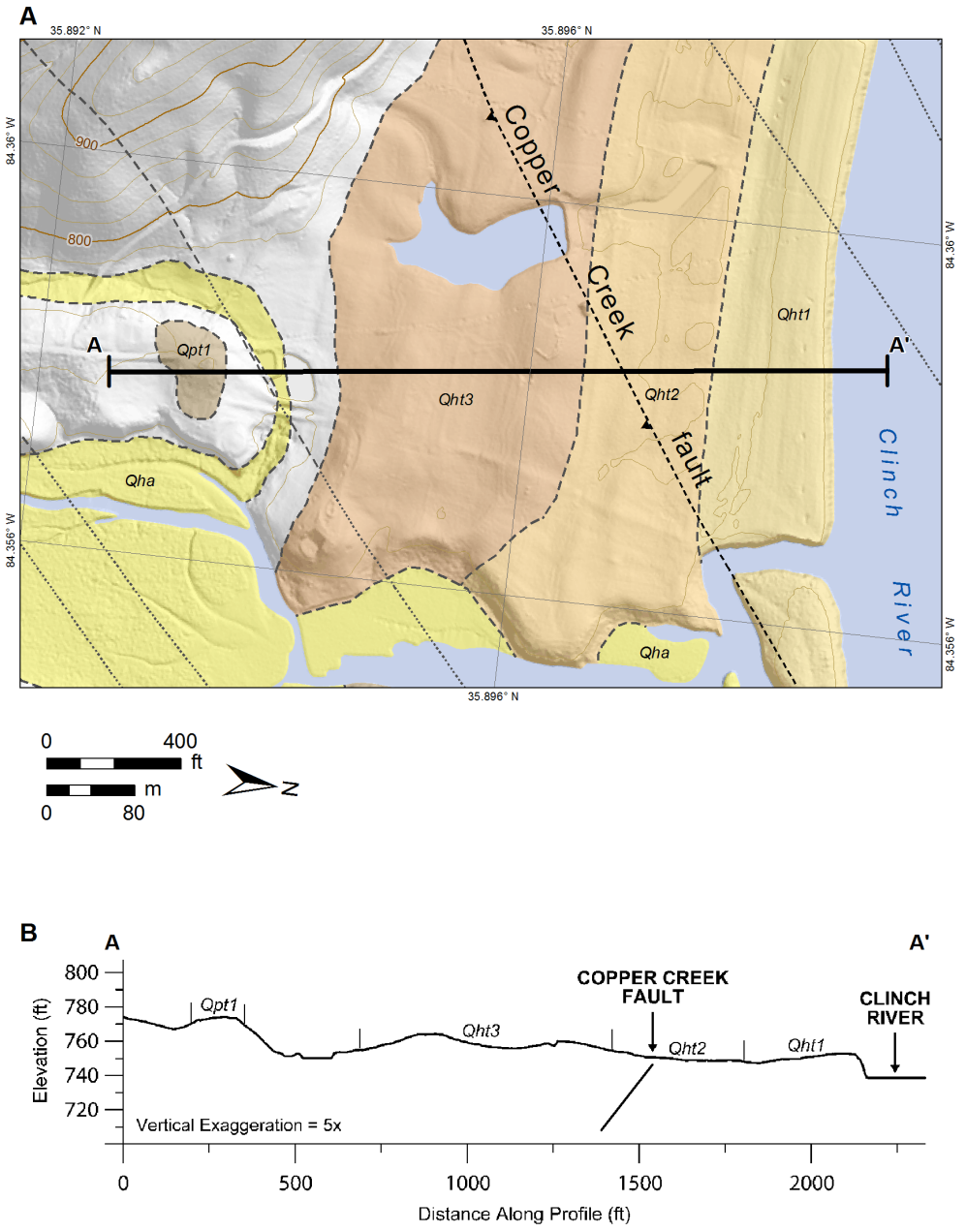

Notes:

A = Map of Clinch River terraces that overlie the Copper Creek fault

B = Topographic profile across terraces and Copper Creek fault

Location of Profile B-B' is shown on Figure 2.5.3-6

Location of Chestnut Ridge fault from Lemiszki (Reference 2.5.3-56)

Figure 2.5.3-3. (Sheet 1 of 2) Geologic Map and Topographic Profile A-A' of Quaternary Fluvial Terraces and Northeastern Projection of Copper Creek Fault

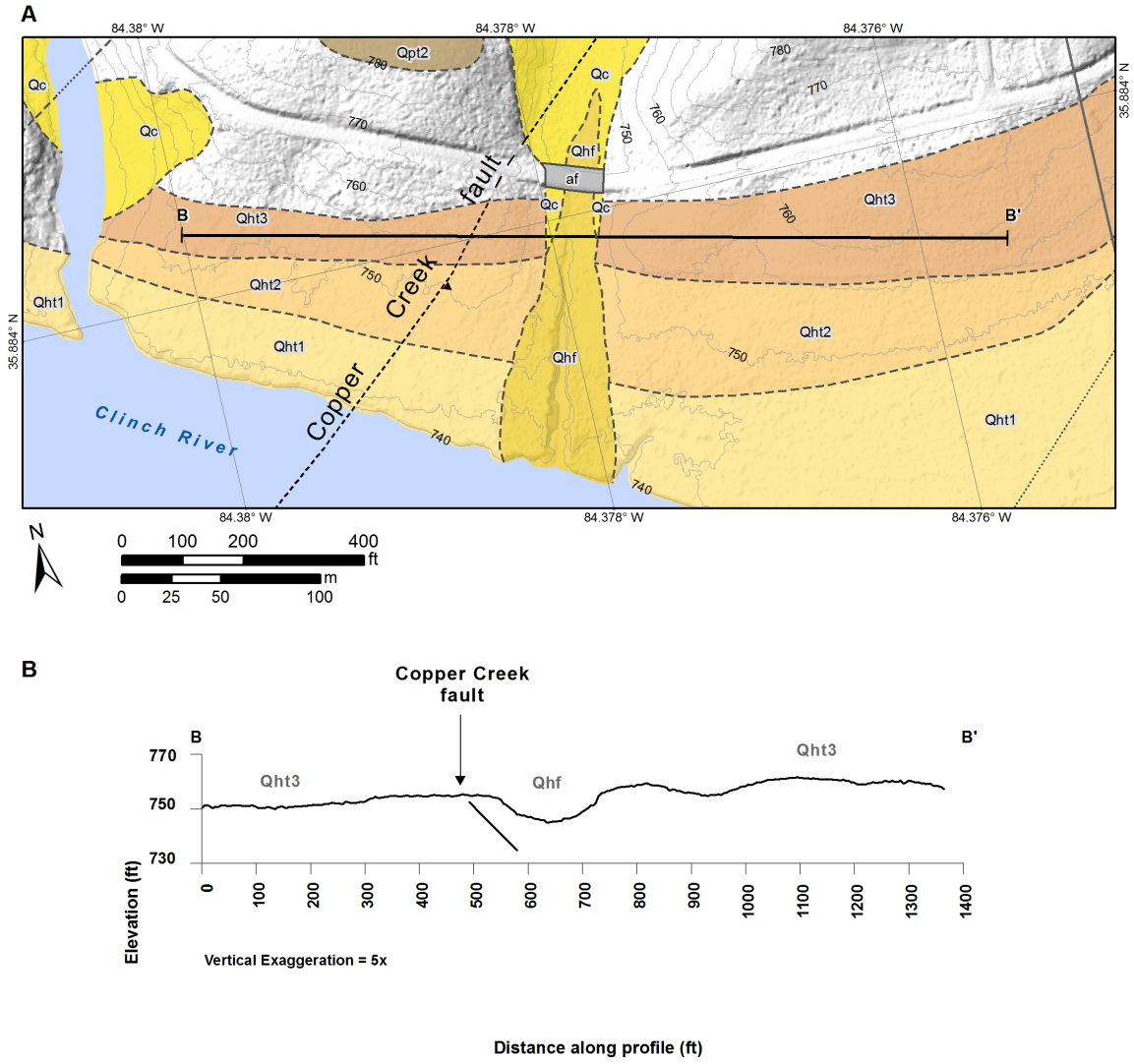

Notes:

A = Map of Clinch River terraces that overlie the Copper Creek fault

B = Topographic profile across terraces and Copper Creek fault

Location of Profile B-B' is shown on Figure 2.5.3-6

Location of Chestnut Ridge fault from Lemiszki (Reference 2.5.3-56)

Figure 2.5.3-3. (Sheet 2 of 2) Geologic Map and Topographic Profile B-B' of Quaternary Fluvial Terraces and Northeastern Projection of Copper Creek Fault

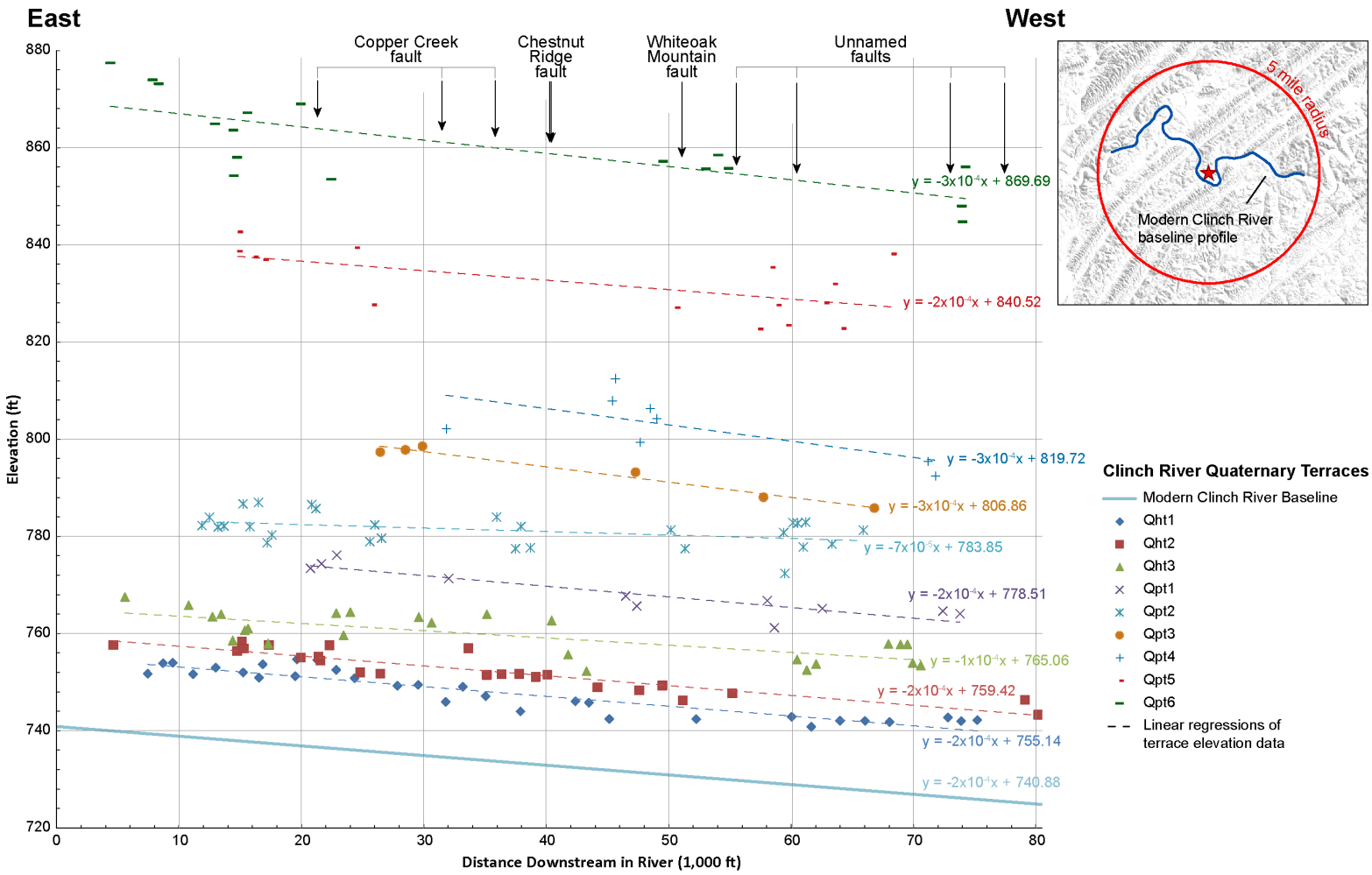

Notes:

See Figure 2.5.3-2 for Quaternary Terrace maps along the Clinch River.

Figure 2.5.3-4. Longitudinal Profiles of Quaternary Terraces Along the Clinch River

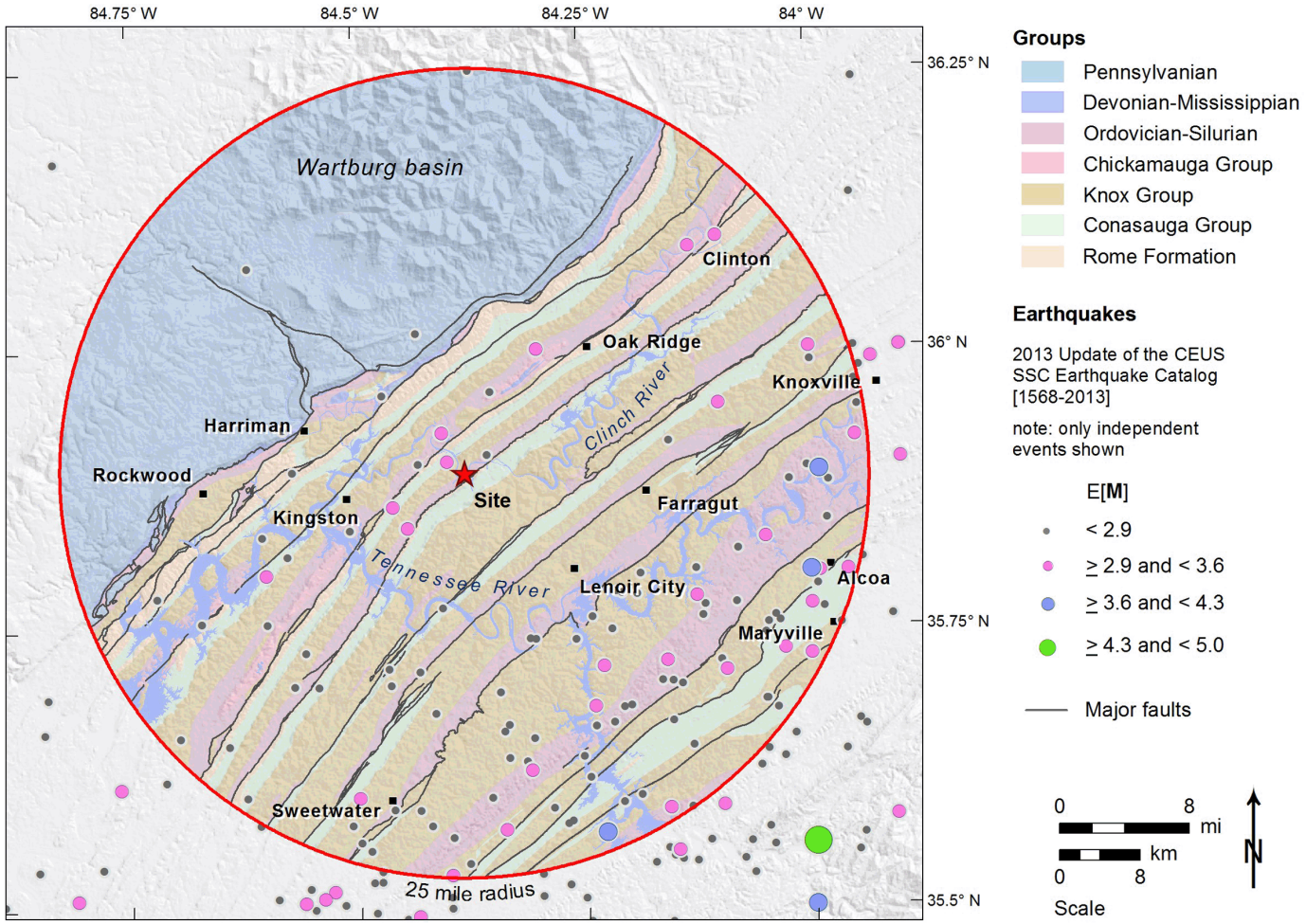

Source: Reference 2.5.3-55

Figure 2.5.3-5. Seismicity within the Clinch River Nuclear Site Vicinity

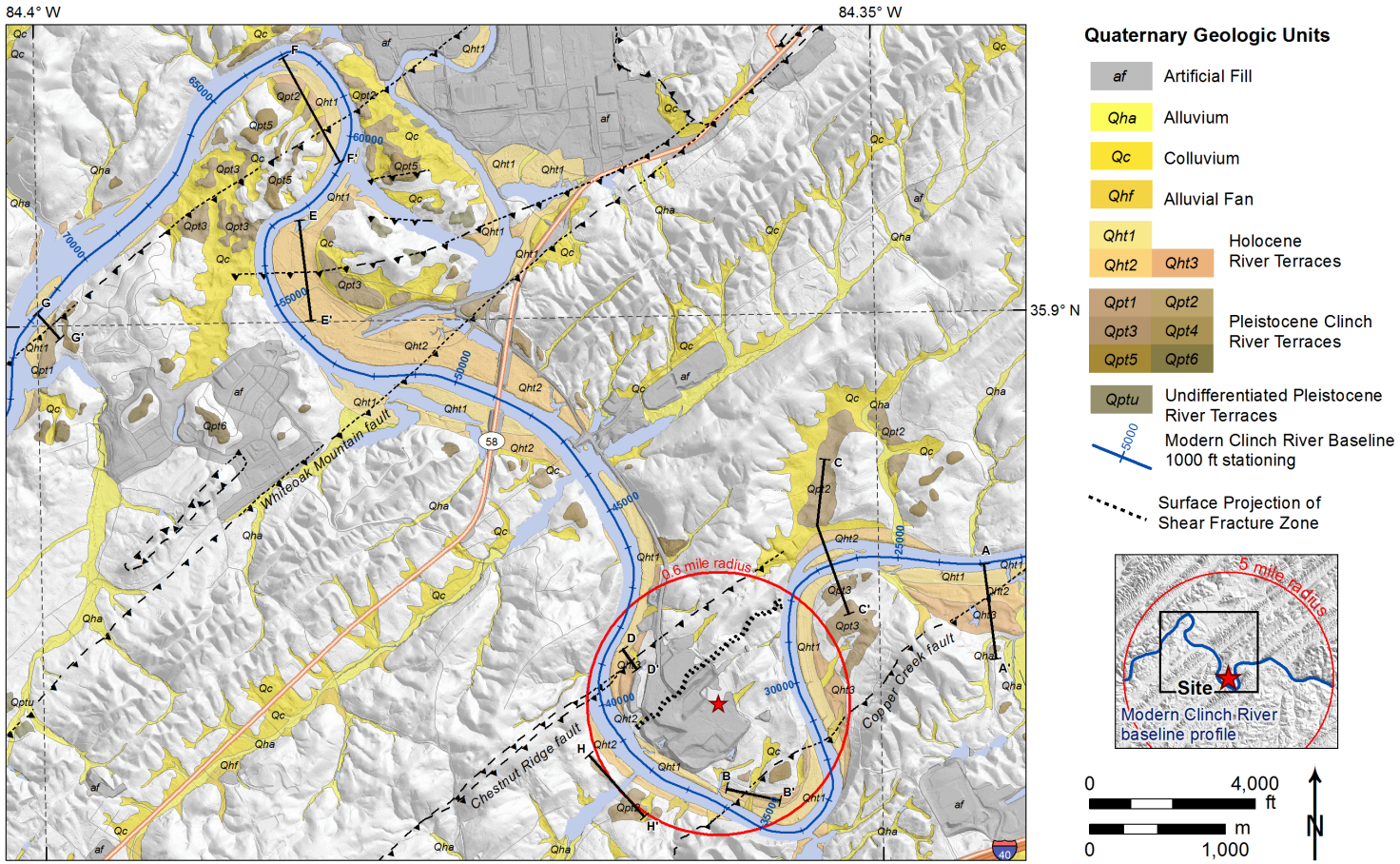

Note: Topographic profiles are shown on Figures 2.5.3-7 through 2.5.3-9

Figure 2.5.3-6. Location Map of Topographic Profiles Across Quaternary Fluvial Terraces and Mapped Faults

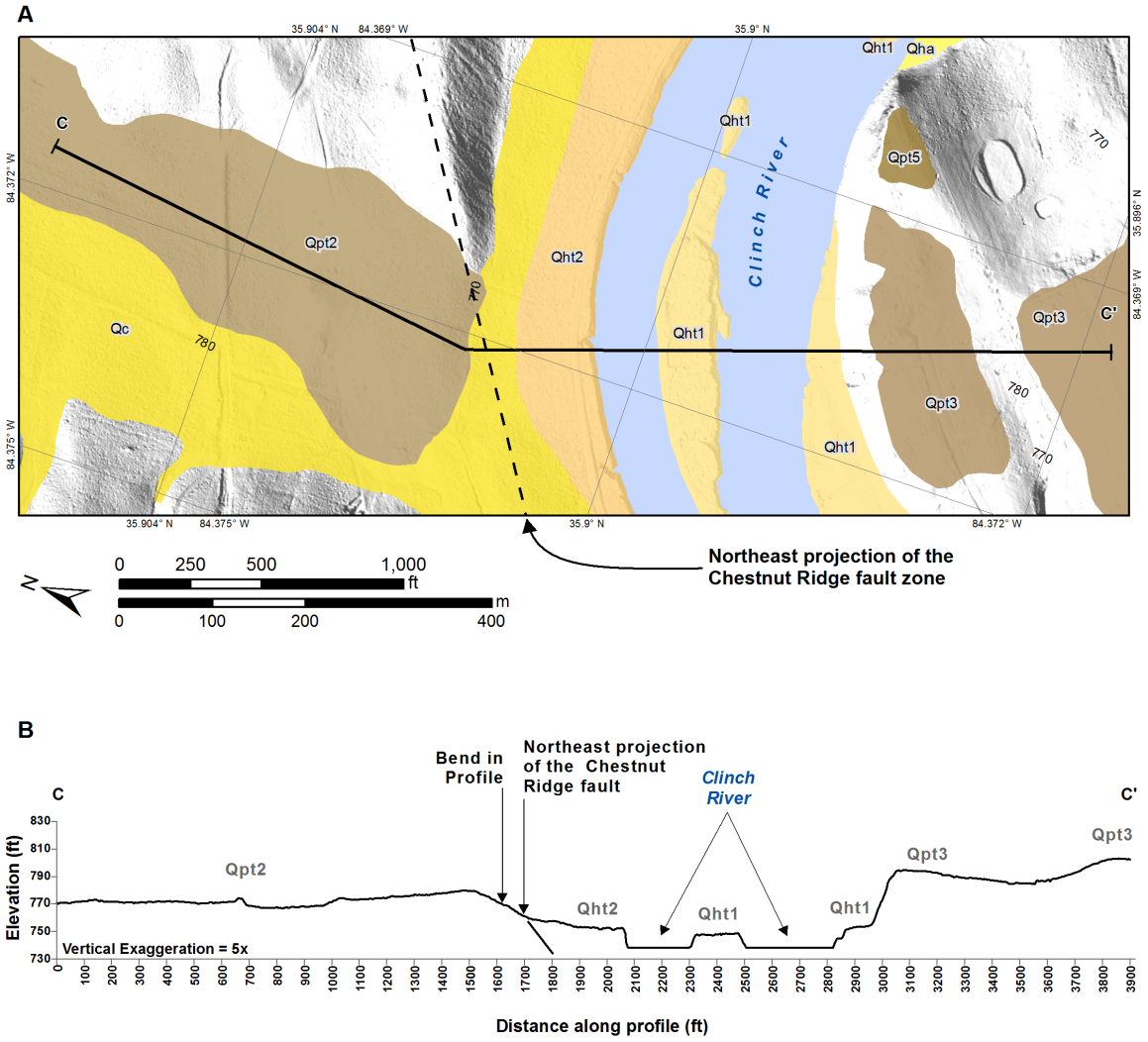

Note: Location of profile is shown on Figure 2.5.3-6

Source: Reference 2.5.3-56

Figure 2.5.3-7. (Sheet 1 of 2) Geologic Map and Topographic Profile C-C' of Quaternary Fluvial Terraces and Northeastern Projection of Chestnut Ridge Fault

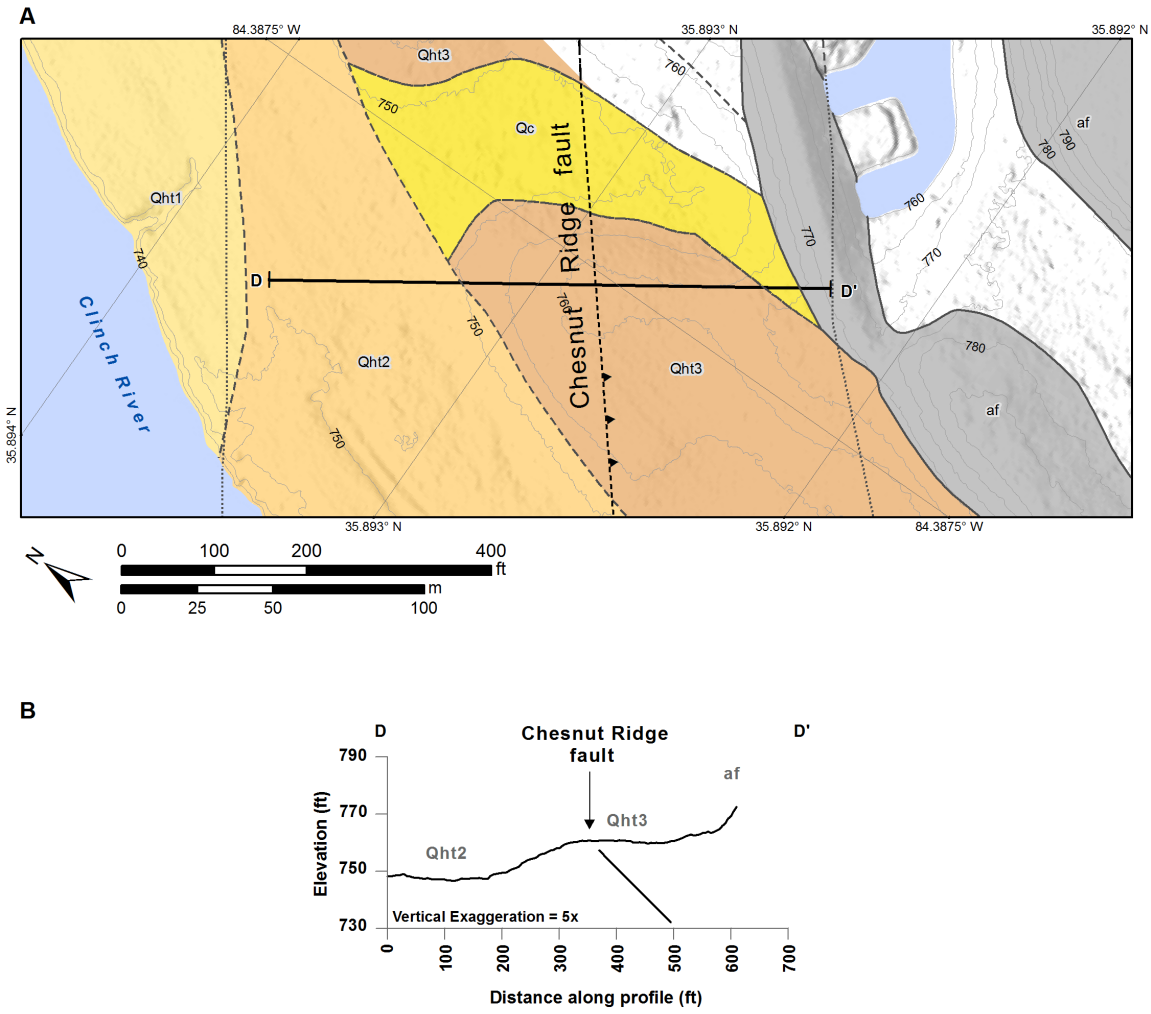

Note: Location of profile is shown on Figure 2.5.3-6

Source: Reference 2.5.3-56

Figure 2.5.3-7. (Sheet 2 of 2) Geologic Map and Topographic Profile D-D' of Quaternary Fluvial Terraces and Chestnut Ridge Fault

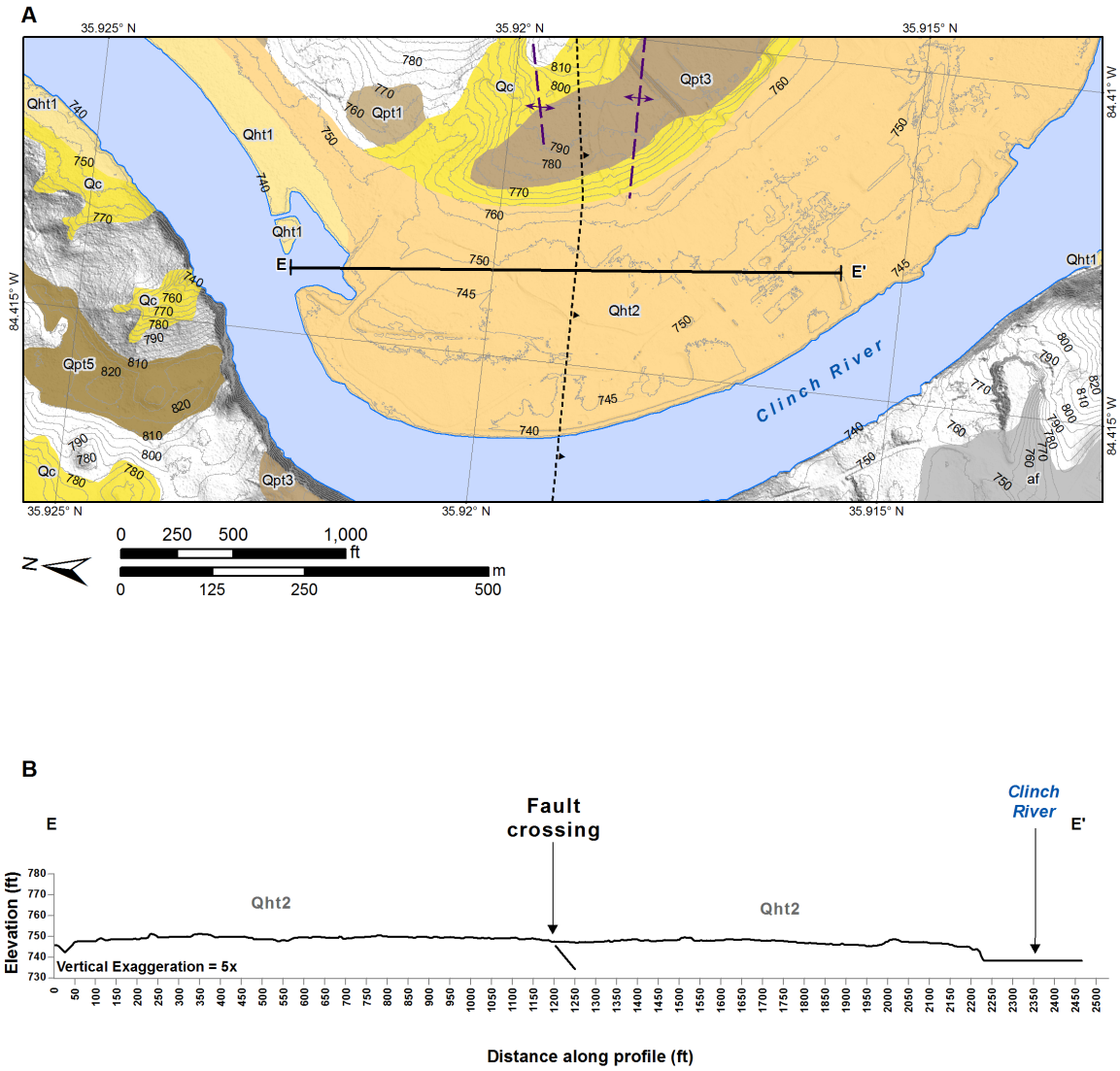

Note: Location of profile is shown on Figure 2.5.3-6

Source: Reference 2.5.3-56

Figure 2.5.3-8. (Sheet 1 of 3) Geologic Map Location and Topographic Profile E-E' of Quaternary Fluvial Terraces and Unnamed Fault

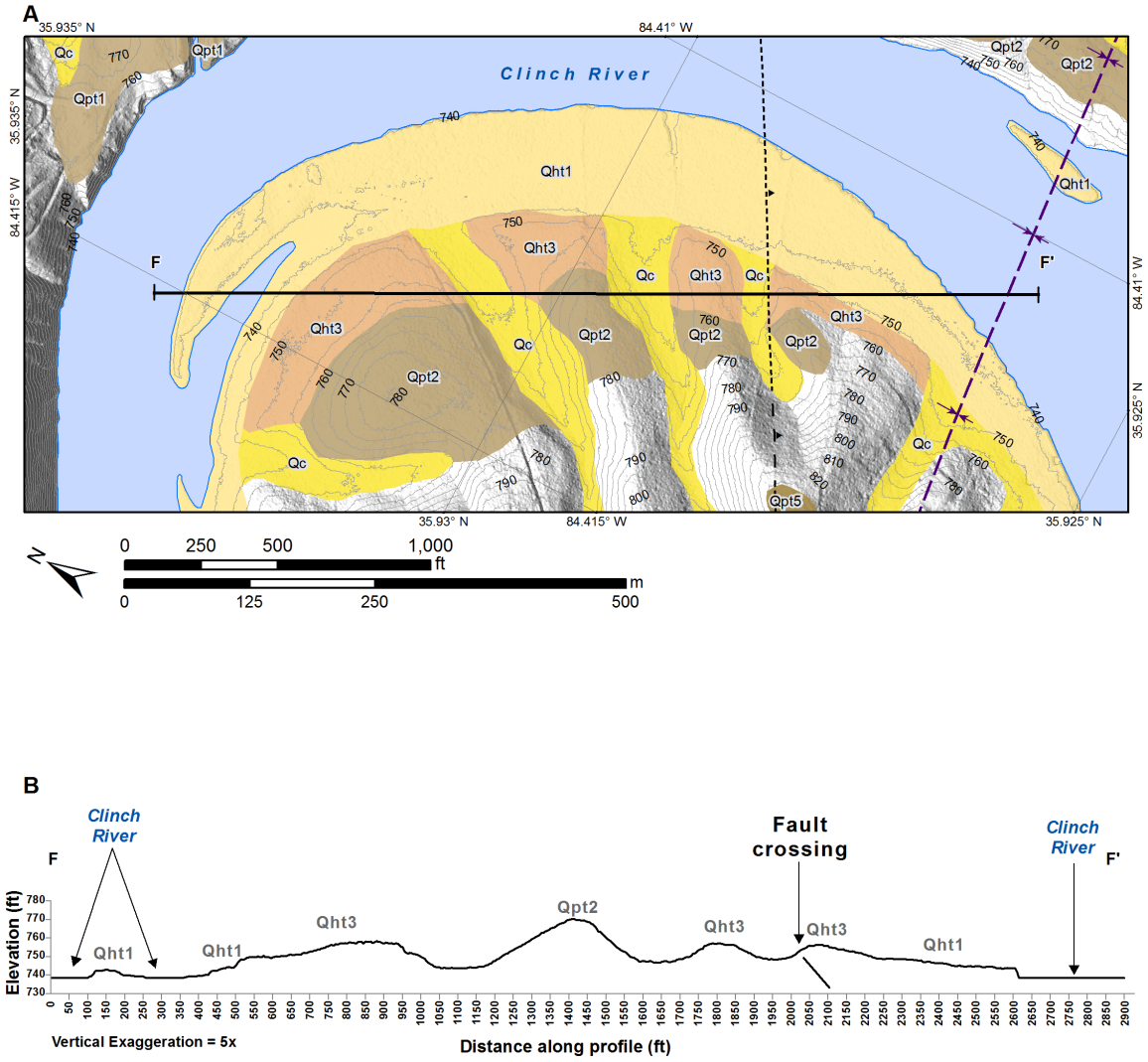

Note: Location of profile is shown on Figure 2.5.3-6

Source: Reference 2.5.3-56

Figure 2.5.3-8. (Sheet 2 of 3) Geologic Map and Topographic Profile F-F' of Quaternary Fluvial Terraces and Unnamed Fault

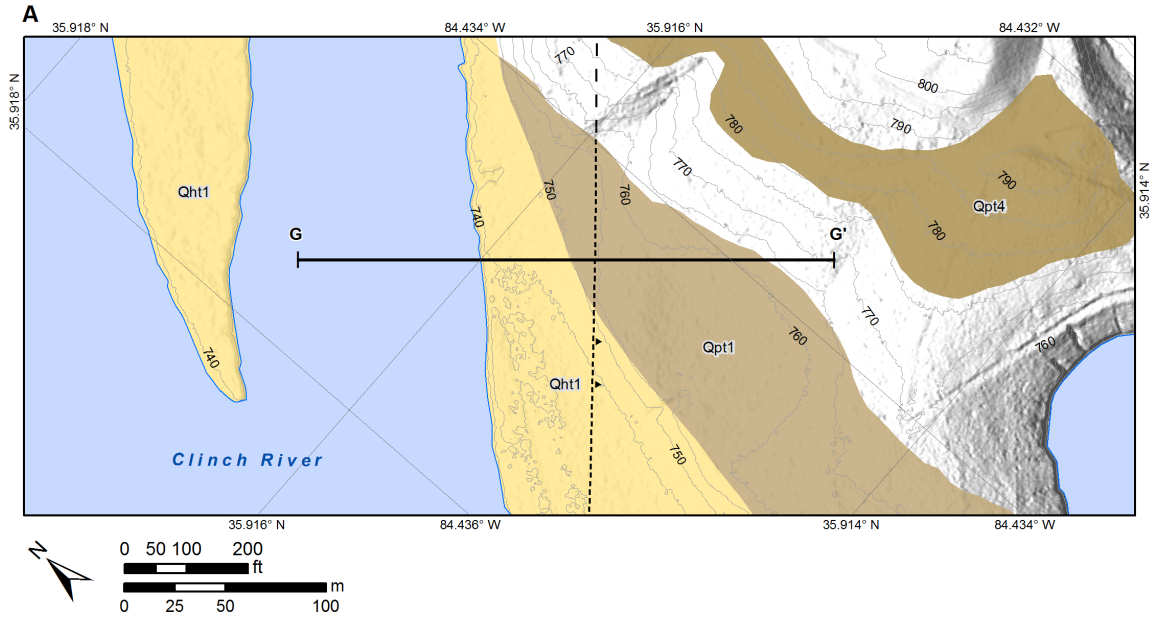

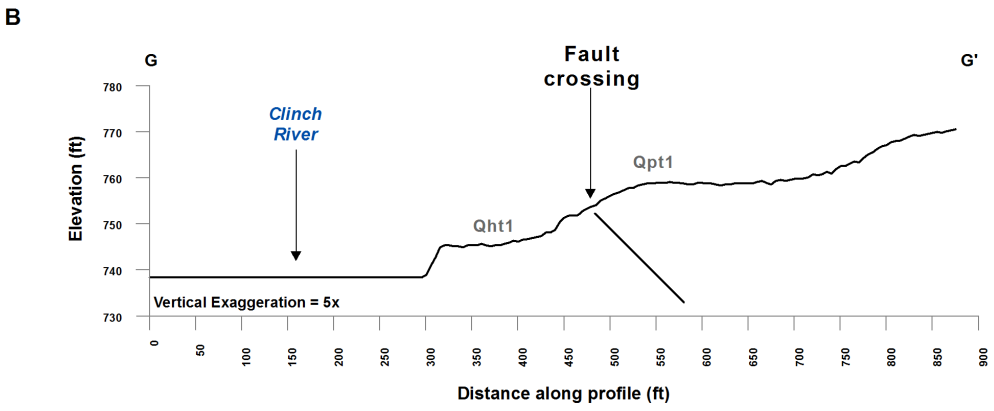

Note: Location of profile is shown on Figure 2.5.3-6

Source: Reference 2.5.3-56

Figure 2.5.3-8. (Sheet 3 of 3) Geologic Map and Topographic Profile G-G' of Quaternary Fluvial Terraces and Unnamed Fault

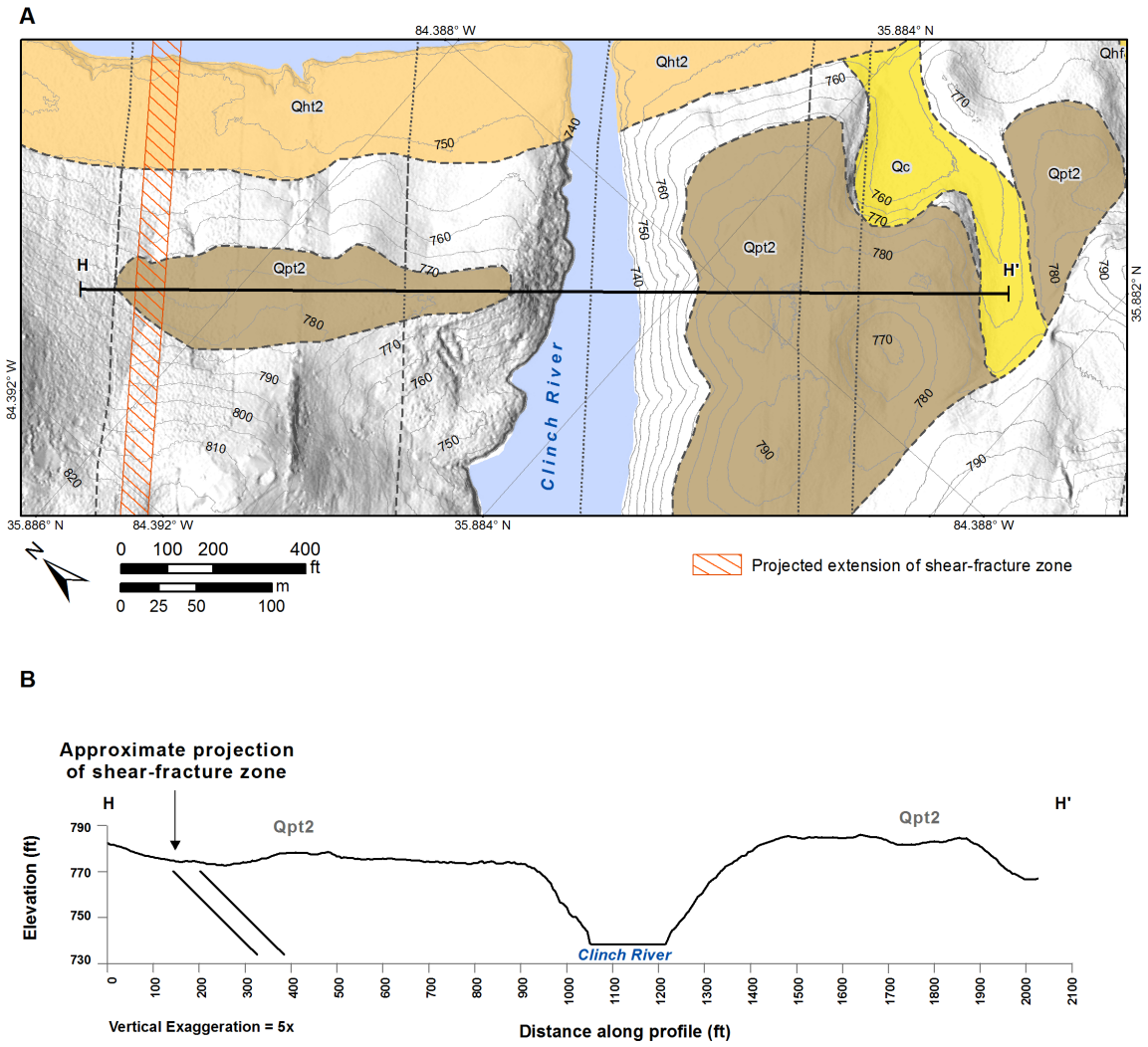

Note: Location of profile is shown on Figure 2.5.3-6

Figure 2.5.3-9. Geologic Map and Topographic Profile H-H' of Quaternary Fluvial Terraces and Surface Projection of the Shear-Fracture Zone

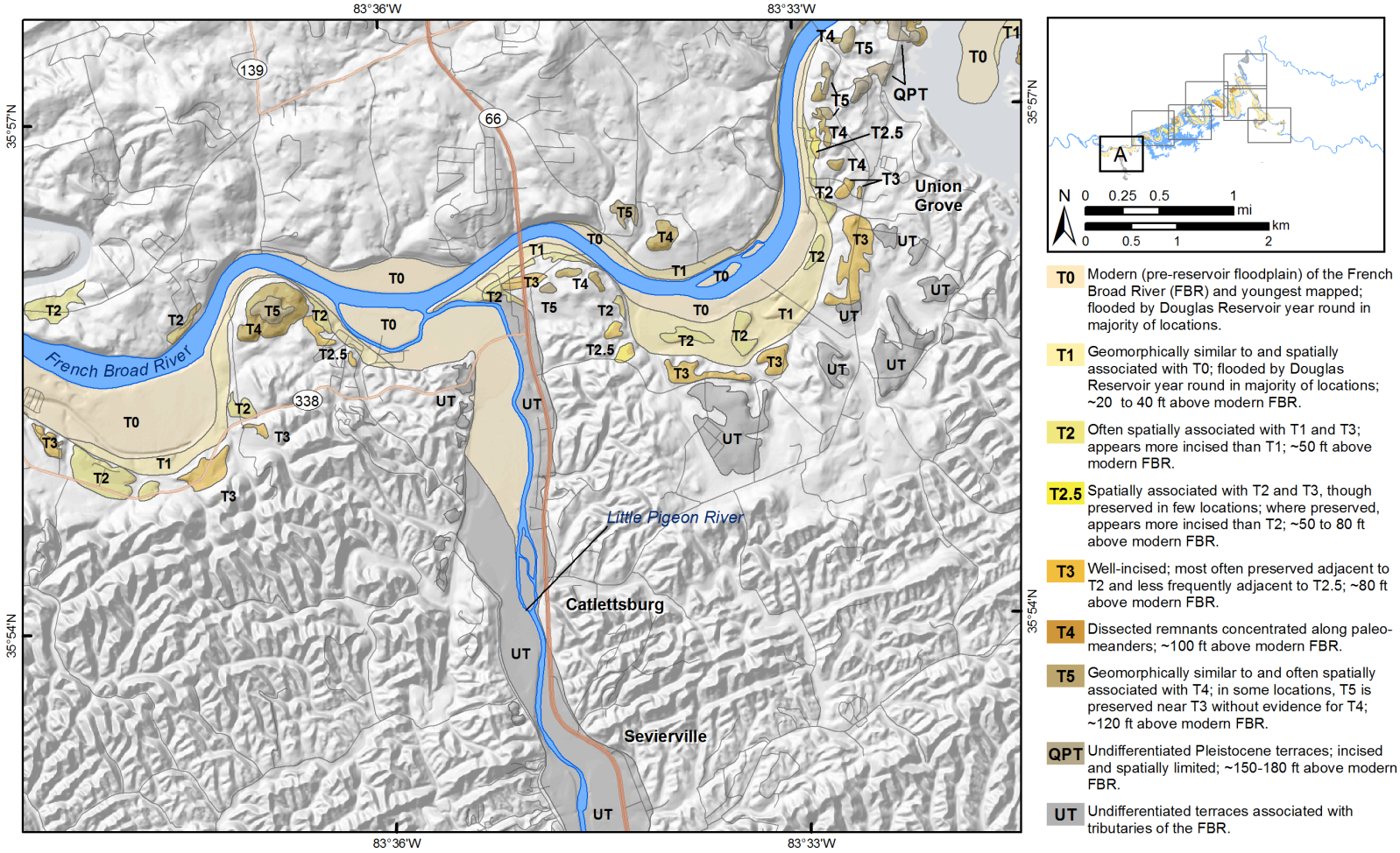

Figure 2.5.3-10. (Sheet 1 of 7) Quaternary Terrace Map of the Douglas Reservoir Area, Location A

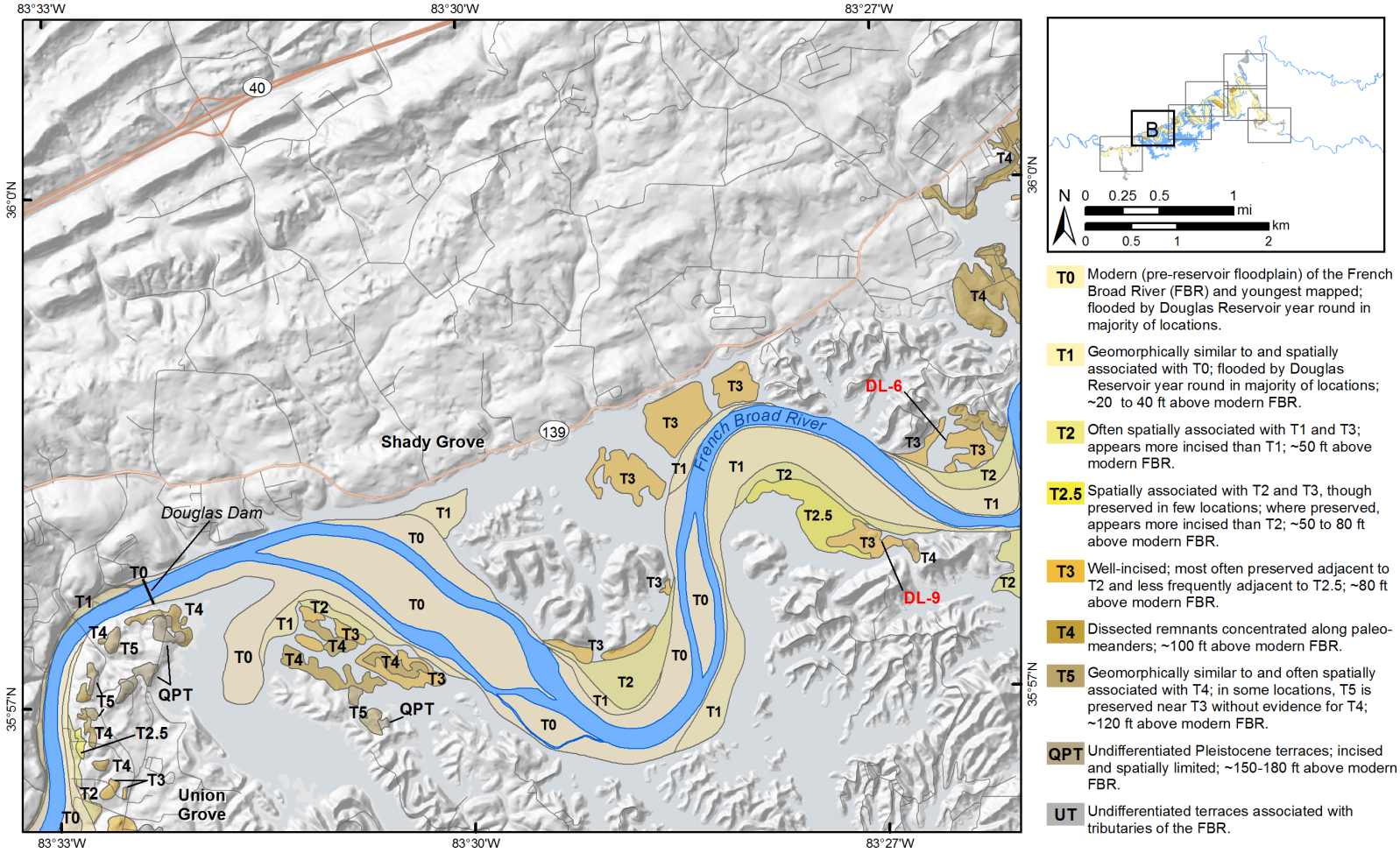

Figure 2.5.3-10. (Sheet 2 of 7) Quaternary Terrace Map of the Douglas Reservoir Area, Location B

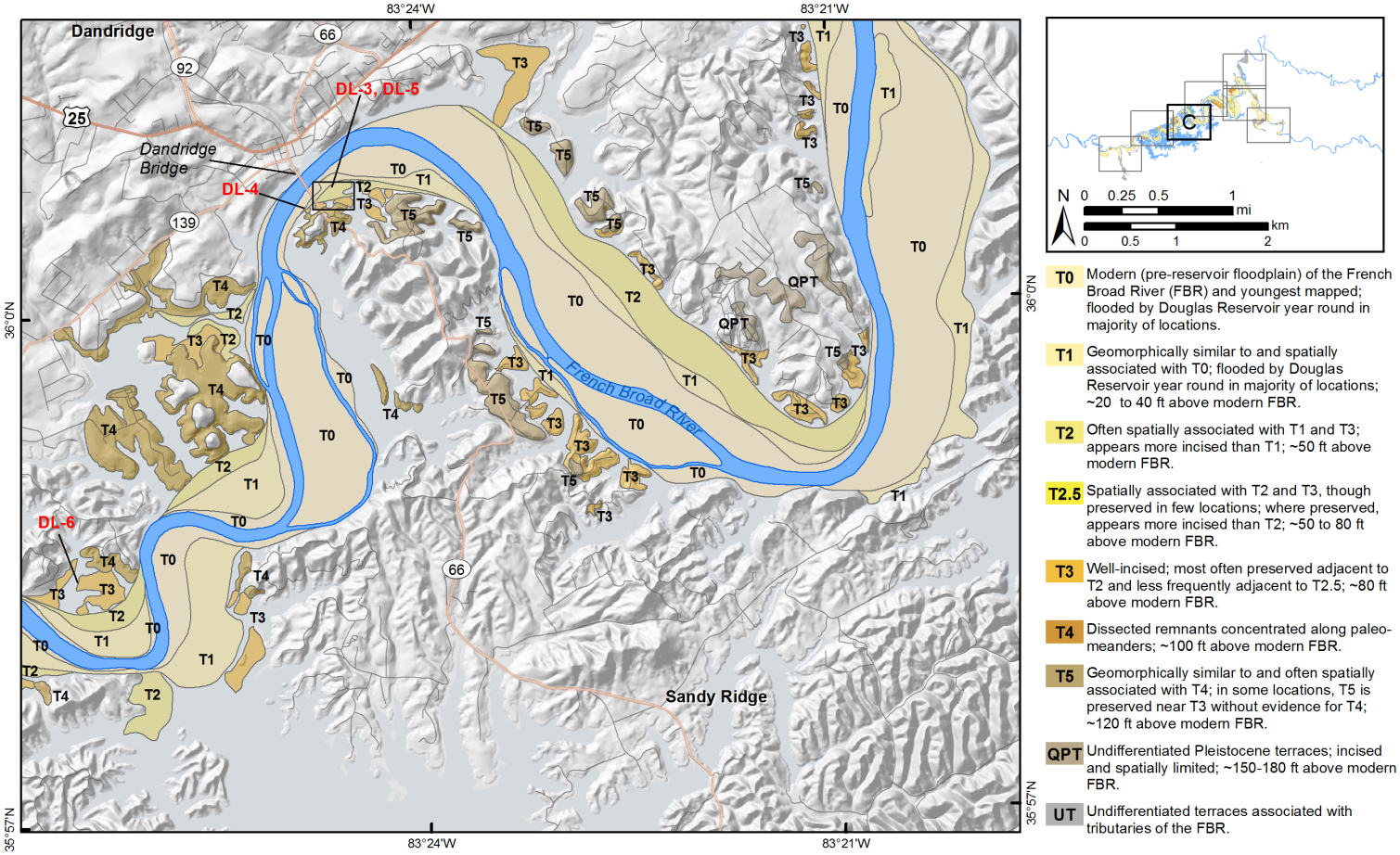

Figure 2.5.3-10. (Sheet 3 of 7) Quaternary Terrace Map of the Douglas Reservoir Area, Location C

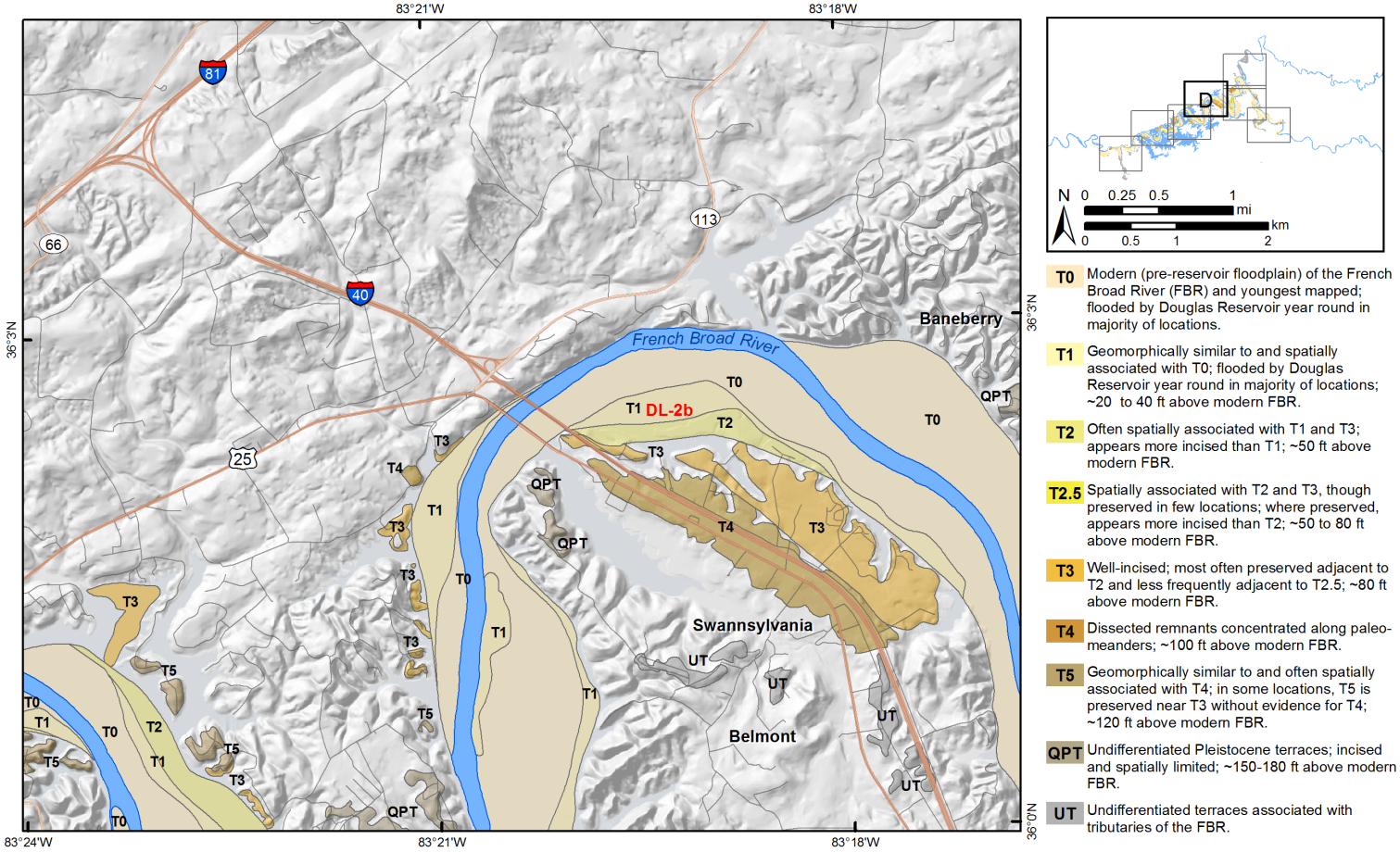

Figure 2.5.3-10. (Sheet 4 of 7) Quaternary Terrace Map of the Douglas Reservoir Area, Location D

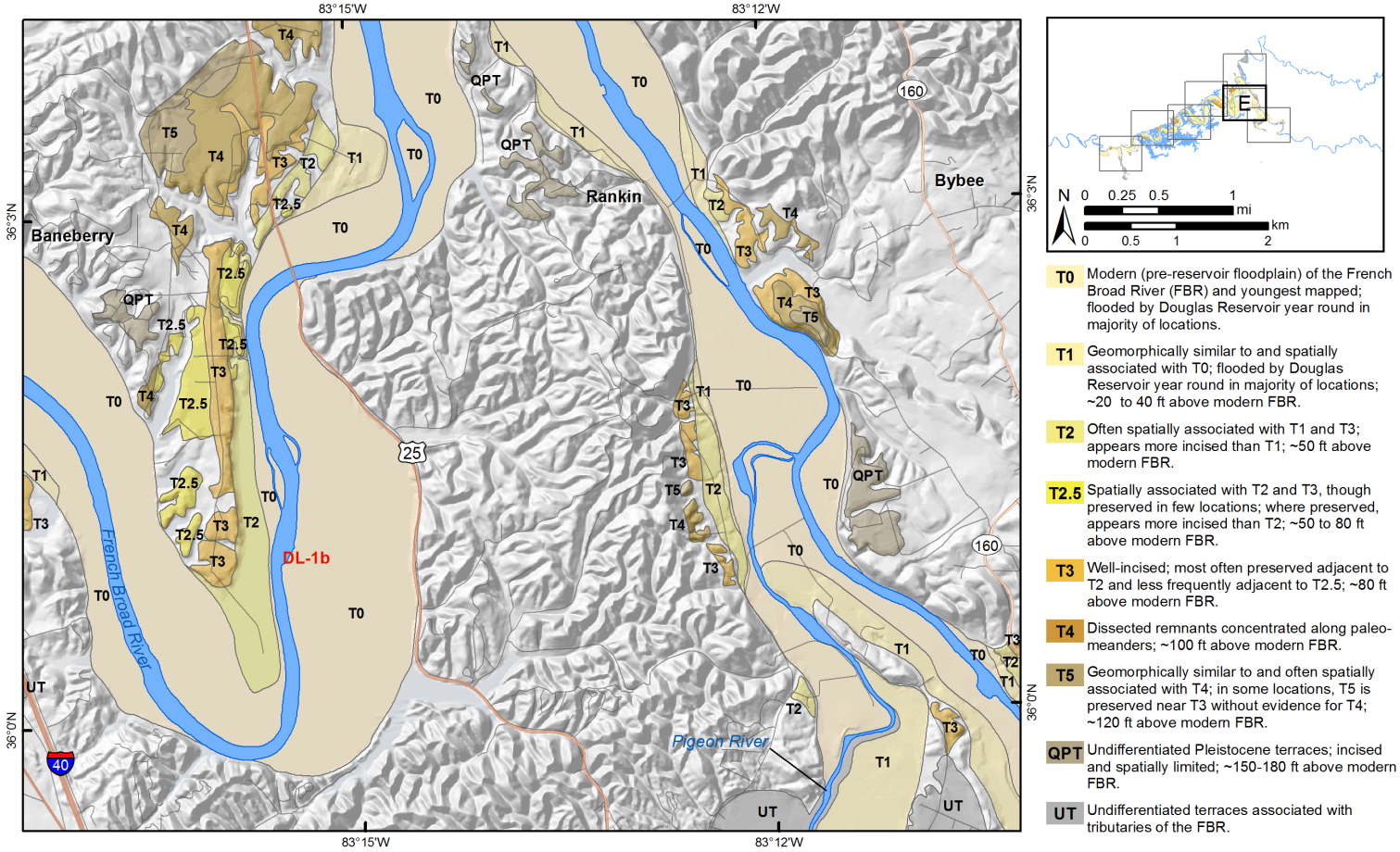

Figure 2.5.3-10. (Sheet 5 of 7) Quaternary Terrace Map of the Douglas Reservoir Area, Location E

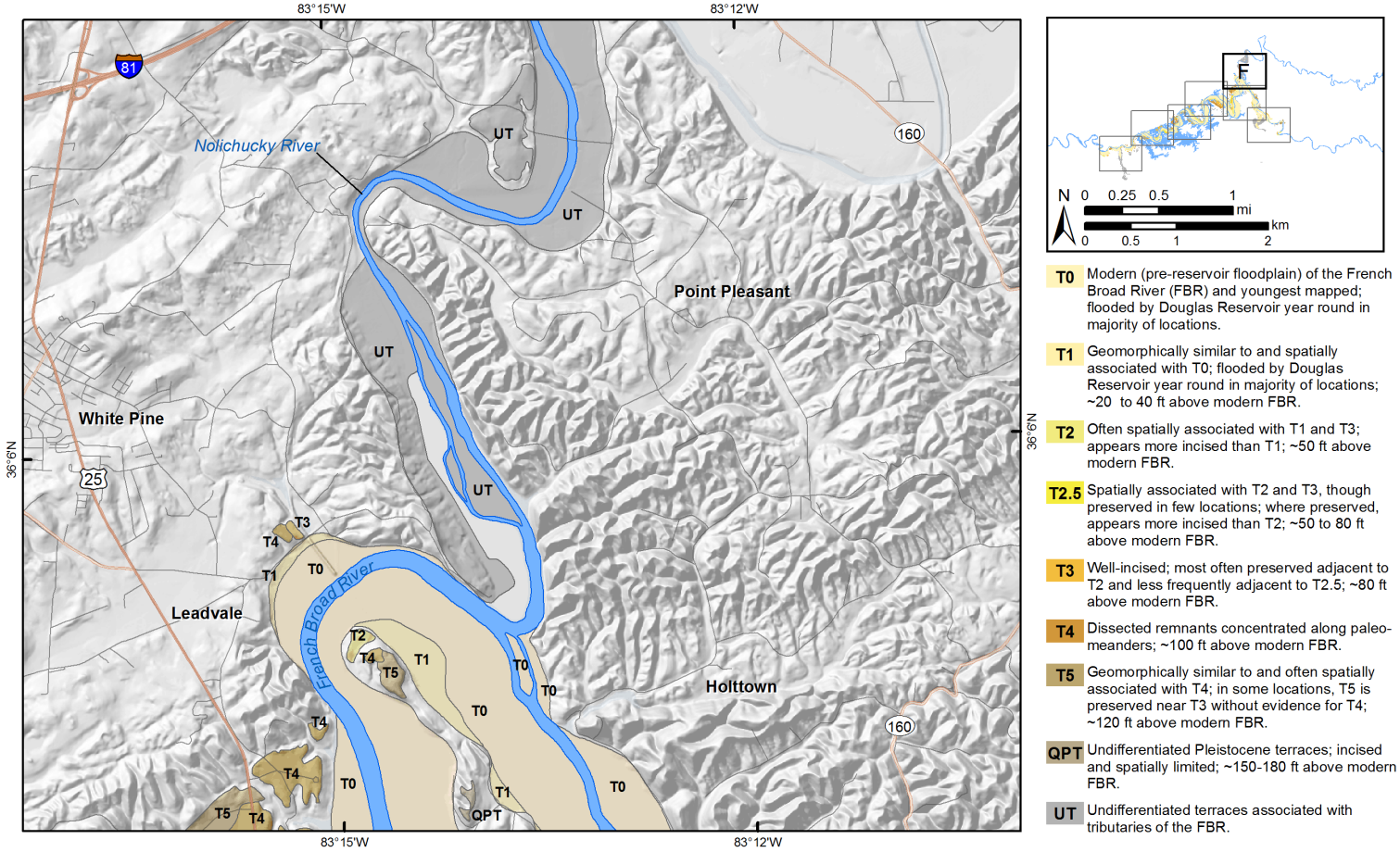

Figure 2.5.3-10. (Sheet 6 of 7) Quaternary Terrace Map of the Douglas Reservoir Area, Location F

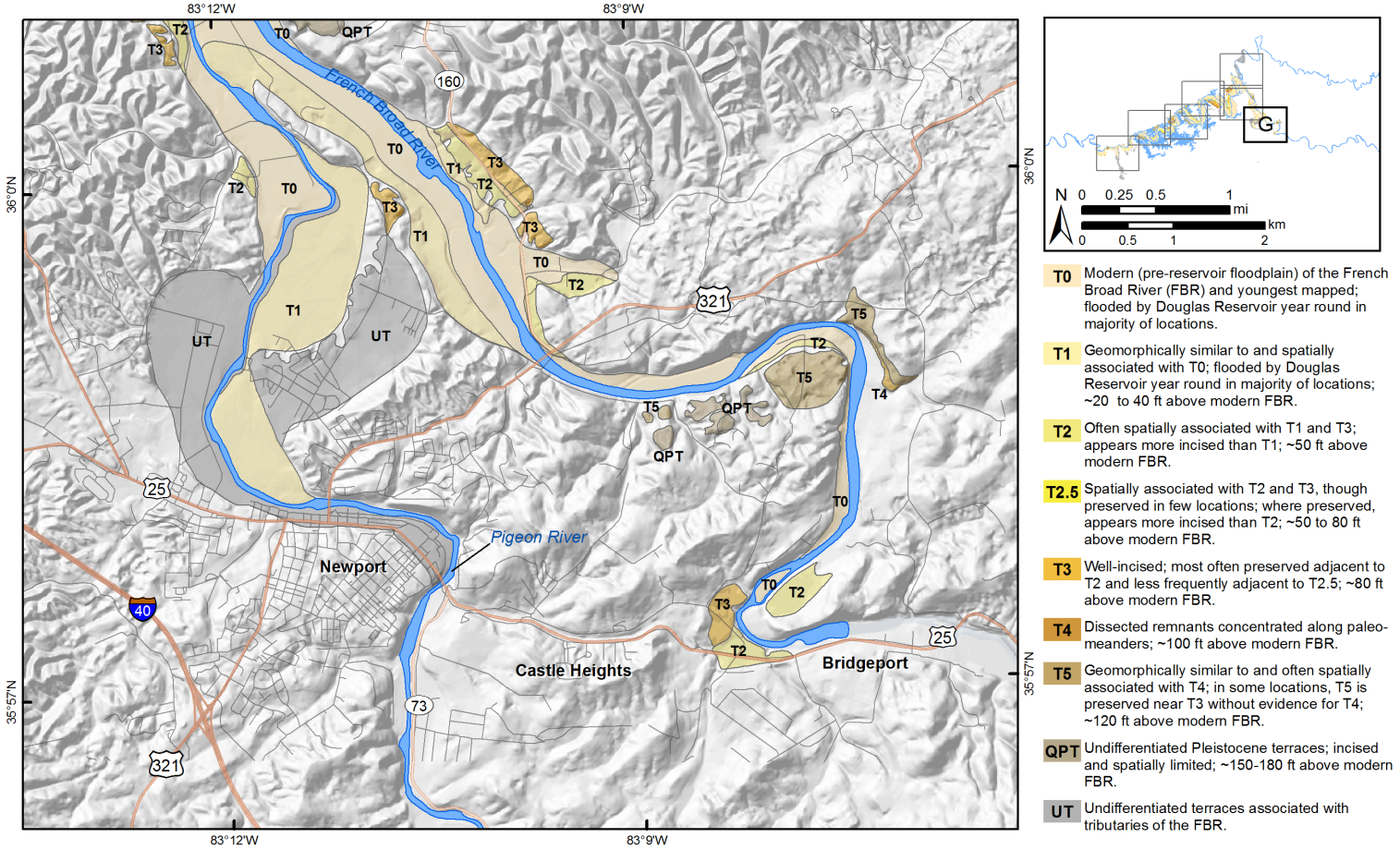

Figure 2.5.3-10. (Sheet 7 of 7) Quaternary Terrace Map of the Douglas Reservoir Area, Location G

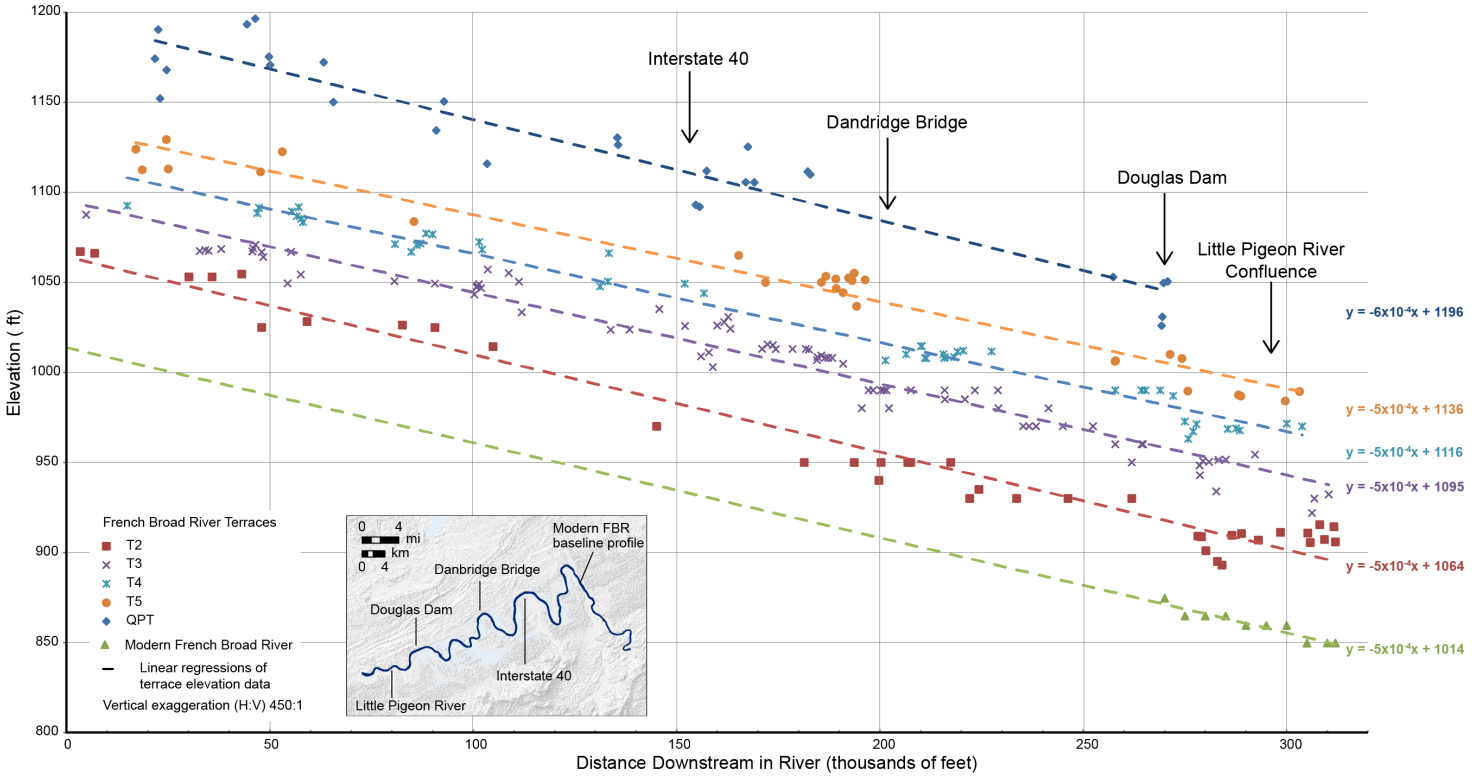

Figure 2.5.3-11. Longitudinal Profiles of Quaternary Terraces Along Douglas Reservoir

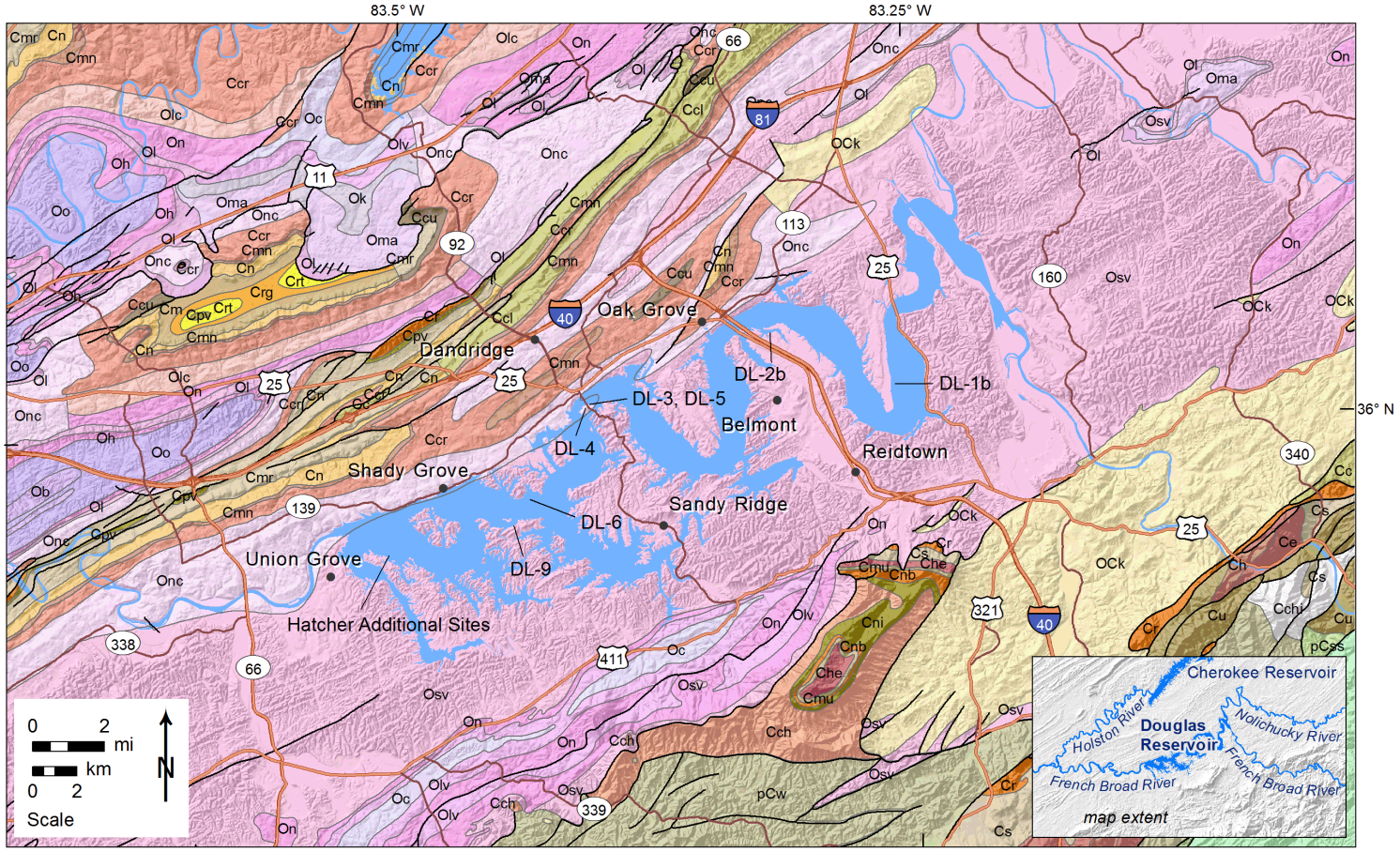

Notes:

Geologic map data from References 2.5.3-55 and 2.5.3-67.

Figure 2.5.3-12. (Sheet 1 of 2) Geologic Map of the Douglas Reservoir Area

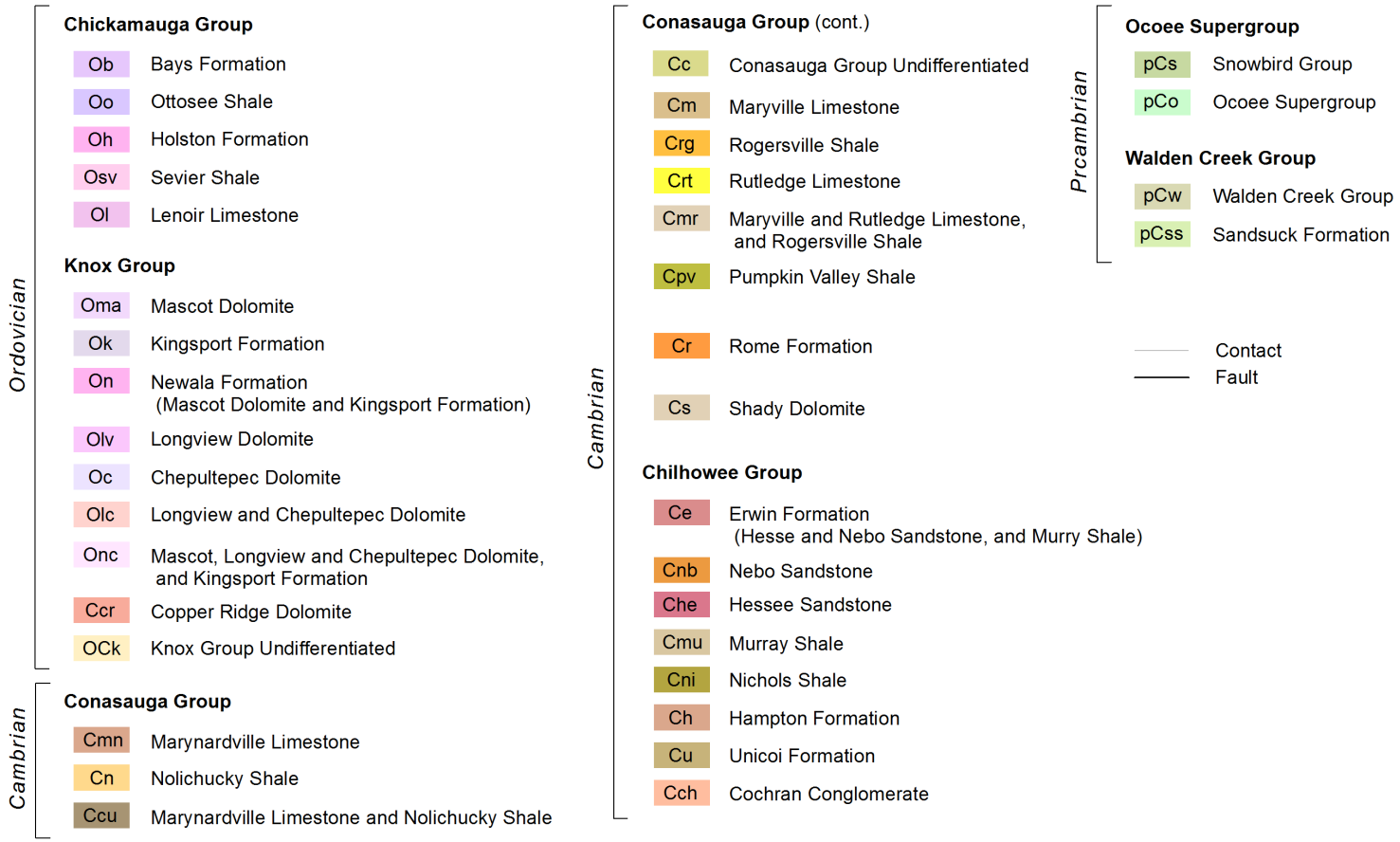

Figure 2.5.3-12. (Sheet 2 of 2) Explanation of Geologic Map of the Douglas Reservoir Area

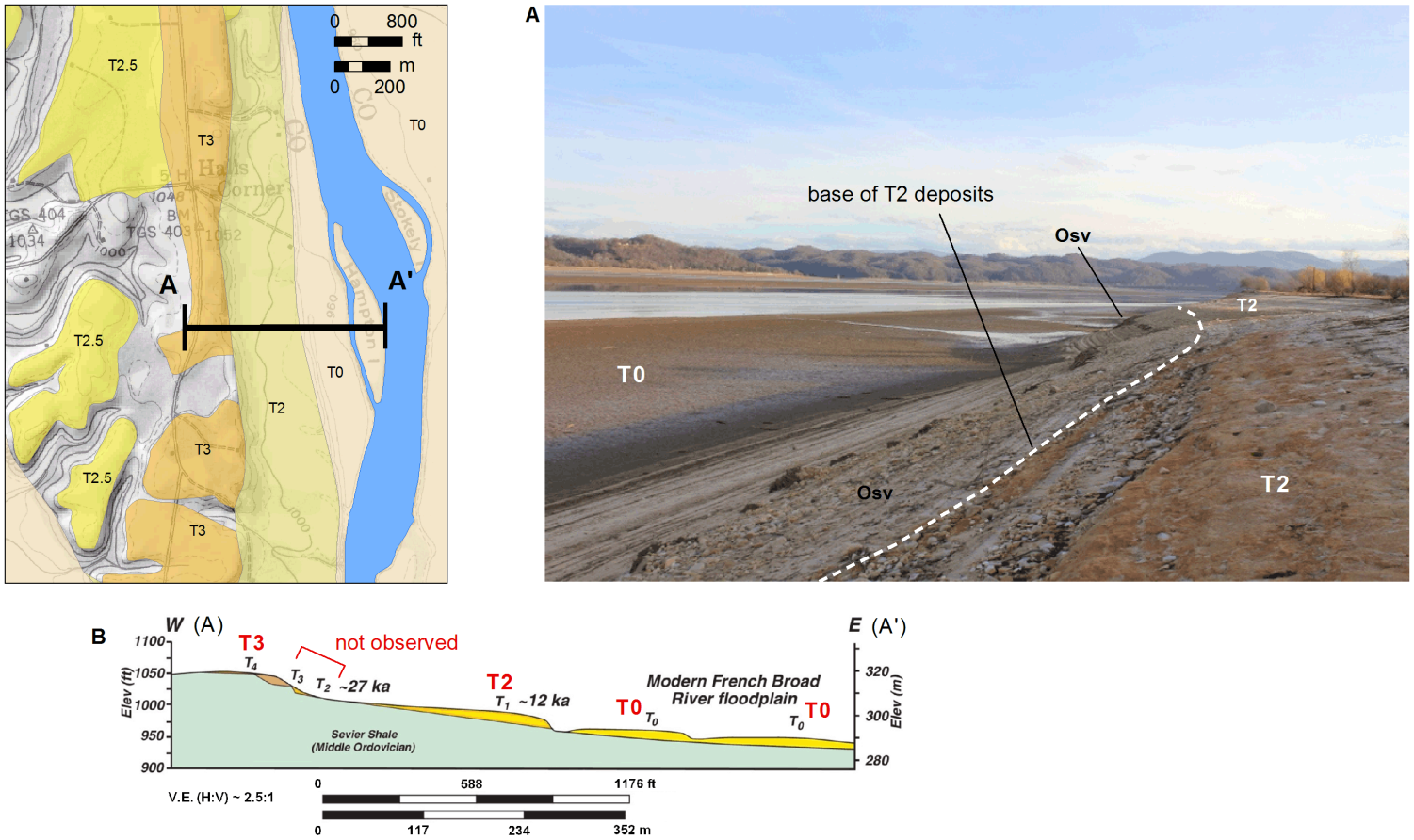

Notes:

A) Exposure of T0 and T2, as mapped in this report, and the base of T2 deposits overlying Sevier shale (Osv), viewed looking south.

B) Cross section A-A' modified from Reference 2.5.3-12: terrace interpretations in black from Reference 2.5.3-12; red from Quaternary terrace mapping presented in Figure 2.5.3-10 and shown in the location map.

Figure 2.5.3-13. Site DL-1

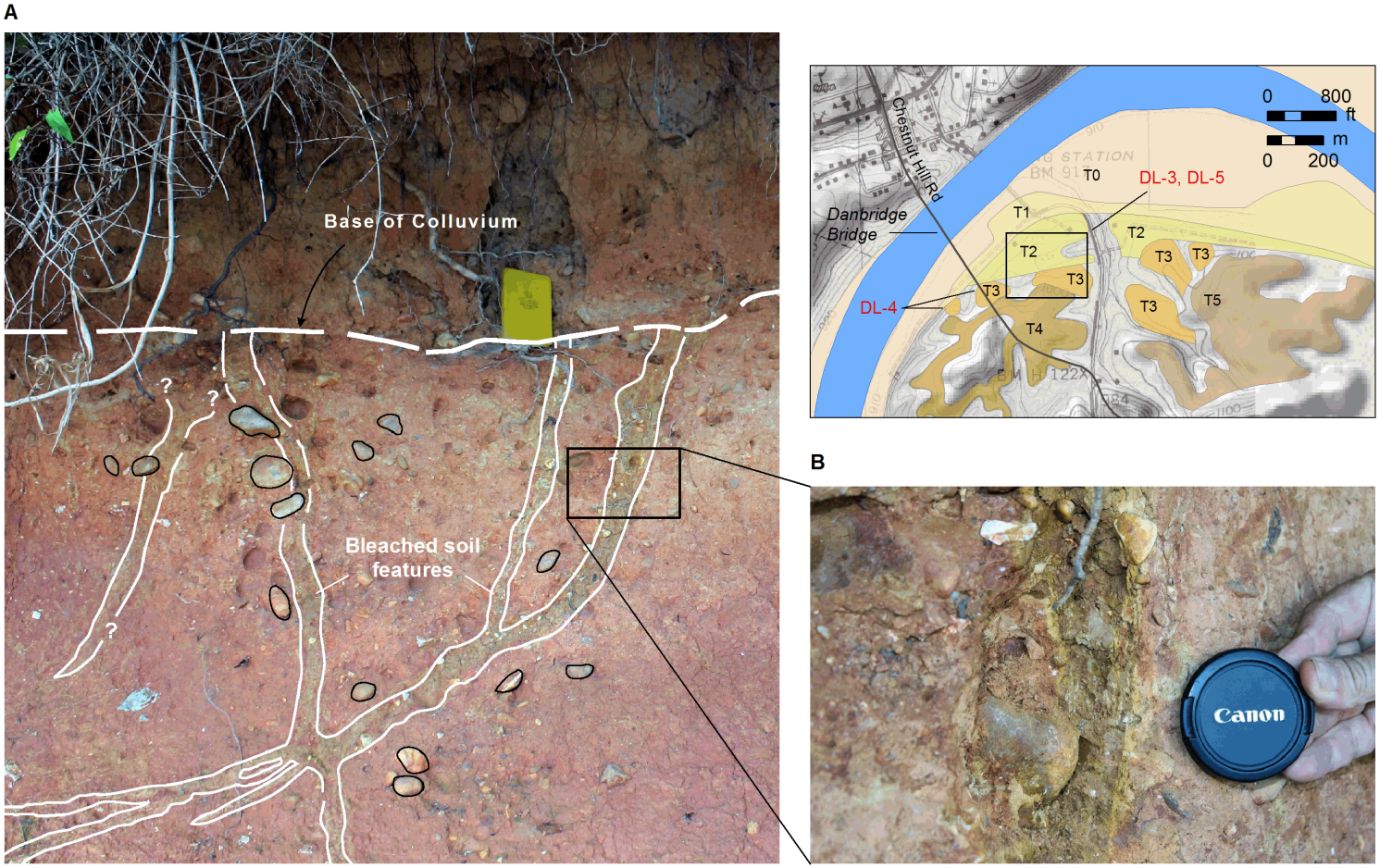

Notes:

A) Photo shows bleached rounded clasts (outlined in black) and bleached soil features truncated at the base of colluvium.

B) Detailed view of bleached soil features showing bleached rounded clasts and soil weathering.

Figure 2.5.3-14. Site DL-4

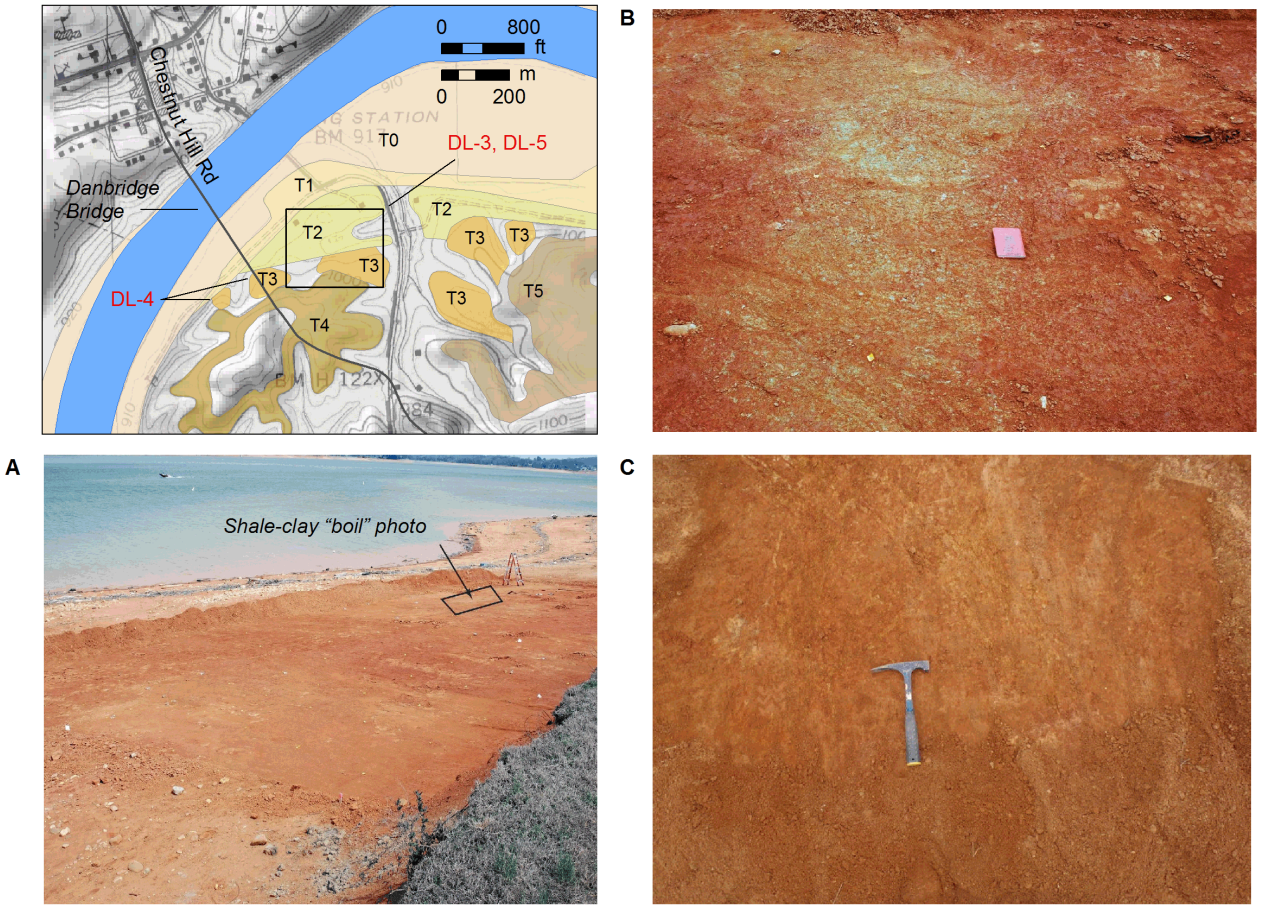

Notes:

A) and B) Images from Reference 2.5.3-12 show shale-clay "boil" exposed in the NE corner of DL-5b (not exposed during field reconnaissance).

C) Photo shows bleached fractures at the site (hammer for scale).

Figure 2.5.3-15. Site DL-5

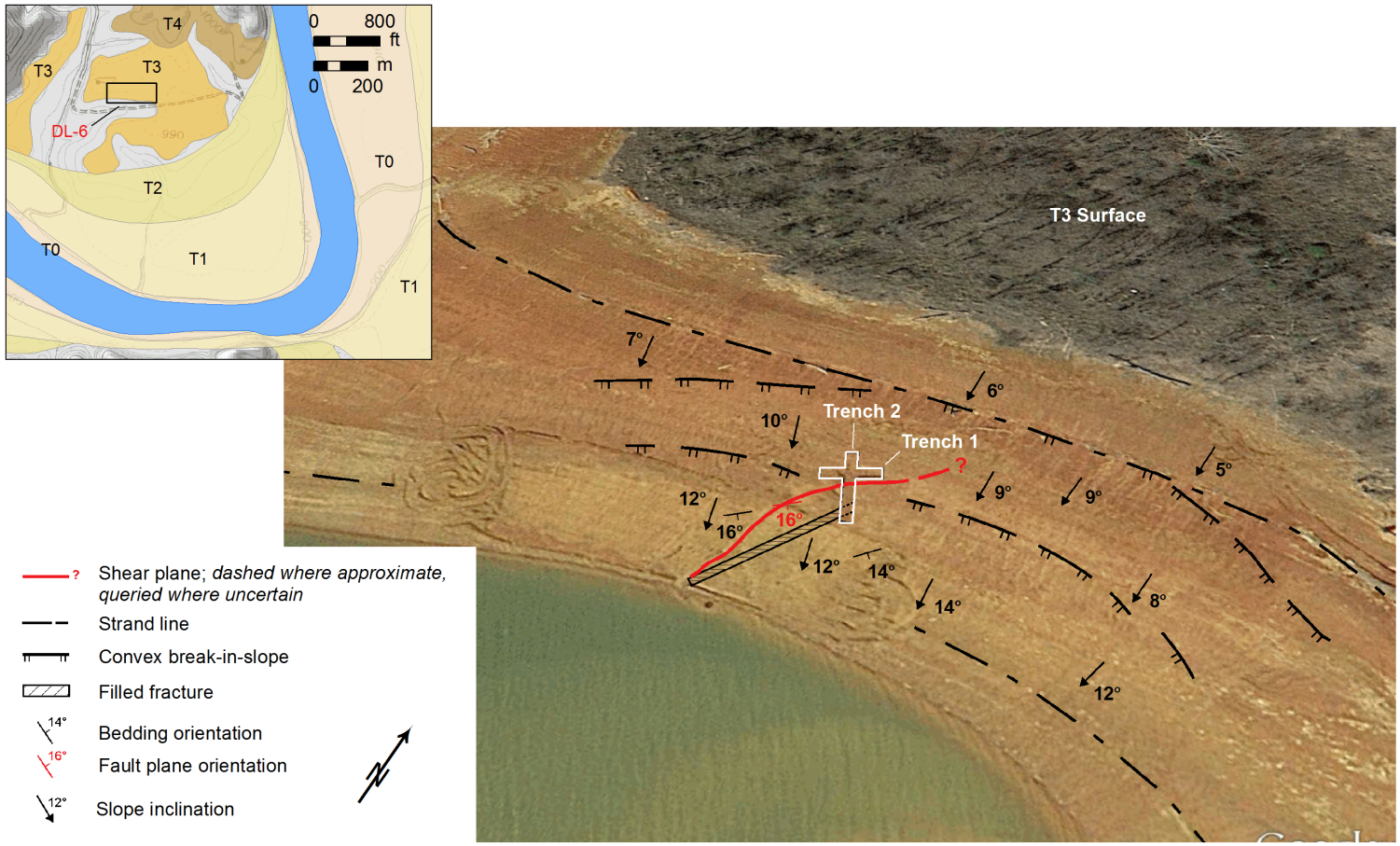

Notes:

Approximate locations of References 2.5.3-12 and 2.5.3-13 trenches, filled fractures, and shear planes below T3 surface. Trench 1 and the section of Trench 2 upslope of Trench 1 were not re-excavated during field reconnaissance. Figure 2.5.3-17 shows log of the NE wall of Trench 2. Bedding orientation and slope inclination as measured during field reconnaissance.

Figure 2.5.3-16. Aerial View of Site DL-6

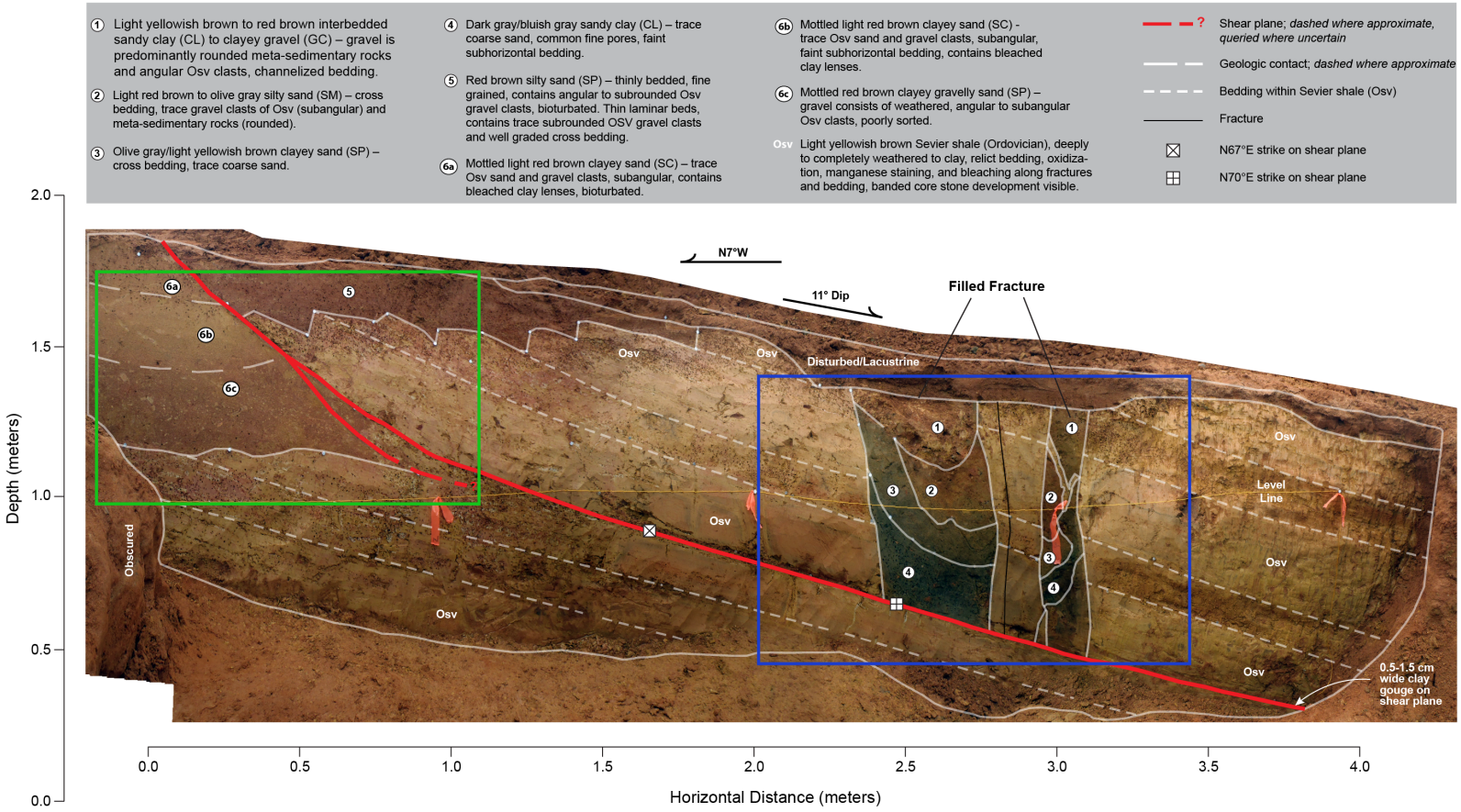

Notes:

White short dashed lines show relict bedding within deeply weathered Sevier shale (Osv) saprolite. Toward the southern end of the trench wall, filled fractures were observed above the shear plane only (blue box; Figure 2.5.3-17, Sheet 2 of 3). At the northern end of the trench wall, contact of Sevier shale with bioturbated silty sand (above shear plane) and mottled clayey and clayey gravelly sand (below shear plane) are observed (green box; Figure 2.5.3-17, Sheet 3 of 3).

Figure 2.5.3-17. (Sheet 1 of 3) Trench Log of Northeast Wall of Trench 2 at Site DL-6

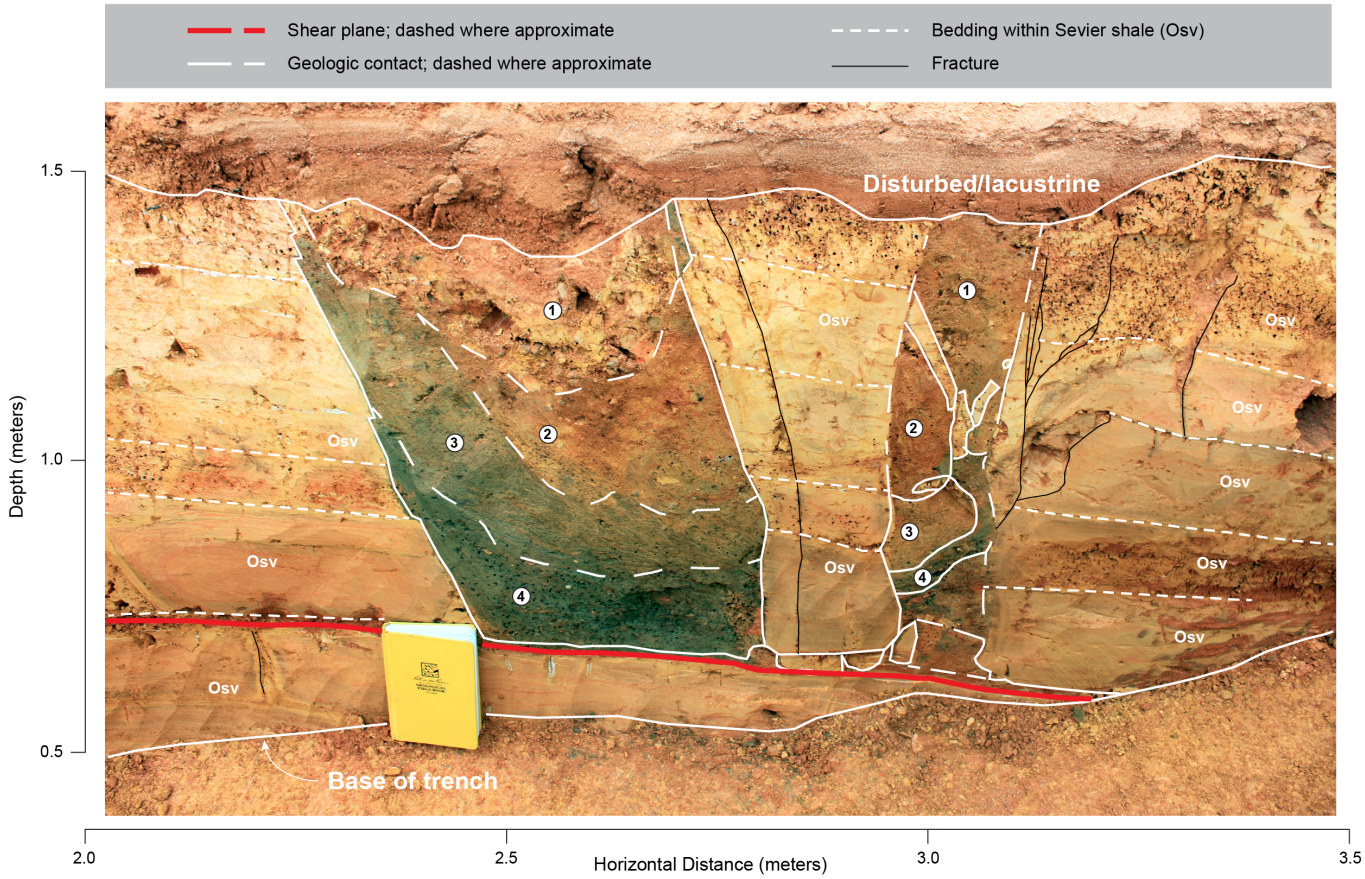

Notes:

Area of figure shown as blue box in Figure 2.5.3-17 (Sheet 1 or 3). Additional excavation below the shear plane did not reveal the potentially offset alluvium filled fracture.

Figure 2.5.3-17. (Sheet 2 of 3) Detailed View of Southern End of Northeast Wall of Trench 2 at Site DL-6

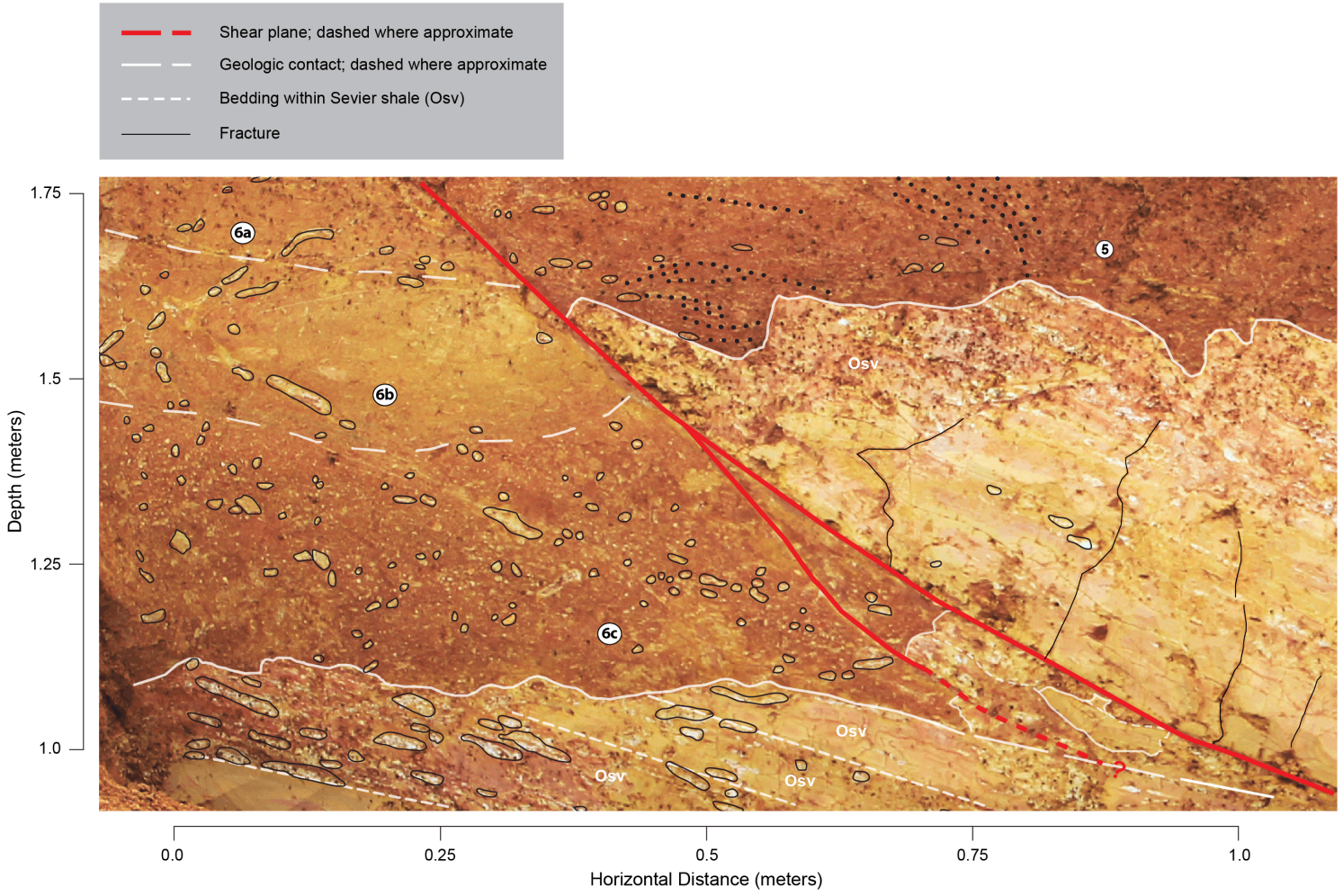

Notes:

Bleached Sevier shale fractures outlined in black. Black dots in Unit 5 show laminar cross bedding. Apparent reverse offset shows incompatibility between Units 5 and 6.

Figure 2.5.3-17. (Sheet 3 of 3) Detailed View of Northern End of Northeast Wall of Trench 2 at Site DL-6

A Event 1 - Oblique downslope movement juxtaposes Sevier Shale above possible channel deposits as shown in Trench 2, East Wall.

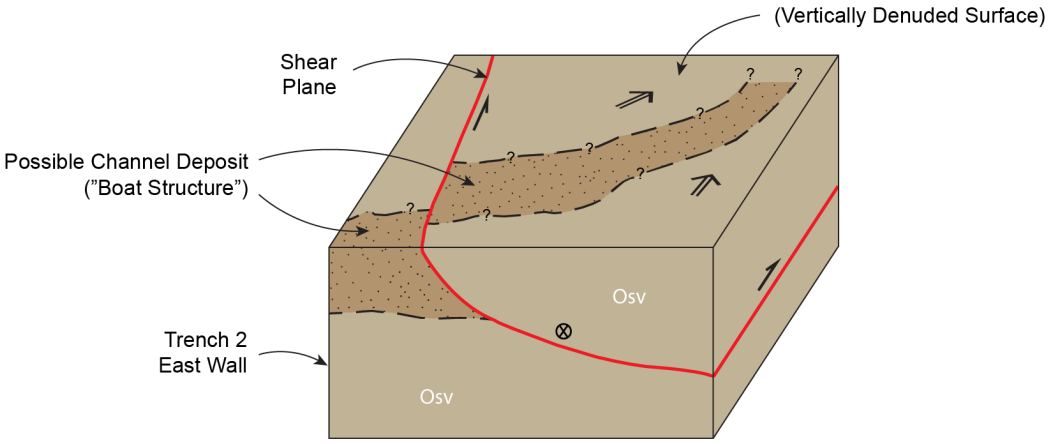

B Event 2 - Later block sliding along pre-existing shear plane creates extensional fracture.

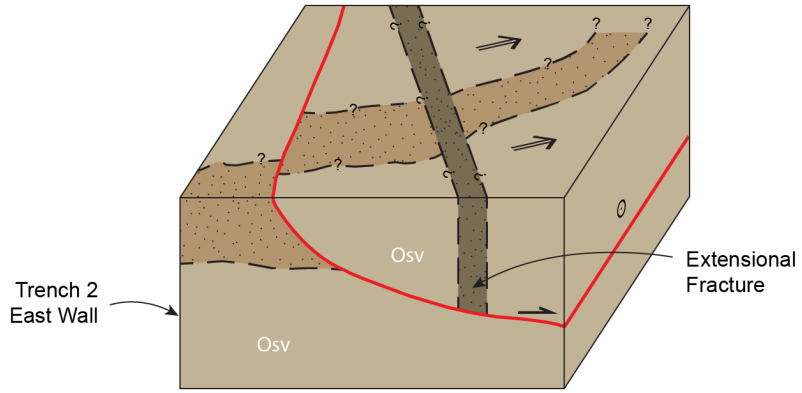

Figure 2.5.3-18. Block Diagram Illustrating Alternative Hypothesis Regarding Features in DL-6

Figure 2.5.3-19. Examples of Closed Depressions Near Site DL-6

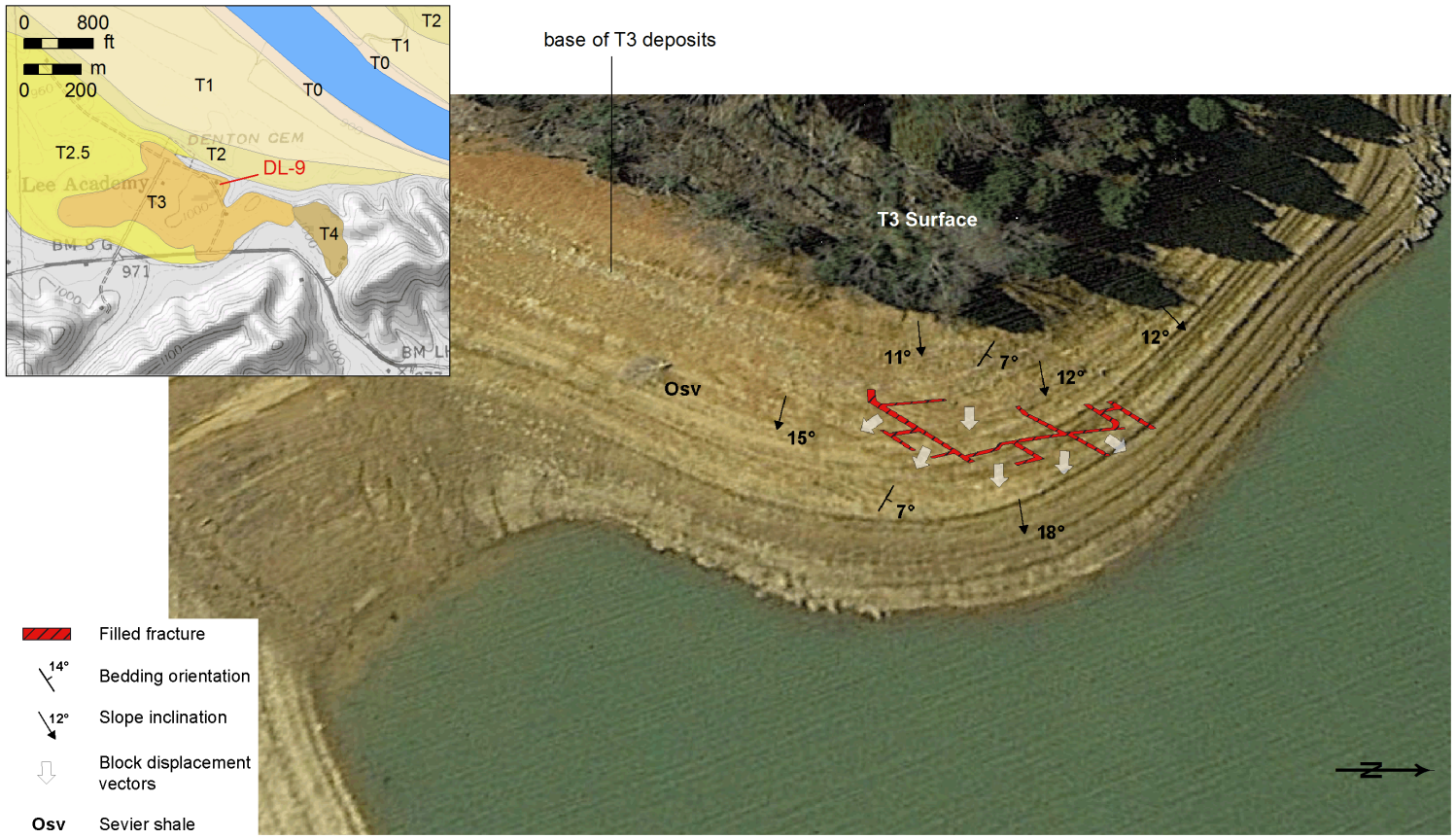

Notes:

Image includes a schematic of filled bedrock fractures mapped by Lettis Consultants International (LCI) and possible gravitational block displacement vectors shown below the T3 surface. Bedding orientation and slope inclination as measured during field reconnaissance.

Figure 2.5.3-20. Aerial View of Site DL-9

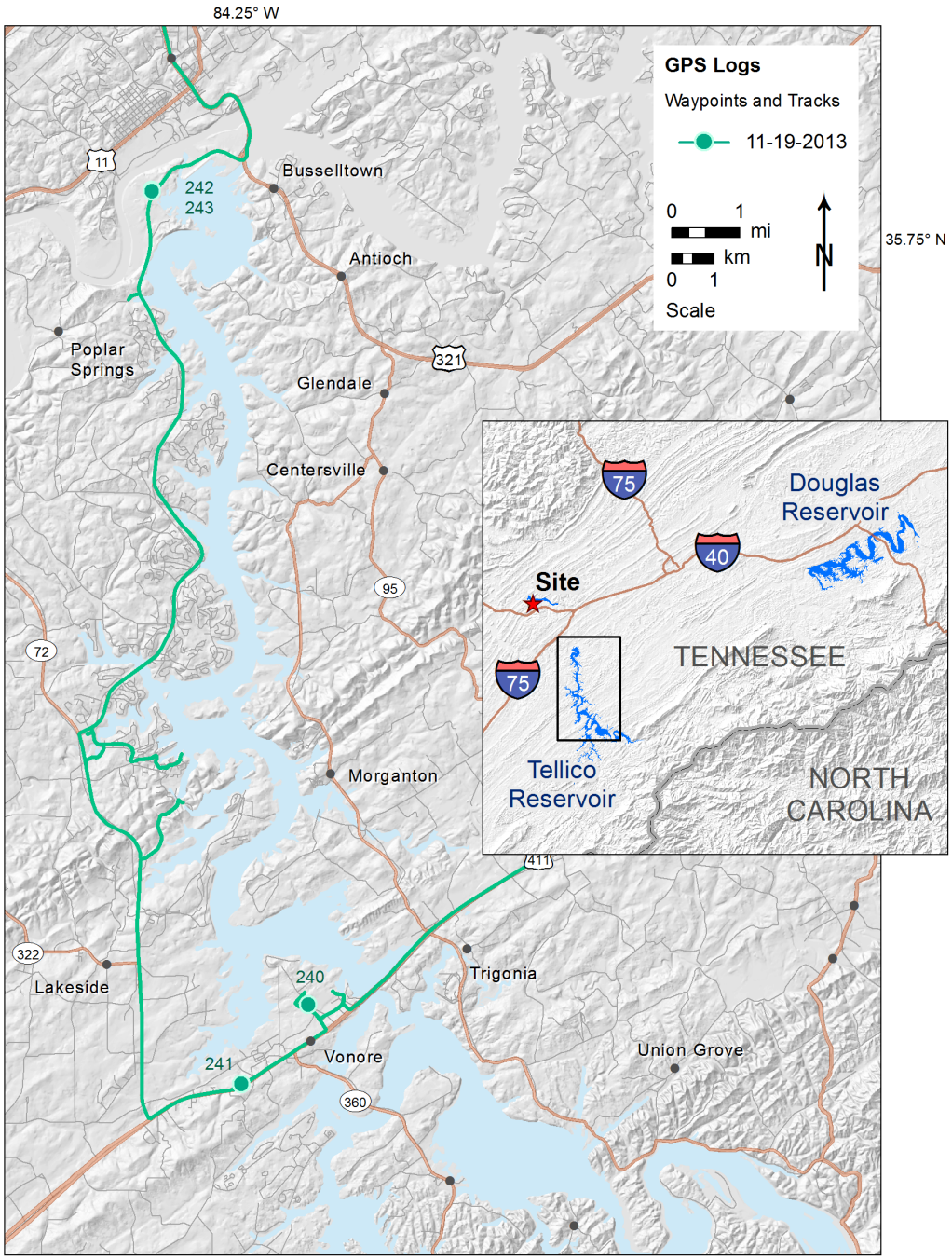

Figure 2.5.3-21. Geologic Field Reconnaissance Waypoint Locations along Tellico Reservoir

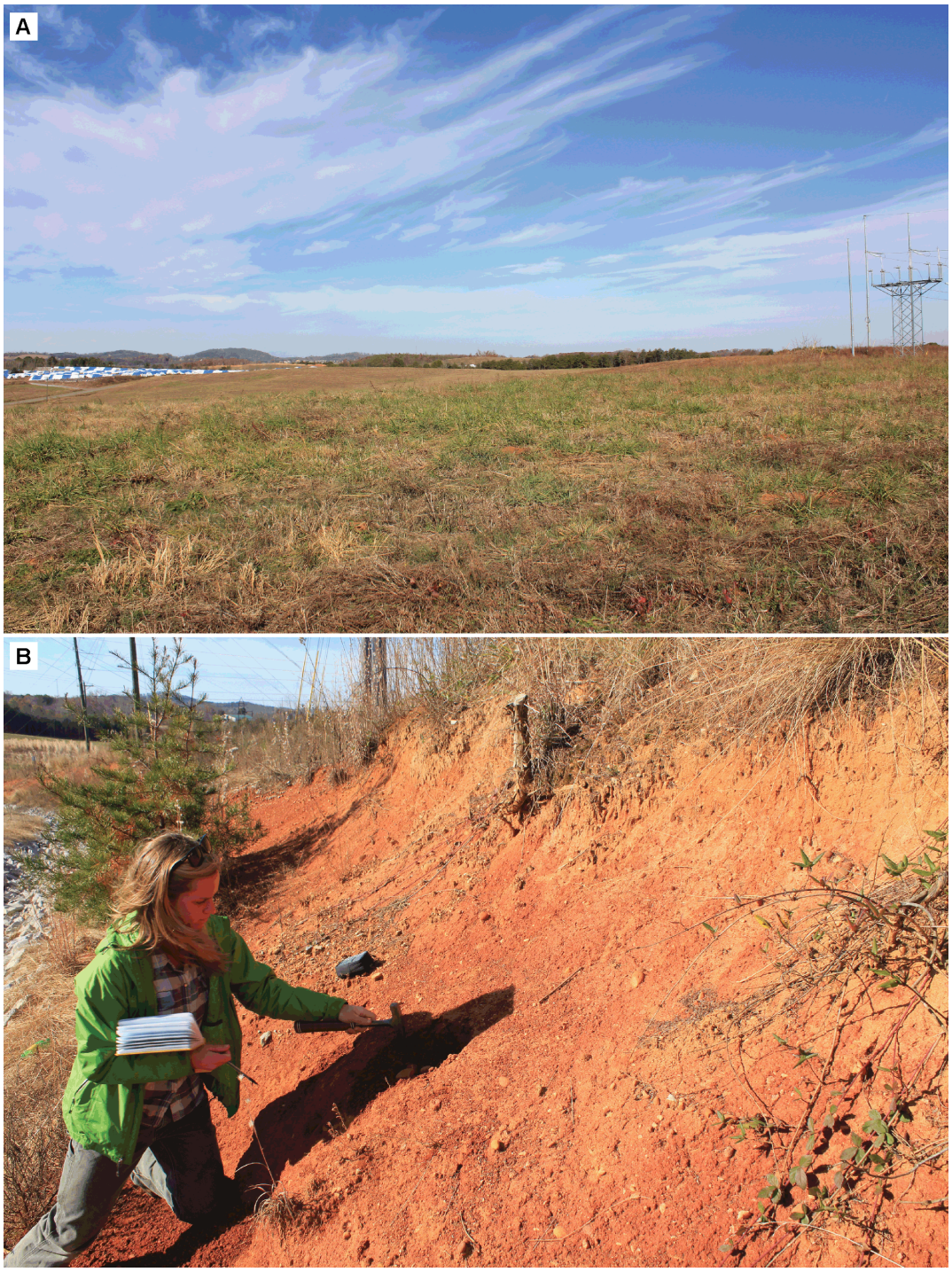

Notes: Photographs taken at Waypoint 240. Photograph A looking west from T9 terrace tread overlooking T7 tread (blue and white buildings). Photograph B showing weathered, rounded gravel deposits in T9 terrace deposit exposure.

Figure 2.5.3-22. Fluvial Terrace Surfaces (A) and Deposits (B) of the Little Tennessee River Exposed along Tellico Reservoir